Final Report –Year One

"Development of Colloidal Polymer Adsorbent for Selective NOM Removal"

By

Mark Clark, Xiang Li, Won-Young Ahn, Neal Sternisha, Andrew Westbrok, Gurjit Sandhu and

Robert Riley*

Department of Civil and Environmental Engineering

University of Illinois

Urbana, Illinois

*Separation Systems Technology

San Diego, California

Prepared for

National Water Research Institute

Fountain Valley, California

April 1, 2004

Executive Summary

This work explored a new idea: Use a common hydrophobic membrane polymer to create a colloidal phase adsorbent for limiting membrane fouling. Based on a disclosure to the University of Illinois by Mark Clark and Bob Riley, this project further developed a new material formed when polysulfone plus two organic solvents (NMP and propionic acid) are injected into water in a stirred reactor.[1] The resulting primary colloidal particles were found to have an average diameter around 60 nm; however, these particles aggregate extremely quickly into larger particles or aggregates of approximately 16 μm in diameter. The larger aggregates are quite stable in a colloidal sense: during an hour period when polysulfone is injected into the water bath, the aggregate size distribution measured in situ does not change with time, only the total mass of aggregates changes (uniformly, as expected for a constant polymer injection injection rate). BET adsorption analysis showed that the aggregates formed via this process are mesoporous, with average "pore sizes" of around 20 nm -- it was shown that the "pores" indicated in the BET analysis are actually the interstices between the primary particles in the aggregates. The total surface area of the material is around 90 m^2, which is about 10% of the surface area of activated carbon. By variation of strong and weak solvents, this work showed that the total surface area and average pore size of the aggregates can be "tuned" to a certain extent, which suggests that the pore size and adsorption performance can be adjusted to specific adsorbate sizes. Preliminary experiments have also been done in comparing the adsorption capacity of the polysulfone colloids with powdered activate carbon, and using the colloids as a pretreatment for membrane filtration, where the adsorbate or foulant in both cases is Suwannee River natural organic matter (NOM). These results are encouraging, although issues having to do

[1] This process has a direct practical and thermodynamic analogy with the phase inversion process of making asymmetric polysulfone membranes; therefore, this project greatly benefited from a previous NWRI-funded project in which Clark, Riley and coworkers investigated membrane formation and performance of a number of different membrane formulations and membrane surface post-treatments.

with purification of the polysulfone particles prior to analysis and use still remain to be overcome.

Future work with the new material should focus on four main tasks. Number one, the material needs to be tested with a wider range of NOM -- both in terms of adsorption capacity and the capacity to limit membrane fouling. Second, work needs to address the best method of applying the new material. It is unlikely that the material will ever be extensively used as a simple additive in the pure colloidal form. It is more likely that a column configuration of some type would be more advantageous, since the column configuration simplifies regeneration. In order to accomplish this, the new material needs to be either bound in another material, or cast in a different form. We have shown in the present work (Section 4.1) that it is possible to cast the polysulfone material as thin fibers, and this would undoubtedly better facilitate implementation in a column configuration. Third, we are very interested in better understanding the exact mechanism of adsorption, and whether the new material can be better "tuned" to specific adsorbates (say, NOM from different water sources). Lastly, recent collaborations have suggested that the new adsorbent can be used to concentrate NOM for advanced spectroscopic analysis of membrane foulants --- NMR and FTIR analysis may benefit from a concentration step utilizing the new material developed in this work.

Funding from NWRI, matching sources, and the University of Illinois WaterCAMPWS expanded the scope of this work. One of the additional studies was a cost analysis of full scale industrial production of the new material, which is included as Appendix I. Finally, a copy of the US patent (6,669,851 B2) describing the new material is also included as Appendix II. The patent application includes information on regeneration of the polysulfome colloids which is not included in the main report.

Nuggets

- US patent (6,669,851 B2) was awarded to the University of Illinois in December, 2003, detailing the formation of the new adsorbent examined in this work.
- Four graduate students (Yingge Wang, Xiang Li, Won-Young Ahn, and Neal Sternisha) and one post-doc (Kerry Howe) were wholly or partially funded by NWRI. The Masters thesis of Xiang Li will be deposited this month at the University of Illinois. Ahn (MS Chemical Engineering, Seoul National University) and Sternisha (MS Chemical Engineering, UIUC) are PhD students whose theses deal with the new material studied in this project.
- Three undergraduate Environmental and Chemical engineering students worked on this project and were paid hourly wages. They include Andrew Westbrook, Ben Harrison, and Gurjit Sandhu. Westbrook completed a Special Undergradaute Research Experience (SURE) project based on his work on the NWRI project, and did another independent study on costs of producing the colloidal polymer (Appendix I). Based on his work on this project, Clark has nominated Westbrook for the University of Illinois Dural Undergraduate Research prize. Ben Harrison, an Australian engineering student, attended the University of Iliniois during the summer of 2003 under the auspices of the International Association for the Exchange of Students for Technical Experience (IAESTE). Harrison was paid an hourly stipend by the NWRI and with matching/supporting funding. Finally, Gurjit Sandhu is an undergraduate Chemical Engineer at the University who is working part-time on the NWRI project.
- Supplementary funding for this project was obtained from the Illinois Board of Higher Education ($32,582), the Department of Civil and Environmental Engineering at the

University of Illinois ($6,500), and the University of Illinois Water CAMPWS ($100,101) -- a National Science Foundation Science and Technology Center.

- Through the NWRI project and the UIUC Water CAMPWS, several side projects related to this project have been initiated. We are collaborating with Andrey Kalinichev and James Kirkatrick of the Department of Geology at UIUC. Kalinichev is an expert on molecular dynamics (MD) simulations, and he is trying to model the association of different ions and foulants with membrane surfaces. We hope that one day this work will help us better understand membrane charge and membrane fouling. Kirkpatrick is an expert on NMR, and we have supplied him samples of the polymer colloids developed in this work to use for concentrating natural organic matter prior to NMR analysis. Since the material developed in this work should preferentially adsorb membrane foulants, we may well have developed an efficient way of concentrating foulants for advanced chemical analysis. We are also collaborating with Timm Strathmann, Assistant Professor in the Department of Civil and Environmental Engineering at UIUC. Strathman has developed and FTIR-ATR capability in his new lab, and will be helping graduate students study organic deposits on membrane surfaces (with and without pretreatment with the polysulfone adsorbent developed in this work). These data should supplement the NMR work going on in the Geology lab at UIUC.
- Numerous publications/presentations resulted from this project. They include the following:

Clark, M.M., Li, X, and R.L. Riley " Polymer Colloid Adsorbent for Limiting Membrane Fouling by Natural Organic Matter," published extended abstract, 226th American Chemical Society (ACS) National Meeting, New York, NY, September 7-11, 2003.

Ahn, W.Y., Sternisha, N., Li, X., Riley, R., and M. Clark, "Development of Polysulfone Colloid Adsorbent to Reduce Membrane Fouling by Natural Organic Matter (NOM)," accepted, Annual Meeting of the North American Membrane Society, June 26-30, 2004, Honolulu, Hawaii

Clark, M.M., "Adsorption of Natural Organic Matter on a Tuneable Colloidal Polymer," Plenary lecture, 12th International Meeting of the International Humic Substances Society, Sao Paulo, Brazil, July 26-30, 2004.

Clark, M.M., "Adsorption on Natural Organic Matter by a Tunable Colloidal Polymer Material," Department seminar, Department of Civil and Environmental Engineering, Rice University, April 16, 2004.

Clark, M.M., "Adsorption on Natural Organic Matter by a Tunable Colloidal Polymer Material," Department seminar, Department of Civil Engineering, University of Minnesota, February 27, 2004.

Clark, M.M., "When Bad Polymers Go Good: A Basic Science Love Story," Department Seminar, Myongji University, Department of Environmental Engineering and Biotechnology, Seoul Korea, November 5, 2002.

Clark, M.M., "When Bad Polymers Turn Good: A Basic Science Love Story," Technical University of Kracow, Krakow Poland, December 17, 2002.

Clark, M.M. "Polysulfone Colloids: Characterization, Stability and Performance in Water Treatment," Department seminar, Laboratoire de Génie Chimique, Université Paul Sabatier, Toulouse, France, December 19, 2002.

Clark, M.M, "When Bad Polymers Go Good: A Basic Science Love Story," department Seminar, Civil and Environmental Engineering, University of Houston, April 4, 2002.

Acknowledgements

Zeta potential measurements and analyses of sonicated particle size were performed at the Illinois Waste Management and Research Center in the University of Illinois. Adrienne Menniti performed the experiments and collected the data. Membrane fouling, BET surface analysis, total organic carbon, and particle size analysis (Lasentech instrument) were performed in the Environmental Engineering and Science (EE&S) lab at the University. Kerry Howe, Shaoying Qi, Lance Schideman, and Rachel Michaud provided training on these instruments. Scanning Electron Microscopy (SEM), Energy Disperse Spectroscopy (EDS), and Transmission Electron Microscopy (TEM) were performed at Beckman Center in the University of Illinois. Scott Robinson provided training and helped in the imaging. Ternary phase diagrams were better understood after discussions with Professor Paul V. Braun of the Material Science and Engineering Department at UIUC. Ken Ishida, of the Orange County Water District, and Harry Ridgway of Aquamem, continue to be valued colleagues and collaborators on all subjects related to organic fouling of membranes and analysis of organic foulants with FTIR.

Finally, a committee from the National Water Research Institute (R. Carnahan, D. Furukawa, and D. Lloyd) was formed to advise this project during a difficult period; their council is greatly appreciated. Ron Linsky's encouragement throughout this project is also greatly appreciated.

1. Introduction

Natural organic matter (NOM) is a source of color in drinking water supplies, and can form disinfection by-products that have a serious health risk. NOM can also complex with heavy metals and pesticides, which greatly increases the persistence and bioaccumulation of these chemicals in the environment (Maartens et al, 1998). NOM has also been regarded as the most important membrane foulant in the treatment of drinking water with technologies like micro- and ultrafiltration; it limits membrane performance and lifetime, and is therefore a critical issue for future application of membranes in water treatment.

Many researchers have shown that the membrane material is extremely important in NOM fouling (AWWA Committee Report, 1999). Howe and Clark (2001) and Howe et al. (2002) have done detailed analysis of membrane fouling by dissolved organic mater (DOM) using water sources from several rivers around the US. In serial filtration tests, fouling of a polyethersulfone (PES) UF membrane could be completely prevented by prefiltration of the lake water with a hydrophobic polypropylene (PP) microfiltration membrane. Since the organic foulant was smaller than the pores of the PP membrane, it was concluded that the foulant adsorbed to the PP membrane pores and was nearly completely removed before the water contacted the second (PES) membrane. The astonishing thing about these tests is that the change in DOM concentration across the MF membrane was barely detectable (~5%). This suggests that the fraction of the DOM that actually causes fouling is a small subset of to the total DOM matrix.

There is a considerable history of efforts to limit organic fouling of membranes using additives like powdered activated carbon (PAC) and metal ion coagulants. (AWWA Committee Report, 1999). However, additives like PAC and coagulants have been used with limited success. In both

cases, there is little about the additives that can be tailored to adsorb or complex the part of the DOM which actually causes fouling. Both materials remove significant mass percentages of DOM, but have no effect or a very small effect on membrane fouling.

With this background in mind, the present work examined a new material that specifically targets NOM foulants (US Patent 6,669,851 B2). The new material is a colloidal form of polysulfone; polysulfone is one of the most common membrane polymers, is hydrophobic, and is particularly prone to adsorptive fouling by NOM (Jucker and Clark, 1994). The idea behind the new material is that adsorbents made from membrane materials will preferentially adsorb the fraction on NOM that fouls membranes. This study focused on the production, characterization, and basic application of the new polymer adsorbent.

2. Literature Review

2.1 Natural Organic Matter

NOM is the main component of organic carbon in aquatic systems (Aoustin, 2001). It is a complex, difficult-to-separate mixture of similar macro-organic molecules derived from the degradation and decomposition of biological organisms, with a broad spectrum of functional groups, sub-structures and molecular weight distribution, strongly depending on its origin and genesis (Stevenson, 1982).

NOM is typically classified as humic substances and non-humic fractions. Humic substances are the more hydrophobic fraction and have a relatively higher molecular weight; the non-humic fraction is more hydrophilic and contains proteins, polysaccharides and aminosugars. Humic substances represent up to 80% of the total organic carbon of natural waters (Buffle et al, 1978) and are of most concern in conventional water treatment, but recent study suggests that the non-humic fraction of NOM could also form a significant amount of potentially regulated DBPs (Wang, 2000). Humic substances are traditionally defined, according to their solubility, as fulvic acids, humic acids, and humin. Fulvic acids are those organic materials that are soluble in water at all pH values. Humic acids are those materials that are insoluble at acidic pH values (pH<2) but are soluble at higher pH values. Humin is the fraction of natural organic materials that is insoluble in water at all pH values (Gaffney et al., 1996). These definitions reflect the traditional methods for separating the different fractions from the original mixture. Fractions isolated from water by sorption on weak-base ion exchange (XAD) resins showed an average NOM composition of 10% humic acid, 40% fulvic acid and 30% hydrophilic acids (Aoustin et al. 2001).

NOM is also characterized as dissolved organic matter (DOM) and particular organic matter (POM). DOM is the fraction that passes through a 0.45 μm filter. It accounts for 80 to 90% of NOM (Aiken and Cotsaris, 1995).

NOM is typically quantified by bulk parameters instead of individual compounds because of its complexity. The most commonly used methods in quantifying NOM in water treatment are total organic carbon (TOC), dissolved organic carbon (DOC), and UV_{254} adsorbance. The molecular structure of NOM has been represented as $C_5H_7O_2N$. By stoichiometry, carbon is approximately half of the total mass, which suggests that the dissolved organic matter (DOM) concentration is roughly twice the dissolved organic carbon concentration (Thurman, 1985). Studies have shown that, water treatment practices such as coagulation or membrane filtration vary in their removal of specific DOM fractions. Measurement of DOC and UV absorbance can also suggest different removal results, since UV absorbance responds disproportionately to NOM aromaticity (Howe, 2001). Typically, in surface waters, the humic content expressed as DOC varies from 0.1 to 50 ppm in dark-water swamps. In ocean waters, the DOC varies from 0.5 to 1.2 ppm at the surface, and the DOC in samples from deep groundwaters varies from 0.1 to 10 ppm (Gaffney et al., 1996).

2.2 NOM characterization and contribution to membrane fouling

2.2.1 Elemental composition and functional groups

The range of the elemental composition of humic materials is relatively narrow, being approximately 40-60% carbon, 30-50% oxygen, 4-5% hydrogen, 1-4% nitrogen, 1-2% sulfur,

and 0-0.3% phosphorus. Humic acids contain more hydrogen, carbon, nitrogen, and sulfur and less oxygen than fulvic acids (Gaffney et al. 1996). DOM functional groups include acidic functional groups like carboxylic acids and phenols; neutral functional groups like hydroxyls, and basic functional groups like amines and amides.

Technologies like Attenuated Total Reflection (ATR) Fourier-Transform Infrared (FTIR) spectrometry and Scanning Electron Microscopy coupled Energy Dispersive X-ray (SEM-EDX) spectroscopy have been used to get insight into the chemical nature and elemental compositions of organic deposits on synthetic membranes. Howe et al. (2002) performed ATR-FTIR on polypropylene MF membranes after filtration of two North American surface waters. The spectra suggested that both organic and inorganic compounds were present. The proportion of those two kinds of foulants varied between the sources. Inorganic foulants appeard to contain aluminum silicates and the organic foulants were enriched in carbonyl or amide functional groups. There was no strong evidence for the presence of carboxylic acid, carboxylate, phenolic, or hydroxyl functional groups in the foulants. In addition, Rabiller-Baudry et al (2002) performed SEM-EDX to measure the atomic composition of skimmed milk fouled PES UF membranes. An atomic ratio, defined as the ratio of a measured atomic composition (C,O,N) to sulfur (S) was used to detect composition change in the foulant; here sulfur was used as an indicator of the membrane material. Atomic ratio ((C+N)/S and O/S) of new, fouled, and water-rinsed PES membrane were compared to get insights into fouling. However, since skimmed milk fouling of membranes is more prominent than NOM fouling, the atomic ratio method may not be as sensitive when used with natural water systems.

2.2.2 Molecular Weight

Apparent molecular weight is an important parameter to characterize NOM because it can provide valuable information for identifying potential treatment strategies (Owen et al, 1995), and because molecular weight affects solubility and hydrophobicity. Various techniques can be used to determine apparent molecular weight (AMW) of NOM. This includes the adsorption/diffusivity model, vapor pressure osmometry, x-ray scattering, ultrafiltration fractionation, and gel permeation chromatography (GPC). The majority of DOM has a typical AMW value of 1000 to 2000 Daltons (Thurman 1985). There is also a small fraction of colloidal organic matter, which is approximately 10% of the DOC, and has an AMW from 2000 to 100,000 Daltons (Thurman 1985). Since molecular size affects solubility and hydrophobicity and large molecules tend to be less soluble than small ones with similar functionality, membrane surfaces would be expected to preferentially adsorb higher-MW organics from solution (Howe 2001). Lin et al. (1999) fractionated a commercial humic acid (Aldrich) into different MWs with GPC, and separated hydrophobic/hydrophilic parts with exchange resins. They found out that the fraction with the largest AMW (6.5–22.6 kDa) of both hydrophobic and hydrophilic fractions exhibited the worst flux decline. Howe and Clark (2002) fractionated NOM according to molecular size by fractionation with regerenerated cellulose membranes and reported that small "colloids" appeared to be important membrane foulants. They believed the size range of the colloids was from 3 to 20 nm. The very small colloids identified by Howe and Clark are not the typical colloidal or particulate matter identified by previous investigators (e.g., Thurman et al., 1985).

2.2.3 Charge Density

DOM is usually negatively charged in aqueous solutions at neutral to high pH. The negative charge comes from the deprotonation of carboxylic acids. Carboxylic acids account for approximately 90 % of the organic carbon in natural water (Thurman, 1995). The pK_a values of the carboxylic acids and phenol groups are listed in Table 2.1. Because of the low pK_a values, carboxylic acids are typically completely ionized at the pH of natural waters. Membrane materials are also usually negatively charged under typical operating conditions. Because of electrostatic repulsion and increased charge density of DOM, adsorption of NOM on membrane surfaces will be reduced. At the isoelectric point, the surface charge and streaming potential vanish, and adsorption reaches a maximum point (Pontie'et al., 1998). The charge density on both DOM and membrane surfaces are related to pH in solution.

Table 2.1 Various pK_as of organic acids

Organic acid	Weak				Strong			
	Phenol (ortho to carboxyl)	Phenol	Phenol (ortho to halogen)	Diketone	Acetic acid	Benxoic acid	Phthalic acid	Oxalic acid
pK_a	13	9.9	8.5	7	4.9	4.2	2.9, 4.4	1.2,4.2

Source: Thurman, E. M., 1985, Organic Geochemistry of Natural Waters, pp89.

2.2.4 Hydrophobicity

Table 2.2 shows that the DOM has a large carboxyl group content. The carboxyl oxygen is polar, which adds to the solubility and hydrophilicity. At natural water pH values, carboxylic acids are typically completely ionized. Polar and ionic groups make the DOM hydrophilic as a whole. Jucker and Clark (1994) found that solutions of humic and fulvic acids with concentrations greater than 1000 mg/L can be prepared without reaching solubility limits. Despite their high solubility, Jucker and Clark found that the hydrophobicity of NOM increases as pH decreases because that carboxyl groups become fully protonated at lower pH. Although

DOM is regarded hydrophilic as a whole, it can be separated into relatively hydrophobic and relatively hydrophilic parts. Using XAD resin, Owen et al identified six fractions: hydrophobic acids, bases and neutrals, and hydrophilic acids, bases and neutrals. The XAD resin is a nonionic methylmethacrylate polymer that adsorbs organic matter from water by hydrophobic bonding (Thurman 1995).

Table 2-2 Acidic Functional Groups in NOM

Carboxyl Groups, meq/g Carbon	Phenolic Groups, meq/g Carbon
9.85	3.94

Source: Ritchie and Perdue, 2003.

The hydrophobic fraction of DOM is important in evaluating of the interaction between DOM and membrane surfaces. Humic acid has relatively more phenolic groups and relatively fewer carboxylic groups; hence, humic acid is relatively more hydrophobic than fulvic acid. Humic acid adsorption on membranes has been studied to greater extent than fulvic acid. Jucker and Clark (1994) reported greater adsorption of humic acid than fulvic acid on a UF membrane; Schaefer et al. (2000) reported more flux decline when filtering humic acid than fulvic acid. The conventional wisdom has been that more hydrophobic compounds have greater adsorption on membrane surfaces. However, hydrophilic compounds have also been found to foul membranes.

Several studies have been done by separating DOM into hydrophilic/hydrophobic fractions using nonionic resins, and then evaluating fouling effects of those fractions individually. Lin et al. (2000) fractionated soil-derived humic acid by adsorption onto a Supelite DAX-8 resin(a hydrophobic resin) and reported that the hydrophilic fraction caused greater flux decline than the hydrophobic fraction durmg crossflow filtration using a polysulfone membrane. Amy and Cho (1999) fractionated DOM by XAD-8 and XAD-4 resin columns and reported that the AMW of

DOM adsorbed to the membrane surface was similar to the hydrophilic fraction. Based on their ATR-FTIR spectrum of fouled membrane surface, they suggested that the hydrophilic neutral and base fraction of DOM was a major membrane foulant in the water of investigation.

Howe (2001) suggested that these conflicting results could arise because the specific mechanism for adsorption on membrane material is not necessarily the same as adsorption on nonionic resins. It is possible that a few specific compounds are responsible for fouling of UF membranes, and that the nature of these compounds varies between source waters (Howe, 2001).

2.3 NOM removal

Table 2.3 shows feasible treatment processes for removal of different NOM fractions. It's clear that membrane technology has the potential to remove a range of NOM fractions and will become increasingly important in drinking water treatment processes.

Table 2.3 Feasible treatment processes associated with different NOM fractions

Fraction	Viable processes
High MW NOM	Coagulation, Membranes (UF)
Medium MW NOM	Adsorption, Membranes (UF or NF)
Lower MW NOM	Membranes (NF), Ozone induced biodegradation (BSF or BAC)
Humic NOM	Coagulation, Adsorption, Membranes
Non-humic NOM	Membranes, Biodegradation (BSF or BAC)

Source: Amy, G. L., 1993.

2.4 Membrane fouling by NOM

Organic-fouled membranes typically exhibit gradual flux-decline during the filtration process which can change DOM rejection behavior. This is due to foulant adsorption/deposition onto membrane surface, which can change the surface charge, hydrophobicity/hydrophilicity, and effective pore size. DOM is thought to adsorb to membrane surfaces by (1) hydrophobic interactions, (2) electrostatic interaction, and (3) specific chemical affinity. The parameters that affect membrane fouling include: (1) DOM and membrane properties such as hydrophobicity, charge density, molecular weight, membrane surface morphology, and (2) important solution parameters such as pH, ionic strength and presence of other solutes such as calcium and silica.

The charge of the membrane may affect performance because charge affects the electrostatic repulsion between charged molecules and the membrane surface (Childress et al, 2000). Membrane surfaces can acquire positive or negative charge because of different functional groups on the surface. The positive surface charge below the isoelectric point is thought to result from the protonation of the basic functional groups, while the negative charge above the isoelectric point would result from deprotonation of the acid groups (Childress et al, 2000). It was reported that contact between membranes and humic substances can change membrane surface charge. This phenomina was observed to be strongly related to the pH value of the solution. Childress et al (2000) did streaming potential measurements of NF--55 membranes contacted with Suwannee River humic acid (SRHA). They observed that SRHA caused the membrane to be more negatively charged over the entire pH range. They believed that this was caused by the adsorption of SRHA on the membrane surface. At relatively low pH, the membrane is positively charged while the SRHA is still negatively charged, and the adsorption of SRHA is favorable because of both electrostatic and hydrophobic interactions. At higher pH values, the SRHA and the membrane are both negatively charged, and adsorption is likely

dominated by hydrophobic interactions. The existance of divalent cations like calcium will also affect the interaction between membrane surfaces and humic substances. This has been explained by invoking mechanisms like electrostatic charge shielding and complexation (Liang and Morgan, 1990; Childress and Elimelech, 1996) and salt bridging (Jucker and Clark, 1994).

2.5 Fouling Control

Since NOM fouling of membranes has been one of the major problems hindering UF application in water treatment, the control of membrane fouling has been intensively investigated. Membrane fouling control typically includes three main categories: (1) the removal of NOM including membrane foulants upstream of a membrane unit, (2) membrane surface pretreatment, and (3) optimization of operating procedures and parameters.

The removal of NOM upstream of a membrane unit can be achieved by adding adsorbents such as powdered/granular activated carbon (PAC/GAC), or metal-based coagulants (or both) to the water. Maartens et al. (1999) and Howe (2001) reported that pre-coagulation with metal-ion coagulants before filtration resulted in a reduction in NOM concentration, but only Howe reported a significant decrease in membrane fouling. Several researchers have shown that the addition of PAC prior to MF or UF processes could increase NOM removal efficiency and slightly reduce membrane fouling (Adham et al, 1991; 1993), while other researches have reported that the flux decline for PAC-treated streams is worse than the original humic substances, and more humic acids were deposited on the membranes (Lin et al, 1999). These contrasting results could be due to differences in the water sources and different types of membranes, or they could simply indicate the lack of membrane foulant removal with PAC or coagulation. New types of adsorbents have been developed to target control of membrane fouling. Chang and Benjamin (1996) developed an iron oxide particle (IOP) adsorbent that

ranged from 0.5 to 50μm in diameter. They reported that IOP pretreatment of influent water could significantly increase the TOC removal efficiencies of the hybrid UF system and at the same time prevent NOM fouling. Two mechanisms of fouling prevention were suggested: (1) IOP sorption of NOM significantly reducing the TOC concentration in the bulk solution and leading to lower NOM concentration in the concentration polarization layer, or (2) IOP cake layer formation on the membrane surface that serves as a protective layer against NOM fouling.

Optimization of operating procedures and parameters includes variation of recovery ratio, variation of pH and ionic strength, and application of hydrodynamic cleaning with high cross-flow velocity. Cho et al. (2000) studied membrane filtration of NOM with controlled J_0/k (initial pure water flux / estimated boundary layer mass transfer coefficient). They reported that as J_0/k decreased, there was less flux decline and increased NOM rejection due to increased concentration polarization. NOM-induced fouling of UF membranes can also be reduced or eliminated by very frequent and brief loop flushing, by frequent loop backwashing, or by using alkaline cleaners. Even with cleaning, there can be a long-term decrease in the backwashing efficiency; in fact, it has been reported that the cleaning procedures can degrade the membrane causing a more open membrane structure and allow passage of larger molecules.

Membrane surface modification has been achieved in different ways. Fane and Fell (1987) showed that the adsorption of surfactants and soluble polymers to form a hydrophilic monolayer on the membrane surface gives membranes a hydrophilic character; this yields fewer hydrophobic sites for foulant adhesion, and can lead to a reduction in foulant adsorption by hydrophobic membranes. Maartens et al. (2000) pre-coated UF polysulfone membranes with the nonionic surfactants Triton X-100 and Pluronic F108. They found that membrane pretreatment by Pluronic F108 significantly reduced the adsorption of foulant species found in humic acid and

natural brown water at the cost of reduced pure water flux through the membranes; Triton X-100-coated membranes were just as susceptible to foulant adsorption as untreated membranes, but had an increased pure water flux. The lower fouling comes from the more hydrophilic character of the pre-coated membranes. The authors believed that the reduction in pure water flux caused by Pluronic F108 adsorption onto/into the membranes was caused by pore restriction with a subsequent decrease in the average pore size. With Triton X-100-coated membranes, the more hydrophilic membrane surface caused stronger interactions between water molecules and the membrane surface and pores. After coating, more and larger molecules dissolved in water tend to move through the membranes, which cause more foulants to be entrapped inside the membrane pores. Combe et al. (1999) researched three methods: (1) Hydrolyzing CA membranes in order to decrease hydrophobicity by reducing acetyl content, where hydrolysis was carried out by treating the CA membrane with a solution of 0.1 M NaOH with 1% MeOH; (2) oxidizing CA membranes in order to decrease hydrophobicity by increasing carboxyl content, where oxidation was carried out by use of a strong oxidizing agent, 35% H_2O_2; and (3) applying an anionic polymer in order to change surface charge. They reported that hydrolysis greatly increased membrane porosity, decreased the negative charge of the membranes, and increased hydrophilicity, but had little effect on adsorption of humic acid. Oxidation had a small effect on porosity, significantly increased hydrophilicity and the negative membrane charge, but the adsorption of humic acid was increased. Only by pre-adsorption of a vinyl acetate/acrylic acid copolymer was the adsorption of humic acid decreased.

2.6 Polymeric adsorbents

Polymeric adsorbents are gaining more and more attention inside and outside the membrane fouling arena. Bai and Zhang (2001) prepared granules with positive surface

charges by coating glass beads with polypyrrole, which has the potential to adsorb humic acid. The coated glass beads have an average diameter of around 600 μm and the surface area increased by approximately 347 times per bead over the uncoated glass beads. The increase in surface area was due to the increase in surface roughness. The uncoated glass beads were relatively smooth whereas the coated surface was rough due to the formation of ring-like structures. Adsorption isotherms were fit by the Langmuir equation and the maximum calculated adsorption capacity is around 0.4 mg humic acid per gram adsorbent.

Macroporous polymeric adsorbents have been used in solid-phase extraction (SPE) to preconcentrate organic contaminants such as phenols and cresols from water samples. The technique was first introduced by Burnham et al (1972). SPE may be classified into three types: (1) reversed-phase SPE, which isolates relatively nonpolar analytes from a polar sample such as water by use of relatively hydrophobic adsorbent particles, such as silica with bonded octadecylsilica groups or an organic polymer with benzene rings; (2) normal-phase SPE, which isolates polar compounds from a nonpolar sample matrix by use of polar adsorbents; and (3) ion-exchange SPE, in which adsorbents containing cation-exchange sites or anion-exchange sites are used to preconcentrate ionic analytes or neutral analytes that can be converted to ionic form by adjusting the sample pH (Yu et al. 2003).

Hosoya et al. (2003) developed a stimulus responsive polymer adsorbent, which can reversibly adsorb humic matter in soil extracts as well as DNA, and this was used as a DNA purification method. The adsorbent was prepared through a two-step swelling and polymerization method, and formed uniformly sized macroporous particles. The prepared polymer adsorbent has a pair of anion exchangeable and cation exchangeable polymeric selectors. The adsorption and

deadsorption of humic matter can be stimulated by changes in both pH and temperature. It was reported that humic acid can be recovered at 50 °C and pH 9.

Ichikawa et al (1995) developed a polymeric fuel adsorbent. The fuel absorbent comprises fuel-absorbing polymer particles uniformly dispersed in a binder matrix, with or without a crosslinking site. The binder is permeable to fuel which allows gaseous or liquid fuel to pass from the ouside of the fuel absorbent to the polymer particles dispersed in the binder (absorption cycle), or vice versa (desorption cycle). The polymer particles can be one or more plastics from groups like polysulfone, or one or more rubbers/elastomers from groups like acrylic rubber. It is suggested that the preferred particle size is about 0.5mm or less.

2.7 Polymer micro/nano-spheres

The production of micro/nano polymer spheres is important in drug delivery systems, in which proteins are encapsulated in biodegradable polymeric devices from which the drug can be delivered. Poly(D,L-lactide-co-glycolide) (PLG) spheres and poly(D,L-lactide-co-glycolide) (PLGA) spheres are commonly used.

Several methodologies for micro/nano sphere fabrication have been described in the literature including precipitation, spraying, phase separation, and/or emulsion techniques. In the spontaneous emulsification solvent diffusion (SESD) method (Niwa et al., 1993), nano-sized particles of PLGA or PLA (polylactide) can be obtained by the use of a binary mixture of a water-miscible organic solvent such as acetone and a water-immiscible solvent such as; the particles are formed in the water phase via an emulsification process and a subsequent solvent-

evaporation with moderate mechanical stirring. The particle formation steps could be described as: (1) the formation of emulsion droplets in the aqueous phase when the polymeric solution is added, (2) quick diffusion of acetone out from each emulsion droplet, drastically reducing its size to nano-order, and (3) the consequent "solvent-evaporation" process, in which the remaining dichloromethane is removed from the system, solidifying the droplets to final polymeric nanoparticles (diameter: 200-600 nm). Murakami et al. (1999) pointed out that this method sometimes causes a severe aggregation in the particle formation process due to a considerable amount of residual dichloromethane. Since the water solubility of dichloromethane is slight, the residue can act as liquid bridge and increase particle collisions. They suggested a modified method in which a mixture of two water-miscible organic solvents is used for the polymer solvent instead of the mixture of water-miscible and water-immiscible organic solvents; a low hydrolyzation and polymerization grade of poly (vinylalcohol) (PVA) was used as the quasi-emulsifier. Their results indicated that the selection of the combination of binary organic solvents is very important for the preparation of nanoparticles. In their preparation of 50/50 (co-polymer ratio) poly D,L-lactide-co-glycolide (PLGA) nanoparticles, the combination of binary organic solvents, acetonitrile and alcohol, enabled the production of nanoparticles without aggregation. They also indicated that alcohol concentration in the binary organic solvents could change phase separation rate, and cause coacervation of PLGA particles. In their research, an alcohol ratio near the cloud point is prefered to increase particle productivity. They further purified the particles by repeated dilution-condensation followed by freeze-drying. The dilution-condensation process was done by (1) concentrating the 500 ml aqueous particle dispersion to 25 ml by ultrafiltration (Minitan system, Millipore, Japan), (2) re-diluting the dispersion to 500 ml, and (3) repeating the process three times. The freeze-drying process was done by passing the condensed aqueous dispersion through a mesh-sieve to remove the aggregates and freeze-drying in a vacuum to obtain the powdered nanopartilces.

Four mechanisms have been suggested in the literature to account for spontaneous emulsification: (1) interfacial turbulence, where local interfacial tension depressions tear droplets of oil away from the oil-water interface, thus dispersing the oil in the aqueous phase; (2) diffusion and stranding, where one of the majority phases of the three component system diffuses into a second phase, carrying and dispersing a third component, insoluble in this second phase; (3) zero or negative interfacial tension, where the interfacial tension is locally negative and the area of the interface tends to increase spontaneously -- leading to the formation of droplets that leave the macroscopic interface, which are again dispersed; and (4) bursting of swollen bilayers, which leads to the pulverization of microdroples of alkane into the aqueous phase.

2.8 Phase inversion process and polymer precipitation curves

Polysulfone (PSf) and polyethersulfone (PES) are widely used as ultrafiltration and microfiltration membrane materials. PSf and PES membranes are usually made with the phase inversion technique by precipitating a cast polymer solution with a non-solvent (normally water); this is called non-solvent-induced phase inversion. NMP is a common solvent for polysulfone because of its high solvency and excellent thermal and chemical stability. The other commonly used solvent is dimethyl sulfoxide (DMSO). Besides water, which is the most commonly used non-solvent, methanol, ethanol, and 2-propanol can also be used as non-solvents. Studies from McHugh and Miller (1995) suggest that phase separation and diffusion dynamics showed much more stability when low molecular weight alcohols were used for the non-solvent quench during non-solvent induced phase inversion. In alcohol-quenched systems, there was no large

precipitation region during the initial stage (as was observed in water-quenched systems) and gel growth was slower.

The miscibility gap, diffusion rates, and processing parameters play big roles in determining the morphology and microstructures of PSf and PES membranes. Typically, the curve obtained by joining titration end-points in liquid-solid phase separation is referred as a polymer precipitation curve. Polymer precipitation curves in the form of a ternary phase diagram provide useful thermodynamic and kinetic information for membrane fabrication. Phase diagrams also provide guideance in making polymer colloids.

There is some literature on polymer precipitation curves for single solvent/polymer/non-solvent systems, including NMP/PSf/water and NMP/PES/water systems, but studies on the precipitation properties of the co-solvent/polymer/non-solvent systems are lacking. According to Won et al. (1998), the addition of co-solvent induces a change in the solvent quality, which affects the interaction between polymer and solvent as well as between non-solvent and solvent, and leads to a change in the characteristics of the dope solution. They studied polysulfone solutions by scattered light intensity measurement and dynamic light scattering. The anomalous behavior of the scattered light intensity at small angles was observed in nascent dope solutions made with NMP and with the mixed solvent NMP/ethyl acetate (EA). They observed that the solution made with NMP maintained constant scattered light intensity and optical clarity during aging, whereas light scattering in the solution made with the mixed solvent increased, the solution becoming opaque over time. They concluded that the behavior of the latter solution demonstrated the occurrence of phase separation, and thus is less stable than the former solution. Their experiments on light scattering intensities of the PSf dope solution showed that there is added instability in the system due to the addition of the co-solvent.

In the formation of membranes, both solid and liquid phase are required to be coherent in order to form a porous sheet, i.e., no break-up of the dope solution and the quench media. If the solid phase is incoherent, polymer colloids will be formed, which is how a colloidal polymer adsorbent, the target of study in this research, is formed.

3. Methods and Materials

3.1 Standard Preparation of Polysulfone Colloidal Polymer Adsorbent

3.1.1 Preparation

P3500 polysulfone (PSf) polymer with a number average molecular weight of 66,909 was used in the production of the colloidal polymer adsorbent (CPA). The following procedure was used to make a 2% PS polymer solution: After 2 gm of PSf was dissolved into 56.0865 gm N-methyl 2-pyrrolidine (NMP, Sigma, purity 99.7%) by shaking in a gyratory shaker overnight, 41.9135 gm propionic acid (PA, Sigma) was added and well shaken until a homogeneous solution was formed.

Three other recipes were used to investigate the effects of different solvents and non-solvents on CPA characteristics. One variation was to change non-solvent from water to isopropyl alcohol (IPA, Aldrich), another variation was to change the non-solvent from water to glycerol (Aldrich), and the final variation was to change the strong solvent from NMP-PA to tetrahydrofuran (THF, Aldrich), which is also a common organic solvent for PSf. The CPA made from different recipes are called Run-I, Run-G and Run-T respectively. Colloidal suspensions made from the original recipe are called the Control. The molecular structures of the chemicals used in making polymer colloids are shown below.

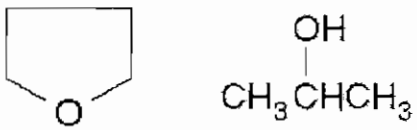

THF

IPA

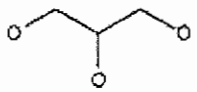

Glycerol

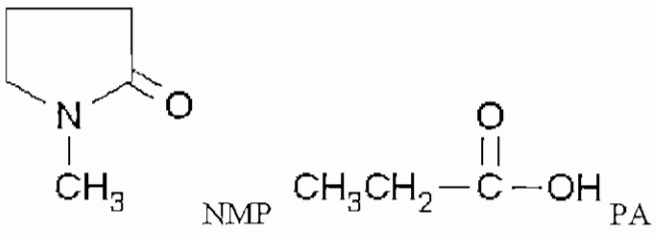

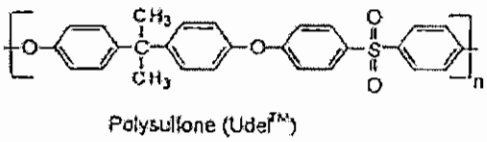

The PSf solution was pumped into a precipitation bath contining Milli-Q water using a syringe pump (Cole-Parmer 74900-00) at the rate of 1.5ml/hr. A schematic of CPA production is shown in Figure 3.1. The diameter of the capillary tube is 180μm. A 1000-ml plexiglass Rushton reactor was used as the precipitation bath. The system was stirred with a 1.5-inch flat-blade disk turbine at a mixing speed of 400 rpm. The concentration of the colloids reached 200 mg/l after 400 minutes of polymer injection.

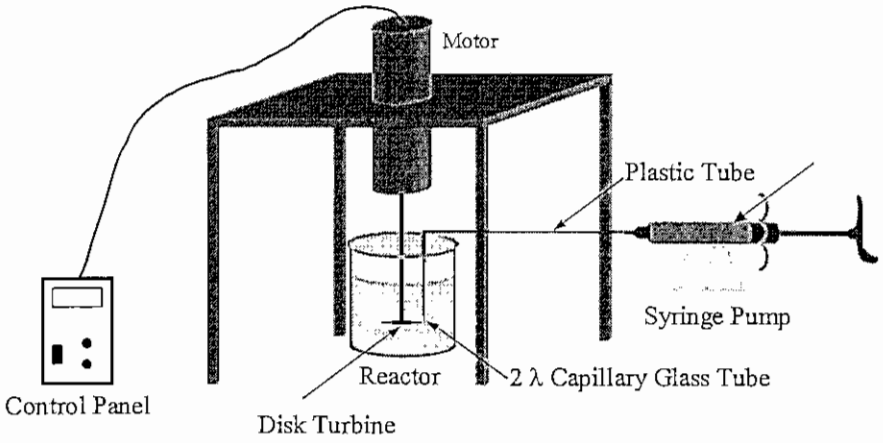

Figure 1. Schematic of CPA production

PSf, NMP, PA, IPA, Glycerol and THF were used as received without further purification. Table 3.1 provided the recipes for all four colloidal systems studied.

Table 3-1 Composition of Polymer Colloids

	Control	Run-I	Run-G	Run-T
Polymer	Polysulfone (2%)	Polysulfone (2%)	Polysulfone (2%)	Polysulfone (2%)
Strong solvent	NMP (56%)	NMP (56%)	NMP (56%)	THF (98%)
Co-solvent	PA (42%)	PA (42%)	PA (42%)	No co-solvent
Non-solvent	Water	IPA	Glycerol	Water

3.1.2 Purification

The colloidal polymer adsorbent is purified by solvent removal. The NMP and PA were removed by dialyzing the colloidal solution against Milli-Q water. Spectro 4 dialysis membrane tubing (Spector Lab.) with a molecular weight cut off of 12,000-14,000 was used. The dialysis was carried out continuously over 14 hours with several changes of the Milli-Q water. A UV spectrometer was used to measure the solvent residue after dialysis. Typical UV absorption spectra from 200 to 500 nm are shown in Figure 3.2. Near maximum absorbance is measured at around 254 nm, making it a good wavelength for characterization. A calibration curve (Figure 3.3) was constructed for UV_{254} absorption at different solvent concentrations, which were measured in terms of total organic carbon (TOC) concentration. After 14 hours, 5 ml of solution was withdrawn from the dialysis tubing for UV absorption analysis. Ninety percent of the solvents were removed with the procedure. The purified colloidal solution was used in the adsorption and flux decline experiments.

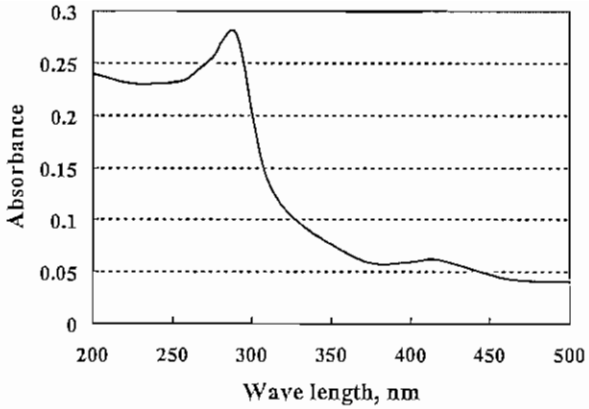

Figure 3.2 Absorption spectra for 1 g/l NMP/PA solution. Molar ratio of NMP and PA is 1:1. The pH of the solution was adjusted to 7 with sodium hydroxide.

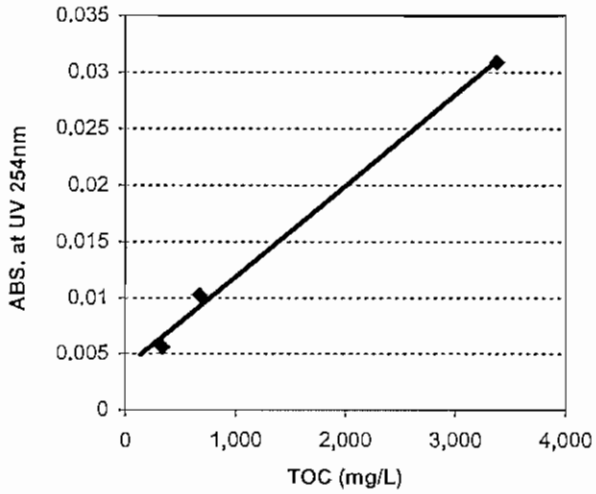

Figure 3.3 Calibration curve of UV adsorption at 254 nm. Solvent (NMP and PA) concentration was measured in terms of TOC concentration.

3.2 Characterization of Polysulfone Colloidal Polymer Adsorbent

The CPA was characterized by the size distribution of primary and aggregated particles, surface area and porosity, and zeta potential.

3.2.1 Concentration limitation

An experiment was carried out to test whether there would be an upper limit to the colloid concentration during standard production; this also tests if the formed colloid structure is affected by increasing solvent concentration in the water bath during continuous injection. An NMP-PA mixture (1:1 molar ratio) of 25 g was added into 75 g water to make a 25% NMP-PA solution, and 0.5 g of the PSf solution was then injected into the bath. In-situ measurement of aggregate size was made with a Lasentec particle sizer, and the results with and without extra NMP-PA were compared (Section 4.2.3).

3.2.2 Primary Particle Size

Polymer colloid primary particle size was determined with SEM and further confirmed by TEM. A Philips XL30 ESEM-FEG (FEI Company., Hillsboro, OR) and Philips CM200 TEM (FEI Company., Hillsboro, OR) were used to make micrographs of the polymer colloids at the UIUC Beckman Center. The SEM uses a field-emission electron gun which is less damaging to sensitive samples. The resolution of the SEM is 2 nm under ideal conditions. Colloids were filtered onto a 0.22 μm MF membrane for SEM imaging. The membrane was air-dried and coated with Au-Pt before imaging. The TEM imaging was done by overlapping a glow-discharged, carbon-stabilized, Formvar-coated copper grid onto a droplet of CPA solution for about 60 seconds to let the colloids diffuse onto the surface of the grid. The grid was negatively stained with 10% uranyl acetate and then dried before TEM imaging.

3.2.3 Aggregate size distribution

A particle-sizing instrument from Lasentec (D600R FBRM, Lasentec) was used to study the size distribution of the aggregates formed in the precipitation batch. The instrument uses a more-or-less non-invasive probe placed in the precipitation bath. The technique is based on back-

scattered laser light. The FBRM does not assume spherical particles. The distance measured by FBRM is a chord length. A chord length is a straight line between any two points on the edge of a particle or particle structure (agglomerate). An illustration is shown below in Figure 3.4. The FBRM typically measures tens of thousands of chords per second, resulting in a robust number-by-chord-length distribution. The chord length distribution is presented as counts in each size range in 5-second intervals. A scan speed of 2 m/s was used in the experiment. The measurement range is 0.5μm to 1000 μm. The aggregate size distribution was measured in-situ during constant rate pumping of 0.5ml polysulfone polymer solution into 100-ml Milli-Q water in a 200-ml Lasentech sample holder. The whole process took 20 minutes and the final colloid concentration was 100mg/l. Two fixed mixing speed of 200 rpm and 400 rpm were used for comparison. Long time-scale stability of the aggregates was evaluated by measuring the size distribution at a fixed mixing speed over a period of 12 hours.

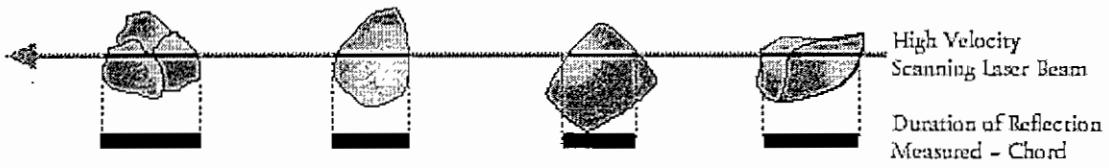

Figure 3-4. (From Lasentec®, a Mettler Toledo Company)

3.2.4 Zeta Potential

A Malvern Zetasizer was used to measure zeta potential of the polymeric colloidal solution. Because the particle size resolution of Malvern Zetasizer is 2 nm to 3 microns, and the aggregate size of the polymer colloids is around 16 microns, the colloidal solution was sonicated with a Cole-Parmer ultrasonic cleaner for 3 hours before measurement of zeta potential. The Malvern Zetasizer measures electrophoretic mobility and the zeta potential is calculated from mobility

using the Henry equation, assuming $f(\kappa a) = 1.0$ (Huckel approximation), where κa is the ratio of the particle radius to the double layer thickness. The solution pH was adjusted to 7.0.

3.2.5 Surface area

Surface area of the polymer colloids was measured with an Accelerated Surface Area and Porosimetry analyzer (ASAP 2405) from Micromeritics (Norcross, GA). The ASAP 2405 system uses nitrogen as the adsorbate and provides full adsorption and desorption isotherms of the loaded samples. The analysis bath was operated at 77.35 K. Approximately 0.6 g of colloids were filtered out of the solution by a 0.2-μm Nylon filter. The colloid flakes were ground and dried at 100°C overnight. The dried colloids were ground again to a loose powder before placement in the adsorption tube. The relative pressure range for the measurements was set from 0.01 to 0.98. The instrument provided the following analysis: BET and Langmuir surface area; BET full adsorption and desorption isotherms; Horvath-Kawazoe micropore volume; BJH mesopore area and volume distribution.

3.3 Adsorption Experiments

3.3.1 Source of Natural Organic Matter

Suwannee River reference Natural Organic Matter (NOM), code number 1R101N, was purchased from the International Humic Substance Society (IHSS). It was isolated using reverse osmosis from the Suwannee River in southwestern Georgia. A 21-mg/l SRNOM solution was made and buffered with sodium phosphate to pH 7.5 for use in adsorption experiments. When making the solution, 21 mg of SRNOM was dissolved into 800 ml of Milli-Q water in a beaker and stirred with a magnetic stirrer for 4 hours. The solution was then transferred into a 1-liter

volumetric flask to obtain the 21-mg/l SRNOM solution. The basic characteristics of SRNOM are listed in Tables 3.2 to 3.4.

Table 3-2 Per Cent Elemental Composition of SRNOM

H_2O	Ash	C	H	O	N	S	P
8.15	7	52.47	4.19	42.69	1.1	0.65	0.02

H_2O content is the %(w/w) of H2O in the air-equilibrated sample (a function of relative humidity). Ash is the %(w/w) of inorganic residue in a dry sample. C, H, O, N, S, and P are the elemental composition in %(w/w) of a dry, ash-free sample. Source: Elemental analyses by Huffman Laboratories, Wheat Ridge, CO, USA; Isotopic analyses by Soil Biochemistry Laboratory, Dept. of Soil, Water, and Climate, University of Minnesota, St. Paul, MN, USA.

Table 3-3 Acidic Functional Groups

Carboxyl Groups, meq/g Carbon	Phenolic Groups, meq/g Carbon
9.85	3.94

Source: Ritchie and Perdue, 2003.

Table 3-4 Number-average and Weight-average Molar Masses and rms Radii (M_n, M_w and R_n) for Samples of Suwannee River Natural Organic Matter

Buffer Ionic Strength M	Buffer pH	Sample Concentration (mg/ml)	M_n g/mol	M_w g/mole	R_n nm
0.275	6.8	9.481	15050±1500	20185±1500	29.9±12.7
0.00688	7.0	8.000	16595±3500	25715±7500	55.8±17.7

Source: Wagoner et al, 1997.

3.3.2 Measurement of NOM concentration

The concentration of NOM in solution was measured in terms of dissolved organic carbon (DOC) with a TOC analyzer (Phoenix 8000, Tekmar-Dorhmann, Mason, OH). The samples were pre-filtered using Amicon YM100 (Millipore Co.) UF membranes in a 50-ml Amicon stirred cell under a pressure of 10 psi to completely filter out the polymer colloids. The permeant from the filtration cell was then collected 40-ml vials covered by Teflon sheets. The TOC analyzer automatically took three replicates measurements in each vial and provided the average value as output. The measurement procedure includes a three-point standard calibration curve as part of the routine measurements. Three standard solutions of anhydrous primary-standard grade potassium biphthalate with DOC concentrations of 1, 2.5 and 5 mg/L were run at the beginning and at the end with every sample set. The data reported by the analyzer were then calibrated to the standards. The typical SRNOM concentration used in the experiments is 7 mg/l, with a measured typical TOC value of 3.5 mg/l after calibration. The measured TOC range in this study is around 0.1~3.5 mg/l.

3.3.3 Adsorption Jar Preparation

Experiments were designed to investigate adsorption capacity of SRNOM by CPA. The CPA solution, SRNOM solution and Milli-Q water with a total volume of 300 ml were poured into a 1-liter glass jar. All the three solutions were adjusted before blending to pH 7.5 with sodium phosphate. The added buffer strength was 1 mM. The solution ionic strength after buffer addition was 5 mM. In each of eight jars, the initial concentration of SRNOM was kept at a constant value of 7 mg/l, while the concentration of PSPC was 200, 120, 100, 80, 60, 40, 20, and 10 mg/l respectively. Blank samples of CPA at each concentration, and a blank sample of SRNOM at 7mg/l were also prepared. A sheet of aluminum foil was placed over the jar before screwing on

the lid. The jars were then placed inside a dark box on a gyrator shaker and were shaken during the entire adsorption period. The adsorption experiment usually lasted for two days, which was assumed to be the time required for equilibrium. The temperature for adsorption experiments was ~25°C. Table 3-5 shows a typical experimental setup.

Table 3-5 Typical Experimental Setup

Concentration of stock SRNOM solution (mg/L)					21		
Concentration of stock CPA solution (mg/L)					200		
Total sample volume in each jar (ml)					300		
(adsorption jars)	Jar 1	Jar 2	Jar 3	Jar 4	Jar 5	Jar 6	Jar 0
Added NOM volume (ml)	100	100	100	100	100	100	100
Added CPA volume (ml)	180	150	120	90	60	30	0
Added water volume (ml)	20	50	80	110	140	170	200
Final NOM conc. (mg/l)	7	7	7	7	7	7	7
Final CPA conc. (mg/l)	120	100	80	60	40	20	0
(blank colloids jars)	Jar 1'	Jar 2'	Jar 3'	Jar 4'	Jar 5'	Jar 6'	
Added NOM volume (ml)	0	0	0	0	0	0	
Added CPA volume (ml)	180	150	120	90	60	30	
Added water volume (ml)	120	150	180	210	240	270	
Final NOM conc. (mg/l)	0	0	0	0	0	0	
Final CPA conc. (mg/l)	120	100	80	40	20	10	

3.3.4 Adsorption Isotherms

SRNOM concentration in the final solution was characterized by DOC measurements as described in Section 3.3.2. The difference in the SRNOM concentration between the solution in the jar and the initial solution was used to determine the uptake of SRNOM by CPA. The data were corrected by the loss of DOC during the pre-filtration with a YM100 membrane (Section 3.3.5). A calibration curve was developed for uptake of DOC by the YM100 membrane, and the equilibrium DOC value was corrected for the loss of DOC on the YM100 membrane. The adsorption isotherm was calculated from the results of DOC analysis and was fitted to the Feundlich model. The model takes the following form:

$$q_e = K_f C_e^{1/n} \quad \text{.....(3.1)}$$

where K_f is an empirical constant related to the capacity of the adsorbent for the adsorbate, n is a constant related to the affinity of the adsorbate for the surface, and q_e takes the following form:

$$q_e = \frac{\text{Mass of adsorbant}}{\text{Mass of adsorbent}} = \frac{(C_0 - C_e)V}{C_s V} \quad \text{.....(3.2)}$$

Here C_0 is the initial DOC concentration of NOM, C_e is the equilibrium TOC concentration of NOM, C_s is the concentration of CPA, and V is the total volume of the solution. In these experiments, C_e is taken to be the corrected equilibrium DOC concentration (Section 3.3.5).

3.3.5 Correction of equilibrium DOC concentration

Before the equilibrium DOC concentration was measured, a YM100 membrane was used to remove the colloids. Since the YM100 membrane will adsorb a small fraction of NOM, the measured equilibrium DOC concentration needs to be corrected before application of Equation 3.2.

A 300 ml SRNOM solution was filtered through a YM100 membrane at 10 psi. The DOC value of the raw solution (C_0') and the permeate (Ce') were measured. The amount of SRNOM that was adsorbed by the membrane is defined as Qe',

$$Qe' = (C_0' - C_e')V, \quad \text{.....(3.3)}$$

where V is the total volume of the solution (300-ml). An adsorption "isotherm" was then established using different SRNOM concentrations (Figure 3.5).

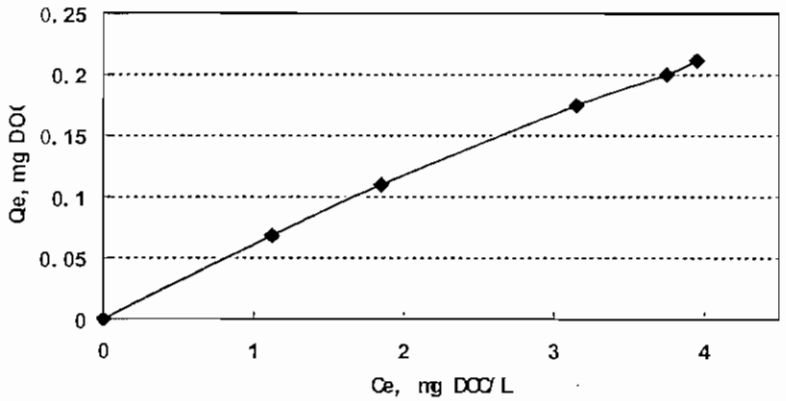

Figure 3-5. Adsorption isotherm of SRNOM by YM100 membrane at pH 7.

Here, if we take Ce' as the measured final equilibrium DOC concentration, then we can obtain C_0' from Figure 3.5 and Equation 3.3. Since C_0' is the DOC value before YM100 membrane adsorption, it is thus equivalent to the corrected C_e in Equation 3.2.

3.3.6 Adsorption Kinetics

The adsorption kinetics for 100, 10, and 1mg/l CPA were measured by taking samples from the adsorption jar at 1, 2, 4, 6, 10, 12, 14, and 20hr, and 1, 1.5, 2, 3, 4, 5, 6 and 7 days. The adsorption kinetics were expressed as the fractional DOC removal over time.

3.4 Membrane Filtration

Membrane filtration of SRNOM was evaluated by flux decline experiments. Filtration performance using fresh SRNOM solution and an SRNOM solution pretreated by CPA were compared. The membranes tested in this research were made of (1) polyethersulfone (PES) with a Molecular Weight Cut Off (MWCO) of 20,000 Daltons (Osmonics) and (2) a regenerated cellulose membrane with MWCO of 30,000 Daltons (Amicon YM30). Polyethersulfone is generally regarded as hydrophobic in the literature. Its contact angle is between 60 to 70 degrees (Cheryan 1998). Regenerated cellulose membranes are generally regarded as hydrophilic in the literature, and the water contact angle of the YM30 membrane was measured as 7.0 degrees in one study (Jucker and Clark, 1994).

3.4.1 Membrane filtration equipment

The membrane filtration procedures used in this research are based on those used previously by Kerry Howe (2001) in the Environmental Engineering Lab at the University of Illinois.

As shown in Figure 3.6, filtration was performed in a 50-ml stirred batch filtration cell with 44.5-mm diameter membrane disks (Amicon Model 8050, Millipore Co.). The effective membrane area of the disks is 13.4 cm^2.

Permeate from the filtration cell is weighed on a top-loading balance (Precisa Model 1000C-3000D, Pag Oerlikon AG, Zurich, Switzerland). The balance has a full scale of 3000 g, resolution of 0.01 g, readability of 0.01 or less, and an integration time of 0.32 seconds. The balance was sampled by a computer at 1-minute time intervals through a serial port. The program "Winwedge" was used to for communication between the balance and the computer.

A nitrogen tank was used for the constant pressure source. The pressure was monitored with digital pressure transmitters (Model PG-4/20, Psi-Tronics, Tulare, CA). The resolution of the digital gauges is 0.1 psi and the accuracy is 0.3 psi. The pressure was adjusted to 30 psi at the beginning of experiments and kept constant during the experiments.

All filtration experiments were done at room temperature, between 23-25°C. All samples and reagent water used for flux experiments were stored before experiments until they reached room temperature. There was no additional temperature control.

3.4.2 Flux calculation

Flux was calculated as:

$$J = 21205.004 \frac{\Delta W}{\Delta t \cdot A} \quad \text{.....(3.4)}$$

where J = flux (gpd/ft^2)

ΔW = difference between two sequential weight measurements (g)

Δt = difference between two sequential time measurements (seconds)

A = effective membrane surface area, 13.4 cm^2

21205.004 = conversion factor

The flux was normalized by percent of initial clean water permeability in order to compare the flux decline of different membranes and different samples. The normalized flux was taken as J/J_0, where J is the measured sample flux, and J_0 is the reagent water flux of the same membrane. J_0 can vary among different membrane samples. The typical value of J_0 for the PES membrane was between 140 and 190 gpd/ft^2.

Accurate temperature and pressure measurements are critical in membrane filtration (Howe 2001). Flux was corrected to standard pressure and temperature conditions with the following equation, adapted from ASTM (1999):

$$J_s = J_M \left[\frac{\Delta P_s}{\Delta P_M} \right] \times 1.024^{(T_s - T_M)} \quad \text{.....(3.5)}$$

where, J_s = flux corrected by standard temperature and pressure (gpd/ft^2)

J_M = measured flux (gpd/ft^2)

Ps = standard pressure (30 psi in this research)

P_M = measured transmembrane pressure (psi)

T_S = standard temperature (25 °C)

T_M = measured temperature (°C)

Preliminary tests of the same equipment by Howe (2001) showed that pressure losses due to equipment and tubing resulted in a differential pressure across the membrane that was about 1

psi lower than the measured pressure at the cylinder. The transmembrane pressure used in Equation 3.5 was corrected for the 1 psi loss.

3.4.3 Membrane filtration procedure

The PES membrane was received in sheets and was cut to size in the laboratory with a circular cutting stamp. The PES membrane had been stored dry in a dark cabinet for about two years before the experiments. The manufacturer indicated that no preservatives or other contaminants had been applied to the membrane, and no initial preparation was necessary. The regenerated cellulose membranes were received as disc membranes of 44.5 mm in diameter. They were cleaned by filtering reagent water at 55 psi for 5 minutes to flush off membrane preservatives. The DOC of the permeate after 5 minutes of filtration varied from 0.1-0.2 mg/l, which was in the same range of the DOC of the fresh reagent grade water.

Flux decline was evaluated over a single one-hour filtration cycle. Previous research has shown adsorptive fouling of membranes to be a fast process. Flux decline due to adsorption is often observed within the first minutes of operation (Lahoussine-Turcaud et al. 1990a).

The PES membrane used here cannot be fully wetted at low pressures (Howe, 2001). Therefore, the routine filtration procedure for the PES membrane was to start with a higher initial filtration pressure of 35 psi for two minutes to insure that the membrane was fully wetted prior to fouling experiments. This procedure was not necessary for the YM30 membrane. Clean water flux was then measured by filtering reagent grade water for at least 30 minutes until constant flux was reached. Flux decline during filtration of NOM solutions was determined in the following way. The sample reservoir was filled with 600 ml sample and filtration was started using a mixing speed "two" on the Amicon mixer. The filtration was stopped when around 500 ml of sample

solution was collected. The remaining sample from the filtration cell was then drained and then the cell was refilled with 50 ml fresh reagent water. The cell was shaken gently, and the water poured out. This procedure was repeated twice. Flux recovery resulting from this "rinsing" procedure was then determined by stirring the membrane for 30 minutes in the filtration cell filled with 50 ml of reagent water. Backflushing was done after rinsing. Backflushing was carried out by putting the membrane upside down in the filtration cell and filtering 100ml Milli-Q water at 15psi. After backflushing, Milli-Q water flux at 30psi was again recorded.

3.5 Scanning Electron Microscopy imaging of clean and fouled membranes

Scanning electron microscope images of clean and fouled PES membranes were made with the SEM described in Section 3.2.2. The membrane samples used for SEM imaging included: (1) a clean PES membrane, (2) a PES membrane fouled by 1 hour filtration of SRNOM, (3) a PES membrane fouled by 1 hour filtration of SRNOM pretreated by CPA for 24 hours, and (4) a PES membrane fouled by 1 hour filtration of SRNOM pretreated by Norit powdered activated carbon. Since the membrane foulants are all made of organic materials, some preservation methods were used since high-vacuum SEM imaging has the potential to alter the appearance of the organic materials and introduce artifacts into the images. The commonly used preservation methods are glutaraldehyde fixation and methanol sequential dehydration. Howe (2001) examined these methods with clean and NOM-fouled PES membranes and concluded that the preservation methods did not significantly improve the images at high magnification. Thus, routine imaging was performed without using these preservation methods. The clean membrane image was made with dry membranes as received. The fouled membranes were extracted after one hour of filtration, rinsed with reagent water in the stirred filtration cell for 10 minutes, and then air dried before application of a Au-Pt coating prior to imaging.

3.6 Elemental analysis with Energy Dispersive Spectroscopy

The SEM was coupled with Energy Dispersive X-Ray Spectroscopy (EDX) for elemental analysis. The SEM in the UIUC Beckman center is equipped with an EDX analysis system. The detection limit of EDX is 1%. The SEM and EDX analyzed the same section of membrane. The EDX results are qualitatively expressed by elemental peaks. To compare the results from different samples, all samples are analyzed under the same conditions. These include the magnification, spot size, and data collection time. Dry SRNOM powder, clean PES membranes, and SRNOM-fouled PES membranes were analyzed. The sample preparation method for membrane samples is as described in Section 3.5. Dry SRNOM powders were analyzed by spreading the powder onto a small area of carbon tape.

3.7 Cloud Point Curve

The phase inversion characteristics of the polysulfone solution used in the production of CPA were investigated with a cloud point curve. The cloud points were determined by titrating polymer solutions with water at 25°C. The detailed methods are described by Lau et. al (1991). The PSf solution with NMP and PA co-solvents was prepared as described in Section 3.1.1 in a 50-ml Erlenmeyer flask. The flask was capped tightly with a rubber septum. The clear polymer solution was then titrated with Milli-Q water, injected through the septum by a microsyringe (Hamilton CR700-200) until turbidity was observed. The cloudy mixture was then placed in a water bath thermostatically controlled at 25 ± 0.3°C for several hours. More distilled water was added if turbidity disappeared at 25°C. The use of a rubber septum reduced the loss of materials from solvent evaporation. The water was added in small increments of 0.02ml. About 25 grams of PSf solution was used in one flask.

3.8 Miscellaneous Laboratory Techniques

3.8.1 Temperature control

The laboratory has a general temperature control, which was adjusted to 25°C. The room temperature variation was always within 1 degree of 25°C. All the experiments were done at room temperature.

3.8.2 Reagent Water Preparation

Reagent water in the Environmental Science and Engineering Laboratories is prepared by deionization using a centralized ion-exchange system, and distributed to the individual laboratories via polypropylene piping. The system typically produces water with resistance around 16 megaohms, and is regenerated before resistivity drops to 1 megaohms. For this research, reagent water was further processed through a Milli-Q Water Purification System (Millipore Co.). The system consists of two carbon cartridges, one ion-exchange cartridge, and a 0.22-μm ultrafiltration cartridge. The reagent water was monitored for DOC conentration. The DOC of the final reagent water varied from 0.1 to 0.2 mg/L.

3.8.3 Glassware cleaning

All glassware used for organic analysis was cleaned thoroughly with soap and water, soaked overnight in a concentrated sulfuric acid bath, and rinsed with reagent water. The cleaned glassware was covered by perforated aluminum foil and baked for at least 3 hours in a 110°C oven.

3.8.4 Buffer

Monosodium phosphate (monohydrate) and disodium phosphate (heptahydrate) were used as the buffer in all the experiments. All solutions were buffered and then ajusted with 1N sodium

hydroxide to pH value of 7.5. A buffer strength of 1mM was used. The corresponding ionic strength was 5.37 mM.

3.8.5 Filtration of colloids for DOC analysis

Because the CPA primary particle size is around 60 nm, they can pass through the 0.45 μm microfilters usually used to filter samples before DOC analysis, destroying the validity of DOC measurement. As a result, all samples were filtered with a YM100 regenerated cellulose membrane (Amicon) before the DOC analysis. It is much more efficient in removing fine colloidal matter than the normal MF membrane filter traditionally used DOC analysis (Table 3.6). Therefore, in this work samples were filtered before DOC analysis at 10 psi with the YM100 membrane. The permeate produced after 30 seconds was collected directly into two 40-ml vials for DOC analysis.

Table 3.6 Removal of CPA colloids by YM100 UF membrane compared to 0.2 μm MF membrane.

CPA concentration (mg/l)	200	100	80
DOC after filtration by 0.2 μm MF membrane (mg/l)	4.8883	2.5330	1.4164
DOC after filtration by YM100 UF membrane (mg/l)	0.8204	0.6393	0.5090

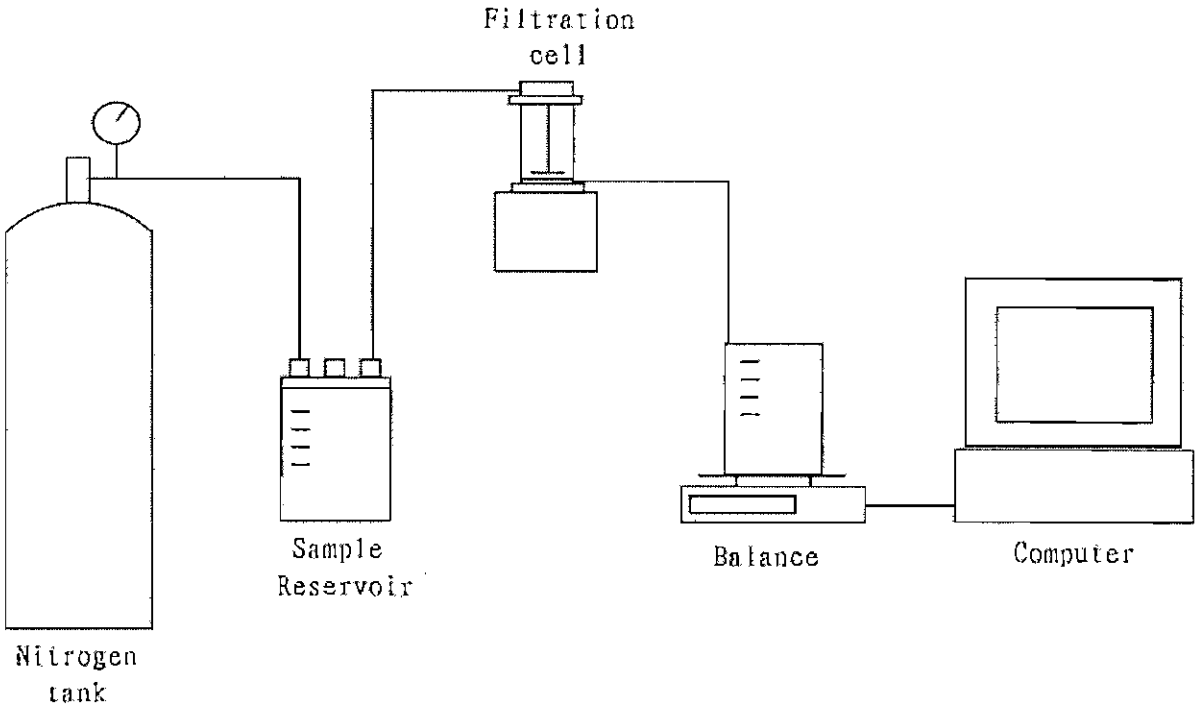

Figure 3-6. Membrane filtration apparatus

4. Results and discussion

4.1 PSf/NMP-PA/Water system

The ternary precipitation curve of the PSf/NMP/Water system was reproduced from Lau et al (1991) as shown in Figure 4-1. The same procedure used by Lau et al was used to characterize the systems examined in this work. The precipitation curves for the PSf/NMP/Water system in this work are also shown in Figure 4-1. (Detailed data from Lau et al. (1991) are compared with similar data from this work in Table 4-1.) Compared with Lau's results, at similar PSf and solvent content, about 20% more non-solvent is needed to start the phase separation in our experiment. The different was most probably because of the difference in PSf molecular weight used in the two experiments. Unfortunately, the PSf molecular weight used in Lau's experiment was not provided.

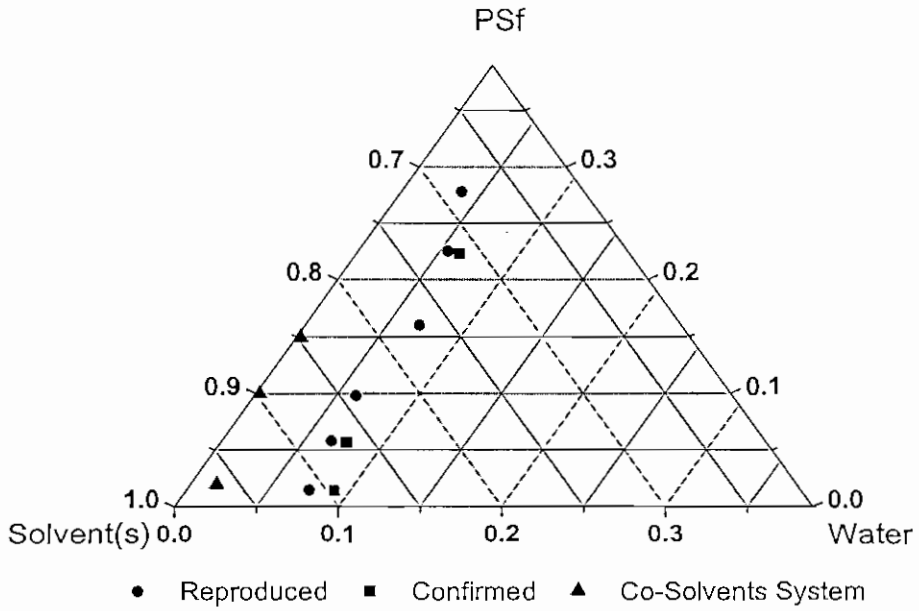

Figure 4-1. Precipitation curves of polymer/solvent/non-solvent systems. Filled circles -- PSf/NMP/Water system reproduced from Lau, et. al. (1991); filled squares -- replication PSf/NMP/water system, this work; filled triangles -- PSf/NMP-PA/Water system, this work.

The co-solvent system was also studied following the same method. The precipitation curve of PSf/NMP+PA/Water system is also shown in Figure 4-1. It was observed that when PA was added as a co-solvent, a very small amount of non-solvent is required to reach the cloud point (Table 4-1). These data show the quick formation of PSf colloids may be related to the instability of the PSf/NMP-PA system towards water (also see Section 4.2.2).

To examine the effect of PA on colloid formation, PSf/NMP and PSf/NMP-PA systems were injected into water following the standard method as described in Section 3.1.1. With the co-solvent system, PSf colloids were obtained (the Control formulation – next section), whereas long PSf fiber were produced through the single-solvent system (Figure 4-2).

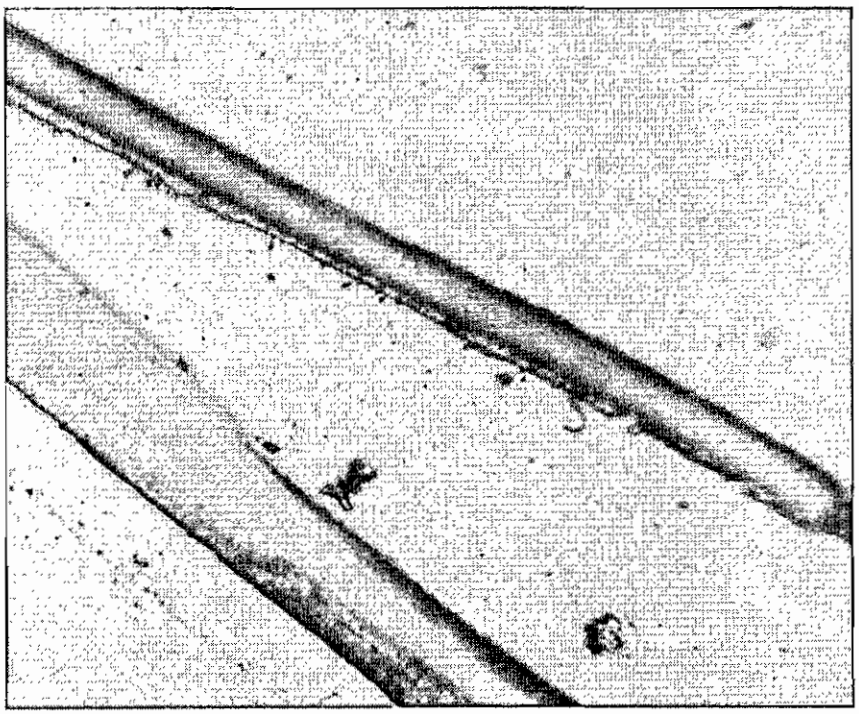

Figure 4-2. PSf fibers made by injecting PSf-NMP solution into water.
160X magnification.

The ability to produce polysulfone fibers opens some interesting possibilities for future implementation of the material, e.g., fibers packed in a column.

	PSf (%)	Solvents (NMP) (%)	Water (%)
Some results from Lau et al (1991)	1.5	91.0	7.5
	5.8	87.5	6.7
	22.5	72.0	5.5
Results from this work	1.4	89.0	9.6
	5.7	86.6	7.7
	22.3	71.5	6.2
	PSf (%)	NMP + PA (%, mole ratiao 1:1)	Water (%)
Co-solvent system	2.03	96.39	1.58
	9.98	89.78	0.24
	14.96	84.85	0.19

Table 4-1 Materials content at the cloud point

4.2 CPA characterization

4.2.1 Particle purification

As we inject the PSf solution into water and PSf colloids are formed, solvents are also transferred to the water phase. The purification of the colloidal polymer is essential to its performance as an adsorbent; if there are organic solvent residues on the polymer surface, it could possibly affect the adsorption capacity for NOM. The purification process was carried out by batch dialysis. As discussed in Section 3.1.2, the solvent concentration after 14 hours of batch dialysis was 9.8 mg/L. The advantages of dialysis are that there is almost no loss of colloids and no effect on the pore structures during purification. The disadvantages are that remaining solvents could not be totally removed by batch dialysis[2] (the remaining solvent could be adsorbed on the surface or inside the pores) and the batch dialysis process is slow. Possible alternatives for CPA purification were considered:

1) Continuous dialysis with dialysis modules. This was not pursued because the equipment was not available.
2) Sedimentation and refill. However, this can cause loss of polymer materials, especially the slowly settling smaller colloids. This was not extensively pursued.
3) Rotary evaporation. The main problem with this method is that because of the high boiling point of NMP, water and PA will be removed first. The remaining NMP will re-dissolve PSf. One solution to this problem might be to continuously add water to the sample during evaporation. However, this was not pursued because the equipment was not available.

All these methods are performed without drying the colloids, and should therefore not affect pore structure and surface area of the produced colloids. However, an additional approach might be to

[2] Near the end of this study, it was discovered that dialysis efficiency could be increased by performing the dialysis at a higher temperature.

vacuum-dry and grind the colloids into a powder. This was also not utilized because of a lack of time. If this were to be pursued, the effects of drying and grinding on the pore structure and surface area of the colloids would need to be evaluated.

4.2.2 Particle size analysis

A milky solution is formed when PSf is injected into water. The milky solution is a suspension of colloidal polymer. Primary and secondary structures of the colloidal polymer were observed. SEM images of a dried CPA layer showed primary particles with sizes between 50 nm to 200 nm, with clear evidence of aggregation (Figures 4-3 to 4-6). The size of primary particles in the SEM images was analyzed with a free software tool, ImageTool ver. 3.0. The analysis area was one quarter of the image. All particle diameters in that area were measured, where the diameter was taken to be the longest distance of span distance of each particle. The typical total particle number in each analysis was around 70. Data for the four systems studied in this work are

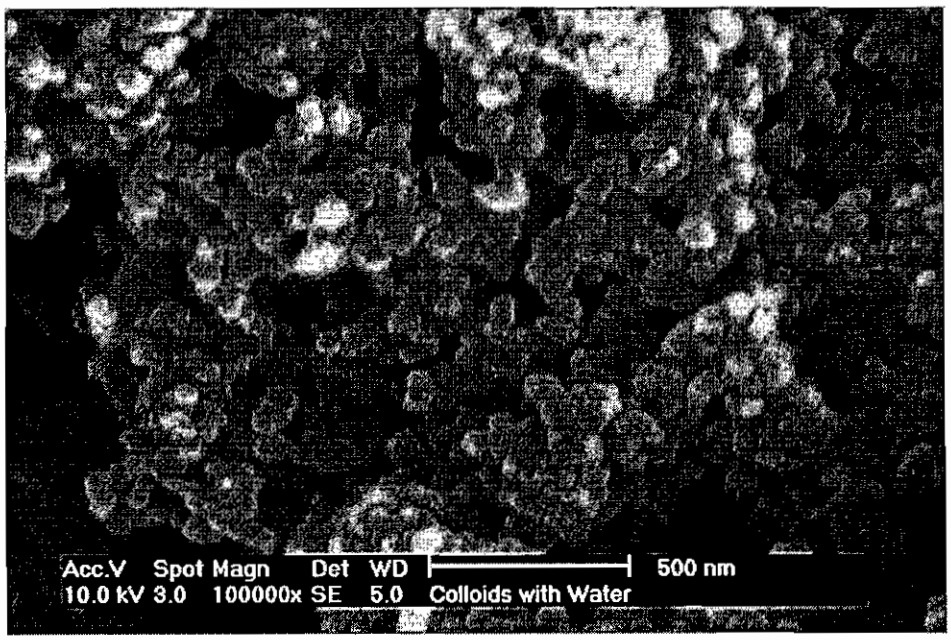

Figure 4-3. SEM image of Control CPA

provided in Table 4.2.

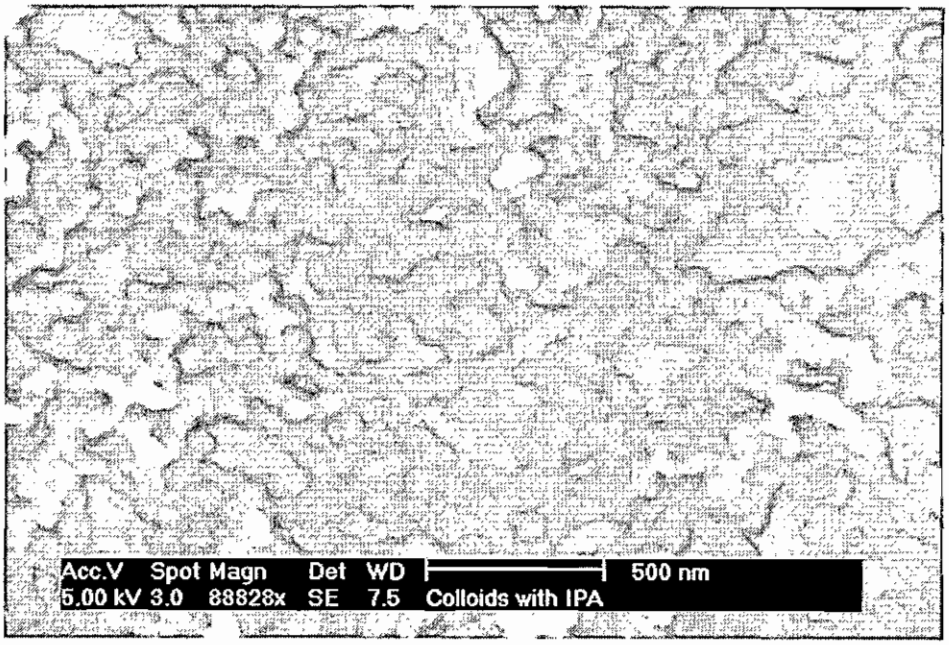

Figure 4-4. SEM image of Run-I CPA

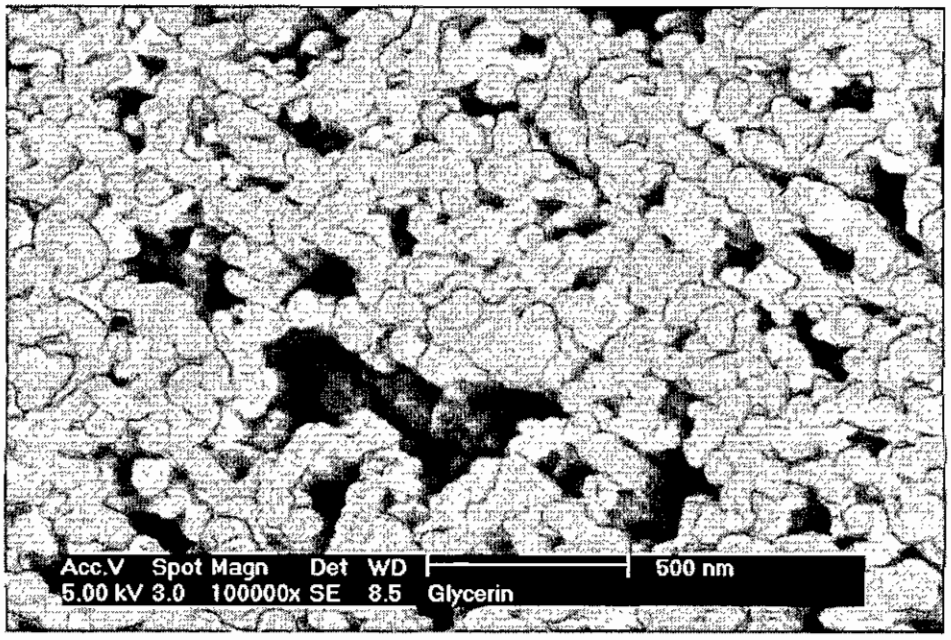

Figure 4-5. SEM image of Run-G CPA

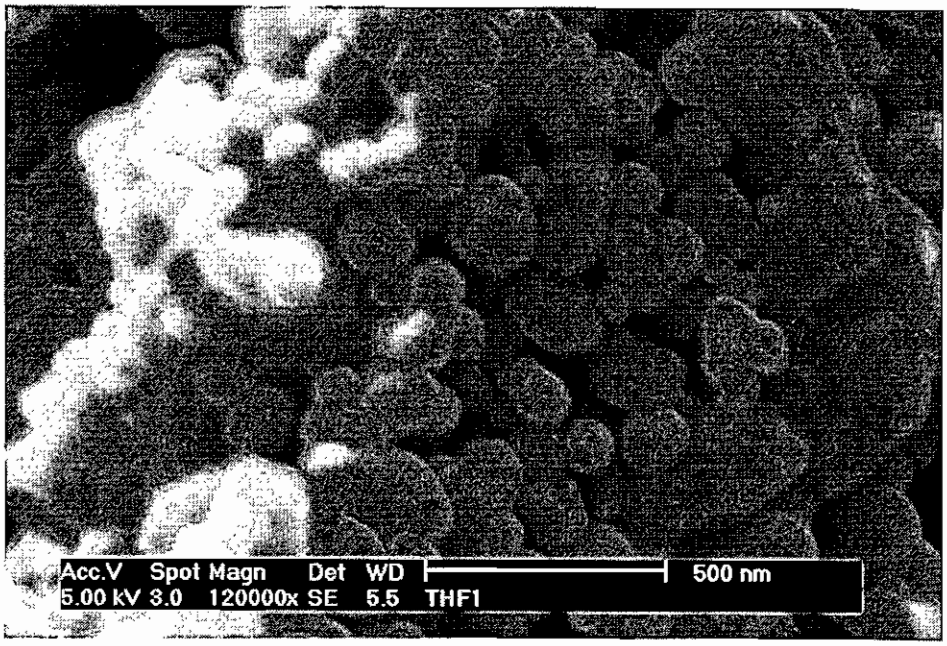

Figure 4-6 SEM image of Run-T CPA

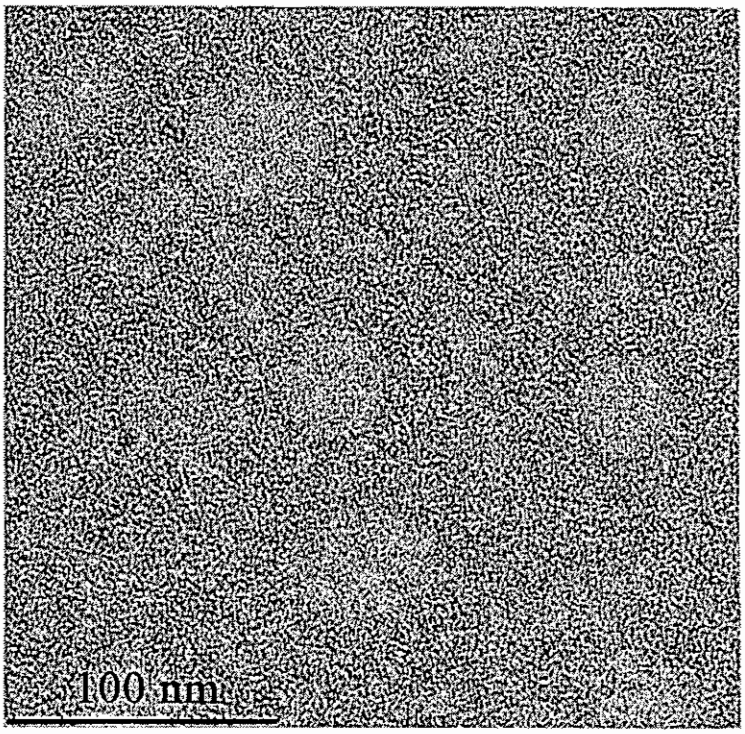

Figure 4-7. TEM image of Control CPA

TEM imaging was done by letting particles diffuse from solution onto the sample grid, thus the resulting image (Figure 4-7) showed the existence of free primary particles in solution, and verified the primary particle size as well.

The size distribution of colloidal aggregates was obtained from the Lasentec particle size analyzer. In-situ size analysis showed that, for a fixed for a fixed mixing speed in the sample vial, the characteristics of the aggregate size distribution did not change over time during constant rate pumping of the polymer solution into the precipitation bath. This is shown in Figure 4-8. The times refer to different times during the addition of polymer solution to the precipitation bath. Notice that the mode of the distribution (around 12 μm), and the shape of the distribution do not change with time. Integration of the area under the curves shows that the particle (aggregate) mass increases linearly with time for constant polymer-solvent injection rate (Figure 4-9). This suggests 2 things: (1) the basic aggregate size distribution is formed very quickly, probably much faster than the 1-minute time scale resolved in the measurements in the figures, and (2) there is no long-time-scale coagulation of the basic aggregates (the shape of the distribution did not change over time). The second idea was further verified by a longer-term mixing experiment, which showed that during 12 hours of continuous mixing at the same speed, the aggregate size distributions did not change, and were the same as those distributions measured immediately after the start of colloid fabrication (Figure 4-10). It should also be pointed out however that the mixing speed in the precipitation bath played a distinct role in the aggregate size distribution. Figure 4-11 compares aggregate size distribution for mixing speeds of 400 and 200 RPM, and shows that the mode of the curve almost doubled when the mixing speed decreased. Morishima et al. (1993) observed similar results when mixing speed was changed. They explained this phenomenon by invoking "quasi-emulsion droplets," which are

thought to appear before all solvent has diffused out of the. The increased mixing speed causes increased shear, which affects mass transfer, alters the quasi-emulsion droplet size, and modifies the final aggregate size. In our case, since the aggregates form very quickly, a "quasi-emulsion state" (if it exists) would have a very short lifetime. This could not be detected in this work because of time resolution limits in the Lasentech analyzer. However, this might be explored in the future with technologies that can be operated with smaller time scale resolution (probably significantly smaller than 1 second).

Changes to the basic recipe (Control) have the potential to affect both the primary particle size and aggregate size, and this was observed in the experimental results. The results are listed in Table 4-2 (recall the recipe matrix, Table 3-1).

Table 4-2 Primary particle size and aggregate median size

		Control	Run-I	Run-G	Run-T
Prmiary particle size (nm)	Average	67	69	87	103
	Range	50-90	50-90	65-125	80-200
Aggregates median size (μm)		16	40	35	7

The primary particle size of Run-I fell into the same range as that of the Control (50-90 nm). The primary particle size of Run-G and Run-T fell into a wider range (65-125 nm for Run G, and 80-200 nm for Run T). The aggregate size distributions from different recipes are shown in Figure 4-12. It was observed that the modes of distributions of the Control and Runs I, G and T were significantly different. The Control mode was located around 20 μm, the Run-I and Run-G modes around 40 μm, and Run-T mode was around 10 μm. The reason for such vararion in

primary particle size and aggregate size distributions should be investigated in the future. Possible reasons are that (1) the diffusion characteristics of the solvents (NMP-PA and THF) are different in different non-solvents (water, IPA and Glycerin), or (2) different solvent systems (NMP-PA and THF) could have different miscibilities and stability levels. The changes in primary particle size and aggregates distributions are expected to cause different surface area, pore structure, and adsorption capacities. Those different were indeed observed.

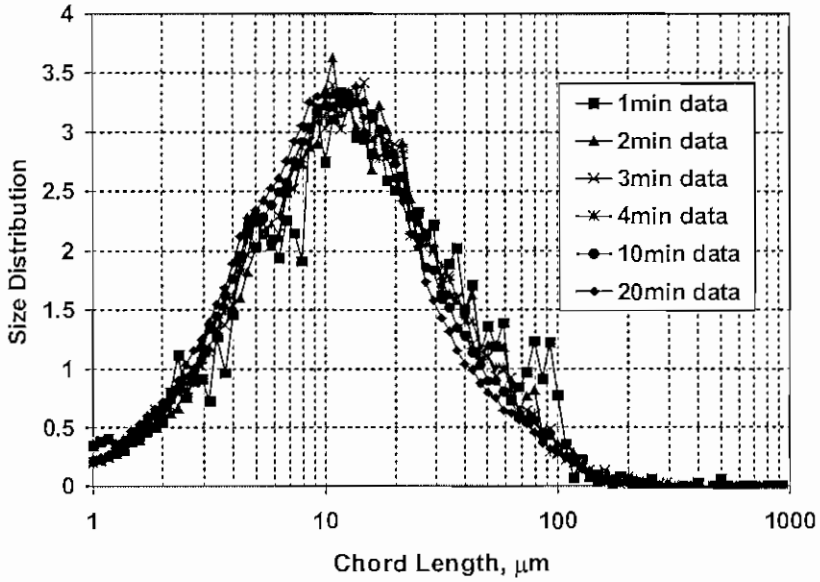

Figure 4-8. Aggregate size distribution at constant polymer injection rate.

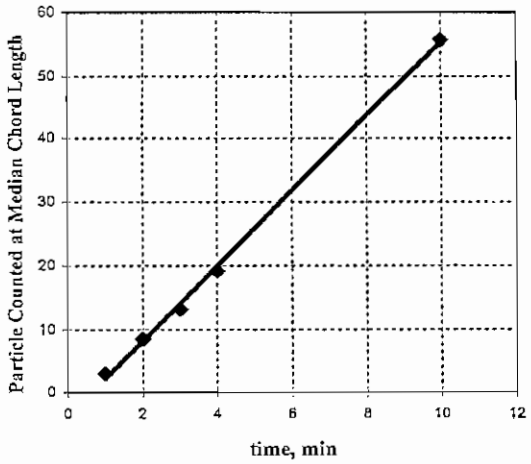

Figure 4-9. Particle number growth over

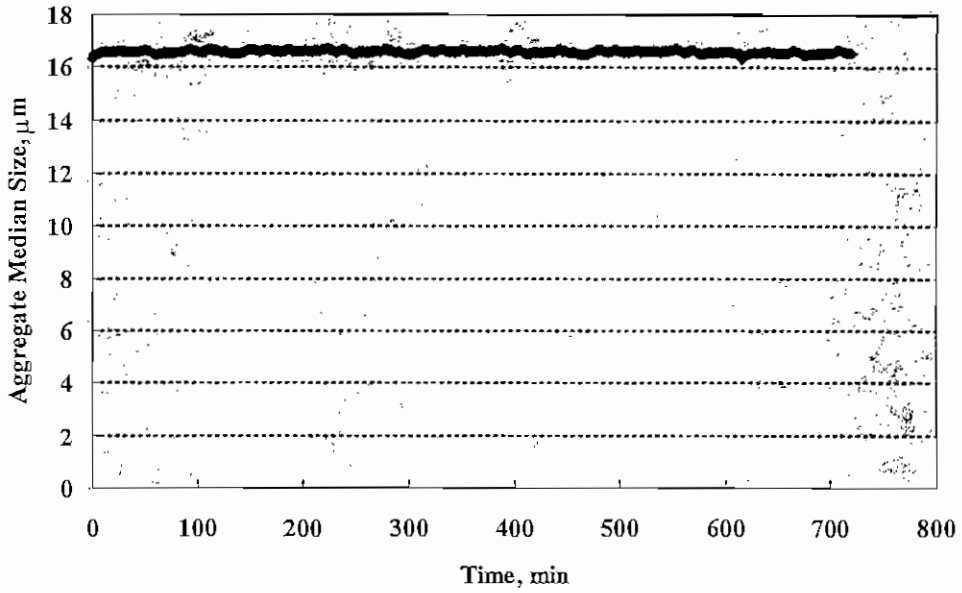

Figure 4-10. Aggregates size (median value) during 12 hours of measurements with continuous mixing.

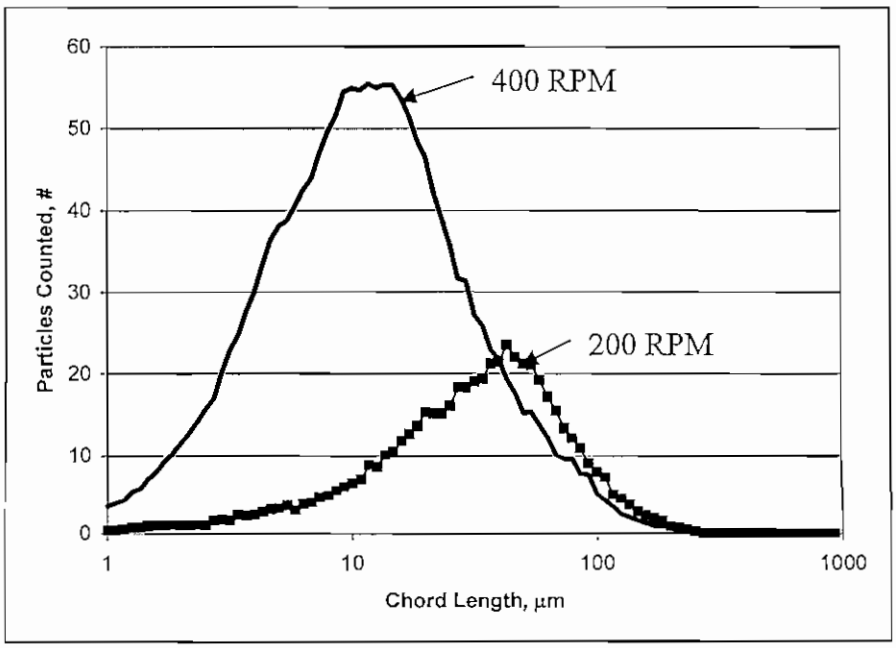

Figure 4-11. Comparison of aggregate size distributions for mixing speed of 200 rpm and 400 rpm. The curves shown here are the measurements after 10 minutes injection of Control PSf solution into the precipitation bath at a constant injection rate. The line with data markers is from a mixing speed of 200 RPM, and smooth line is from a mixing speed of 400 RPM.

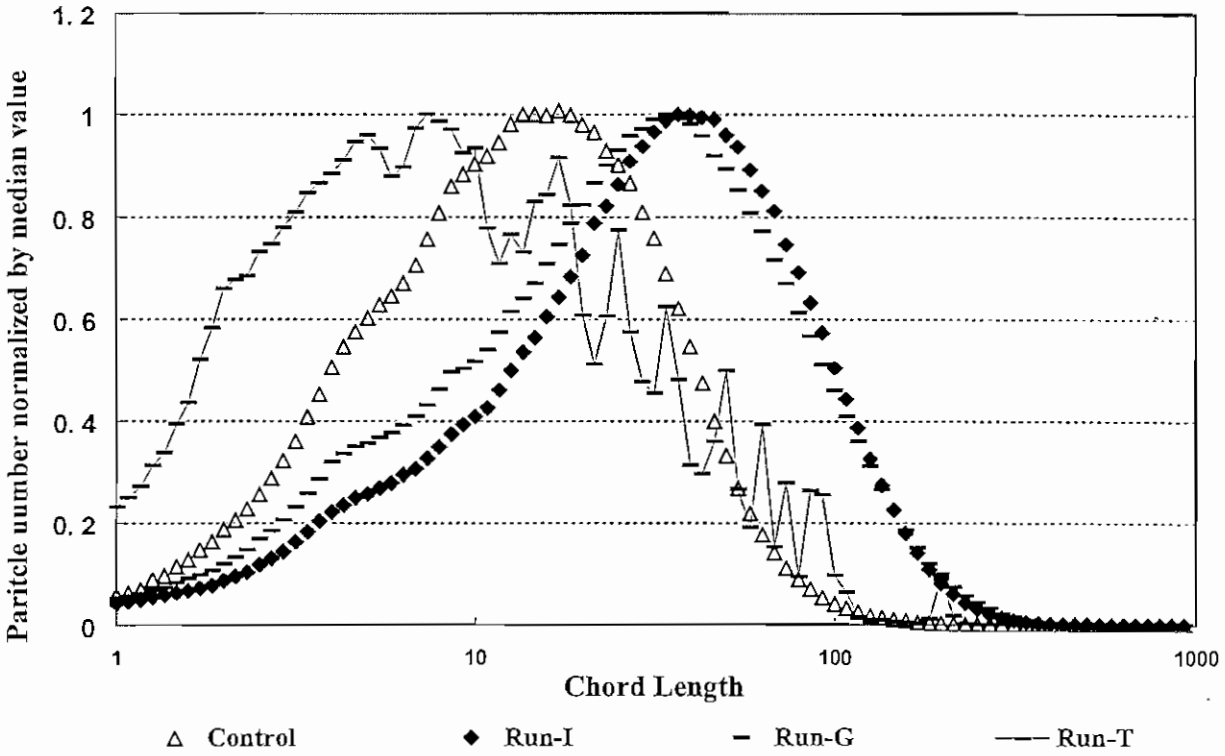

Figure 4-12. Particle number growth over time at constant polymer injection rate.

4.2.3 Concentration limitation

The typical ultimate colloid concentrations achieved during fabrication are in the range of 200 to 1000 mg/l. However, during the process of making CPA, solvents accumulate in water at the same rate as colloids are produced. To test whether there is a limitation of the colloid concentration with the standard production method and to see if solvent concentration affected the colloid structure, a bath with an initial concentration of 25% NMP-PA was prepared, and the PSf control formuation was injected to this solution (Section 3.2.1). The in-situ measurement of aggregate size (Figure 4-13) showed that the product is similar to the one made with zero initial solvent concentration. This is probably consistent with the cloud point curve for the co-solvent system (Figure 4.1), from which we observed that a very small amount of water can cause phase inversion. This experiment suggests the colloids can be continuously produced up to concentrations greater than 5 gram/L.

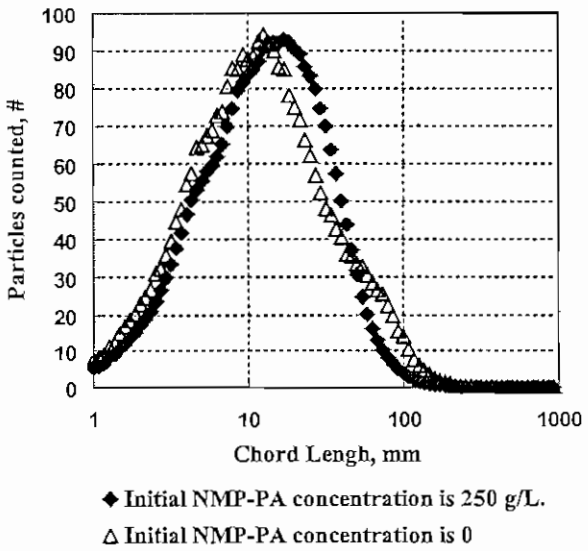

Figure 4-13. Concentration limitation test. In-process measurement of chord length distribution of particles made in the precipitation bath with clean water and with an initial solvent concentration of 250 g/l.

4.2.4 Zeta potential

Zeta potentials of the sonicated particles are listed in Table 4-3. All three measured values are around -25 mV, which is comparable to the surface charge of polysulfone membranes (Jucker and Clark, 1994). It is not clear why polysulfone colloids and membranes achieve a negative charge in simple electrolytes at near-neutral pH values. This is indeed an unresolved issue in electrokinetics measurements with membranes, which deserves further study.

Table 4-3 Zeta potential of different CPAs. Zeta potential is calculated from mobility using the Henry equation, assuming f(ka) = 1.0 (Huckel approximation)

	Control	Run-I	Run-T
Zeta potential (mv)	-25.7	-26.3	-23.9

4.2.5 Surface area

Based on N_2 adsorption experiments and the BET model, surface area and pore size for the Control, Run-I and Run-T recipes were determined (Table 4-5). Figures 4-14 to 4-16 are the BET isotherms (relative pressure p/p0 vs. volume N_2 adsorbed). All three isotherms show a hysteresis loop between adsorption and desorption, which indicates a Type-IV BET isotherm and which is typical of mesoporous materials (pores of 1-50 nm -- Gregg and Sing, 1967). There is no evidence of micropores (<1 nm). Micorpores will give characteristic of the Type-I BET isotherm, but that was not observed in this work.

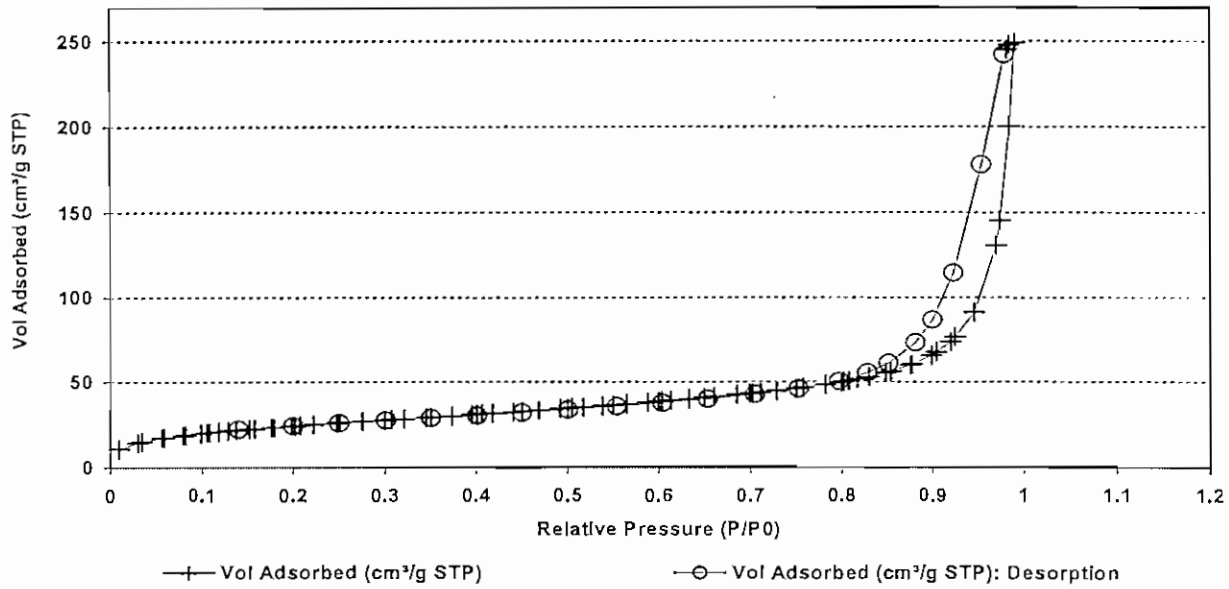

Figure 4-14. BET isotherm of Control.

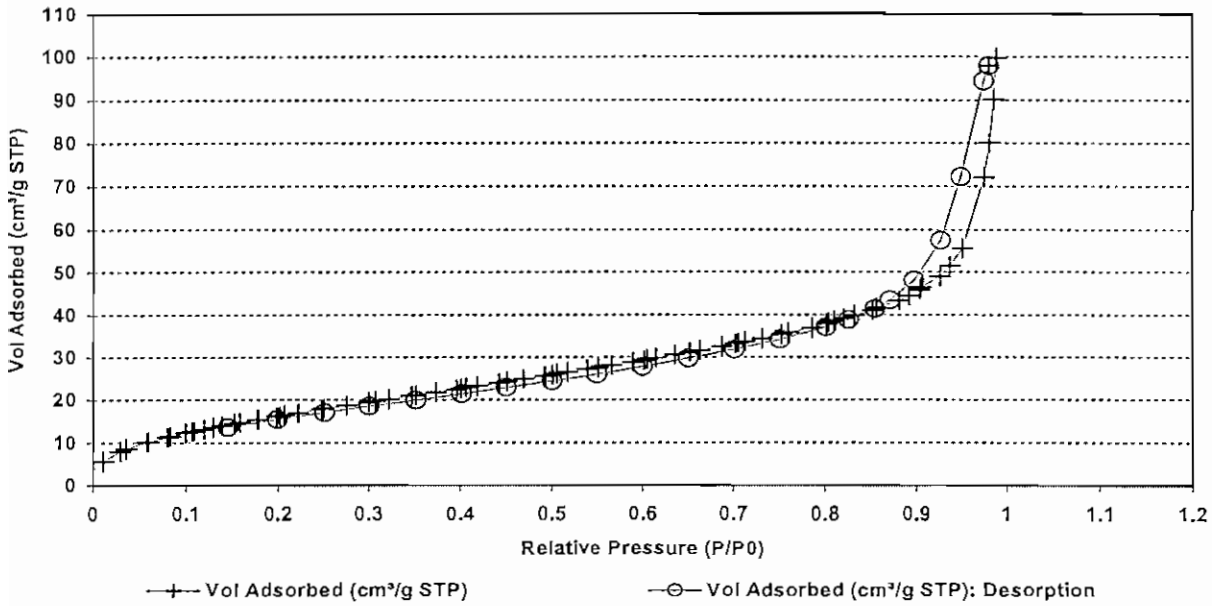

Figure 4-15. BET isotherm of Run-I.

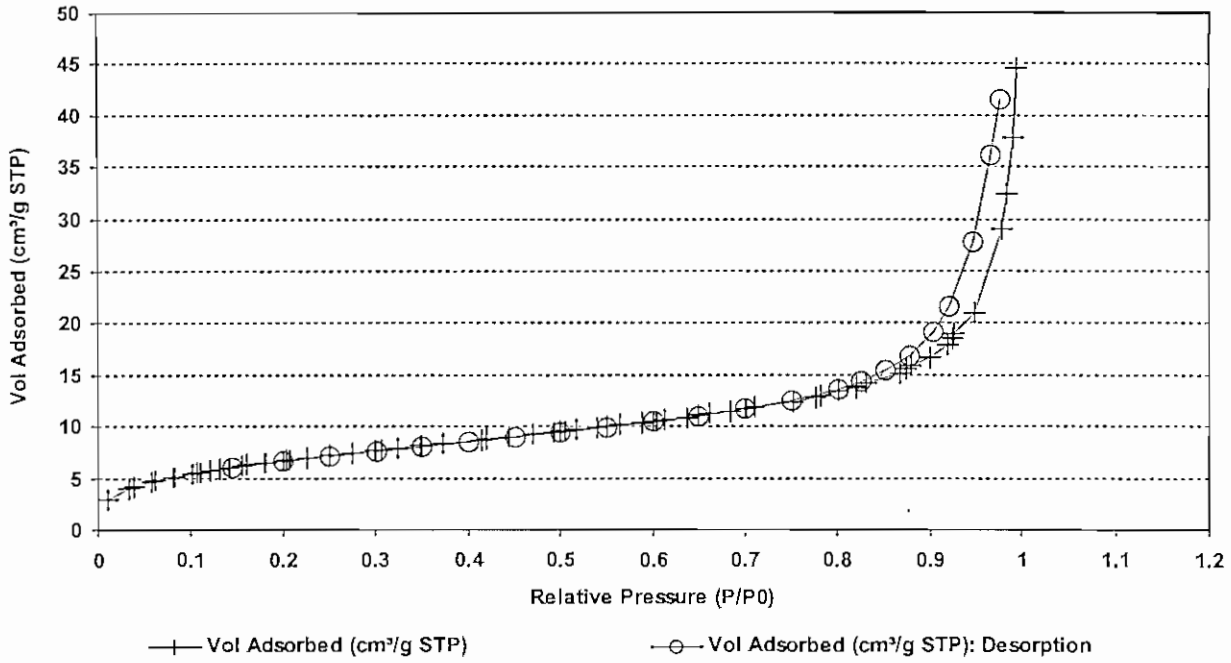

Figure 4-16. BET isotherm of Run-F.

One commonly used model for mesopore calculation is the BJH model. The BJH model accounts for capillary condensation in the pores using the classical Kelvin equation. The Kelvin pore radius is given by:

$$r_k = -\frac{nV\gamma}{RT\ \ln(\frac{P}{P_0})}\cos\theta \qquad (4\text{-}1)$$

where,

r_k—Kelvin pore radius;

P/P_0 —relative pressure;

γ—liquid surface tension;

V– molar volume of the liquid;

n—2 for desorption; 1 for adsorption;

Θ—angle of contact between the liquid and the walls of the capillary, taken to zero when the adsorbate is nitrogen.

The BJH pore radius is given by:

$$r = r_k + t \tag{4-2}$$

where,

r—BJH pore radius from corrected Kelvin equation;

t—adsorbed layer thickness, which is given by;

$$t = \sigma\left(\frac{-5}{\ln(p/p_0)}\right)^{1/3} \tag{4-3}$$

where, σ—occupation area of one particle.

The nitrogen adsorption data were fitted with the BJH model, and pore size distributions and pore surface area were calculated. The parameters used in the modeling are adapted from Gregg and Sing (1967) and are provided in Table 4-4. Adsorption pore size distributions were plotted as pore size vs. incremental adsorbed volume, and adsorption pore size vs. cumulative adsorbed volume, as shown in Figure 4-17 and Figure 4-18. Pore size was calculated from Equations 4-1 to 4-3, and the volume adsorbed is the measured value. The results are summarized in Table 4-6.

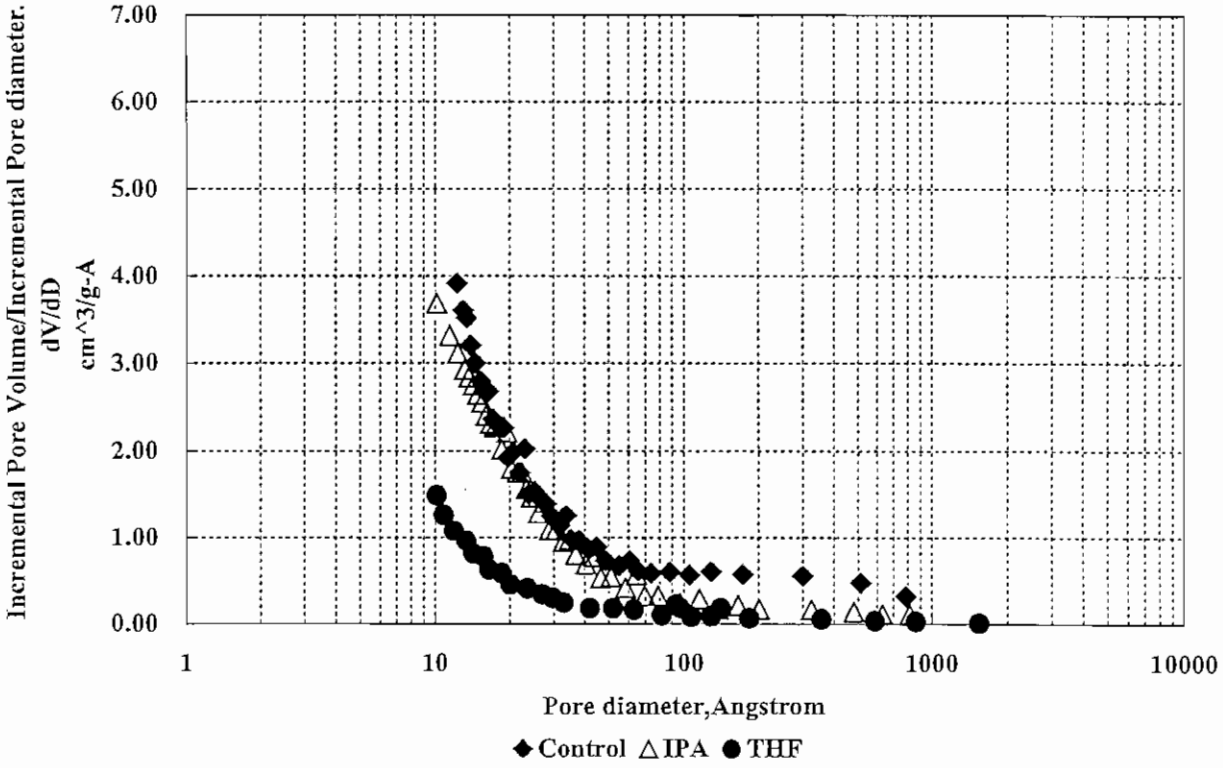

Figure 4-17. Adsorption incremental pore size distribution by BJH model.

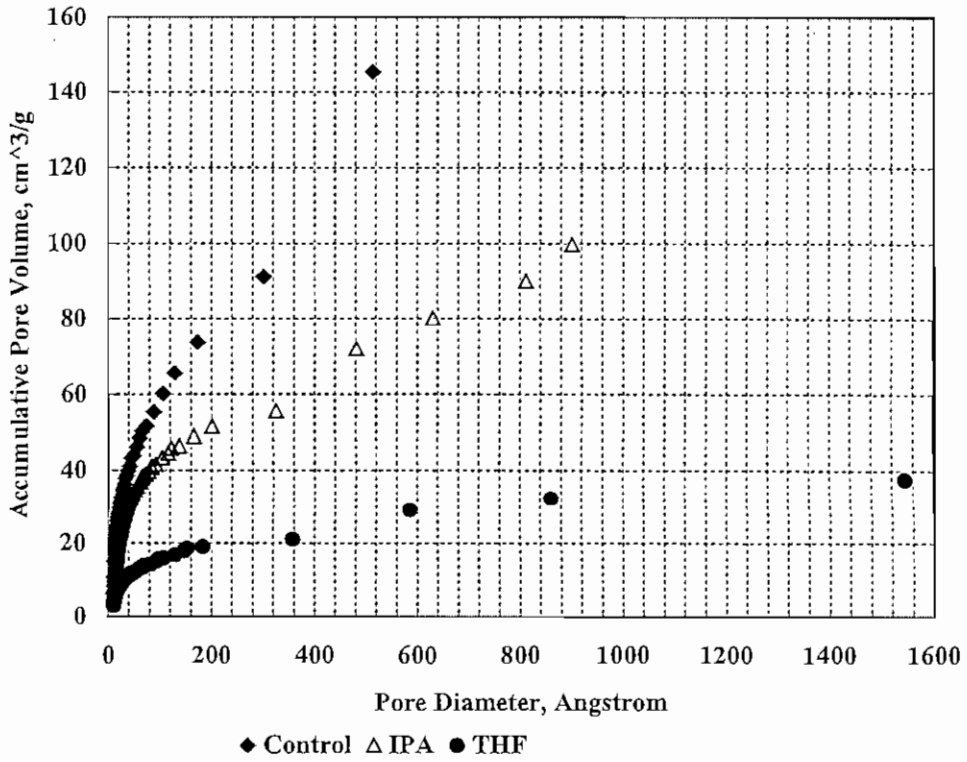

Figure 4-18. Adsorption accumulative pore size distribution by BJH model.

Following discussions in Section 4.2.2, changes in primary particle size and aggregate size will lead to changes in the total surface area. The increase in both primary particle size and aggregate size will lead to a decrease in total surface area. This was verified in these experiments. The surface area of Run-I was decreased by 30% compared to the Control because of a roughly 50% increase in the aggregate size; the surface area of Run-T was decreased by 70% compared to the control because of a roughly 50% increase in the primary particle size. From this result it seems that the changes in primary particle size have bigger effect on surface area than the aggregate size.

Table 4-4 Parameters used in BJH modeling

V	γ	σ
cm^3/mol	mN/m	Angstrom
34.68	8.72	3.54

Table 4-5 BET model summary

BET model	Control	Run-I	Run-T
Surface area (cm^2/g)	89.8	62.5	25.0
Adsorption average pore diameter (nm)	9.00	7.14	7.18

Table 4-6 BJH model summary

BJH model		Control	Run-I	Run-T
Surface area of pores* (cm^2/g)	Adsorption	88.2	72.4	24.0
	Desorption	85.3	68.4	24.0
Average pore diameter (nm)	Adsorption	20.66	30.27	31.68
	Desorption	28.26	38.37	29.80
Pore range (nm)	Adsorption	1~80	1~90	1~154
	Desorption	1.5~203	1.5~185	1.5~331

* The values showed in the table are accumulative surface area of pores from 17 to 3000 Angstrom.

Equations 4-1 to 4-3 tell us that low relative pressure gives information on the smaller pores (r is propotional to $1/\ln(p/p_0)$). A lack of pore size information in the lower range (< 10 Å) can be seen from Figure 4-17 with all samples, which means that the relative pressure was not adjusted low enough. To obtain the whole information in the lower range of pore size, the relative pressure in future experiments need to be adjusted to the range from 10^{-7} to above 0.99 (micropores are expected to be detected in that pressure range if they exist).

In summary, the BET surface area of the Control is around 90 m^2/g. The observed pore range is from around 10 to 800 Angstroms, where pores less than 50 nm (mesopores) are dominant (Figure 4-17 and 4-18). The surface area of CPA is roughly 10% of that of PAC, which is typically on the order of 800 to 1000 m^2/g.

4.3 CPA performance

4.3.1 SRNOM adsorption isotherms

Two repeated isotherms for SRNOM adsorption by the Control CPA, and one isotherm for SRNOM adsorption by Norit PAC, are shown in figure 4-19. CPA exhibited a similar adsorption capacity to PAC. The K and 1/n values in the Freundlich equation are listed in Table 4-7. The K values have good repeatability with a variation of around 4%; the 1/n values are not as repeatable (about 30% variation).

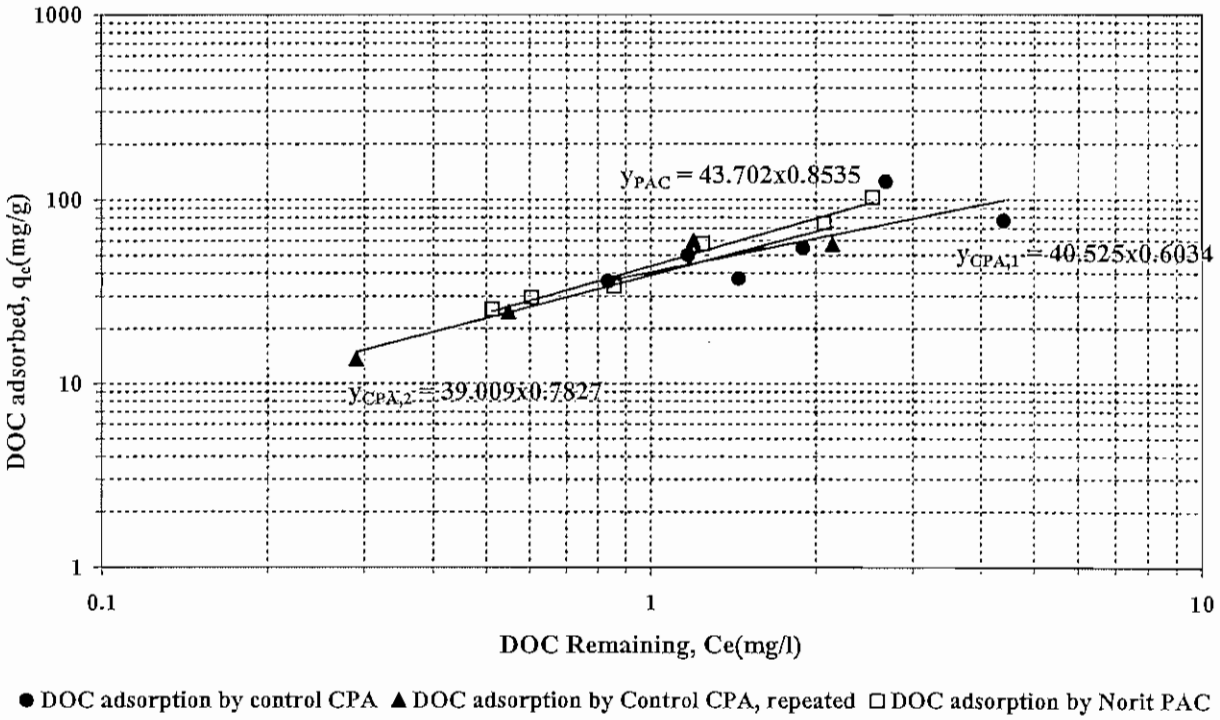

Figure 4-19. DOC adsorption isotherms. Adsorbents are PAC and CPA. Initial SRNOM concentration is 7 mg/l. PAC concentrations are from 120 mg/l to 10 mg/l. CPA,1 concentrations are from 120 mg/l to 10 mg/l. CPA,2 concentrations are from 200 mg/l to 30 mg/l. Solution conditions are pH =7.5

Table 4-7 Fitted parameters in Freundlich equation

	Norit PAC	CPA (Control)	CPA (Control)
K	43.702	40.525	39.009
1/n	0.8535	0.6034	0.7827

The adsorption capacities of PAC and CPA are comparable. Considering the fact that PAC has a typical adsorption surface area of 1000 m^2/g whereas CPA has only around 100 m^2/g of surface area, CPA must have other features that make it a good adsorbent for NOM.

1) As discussed in Section 4.2.5, mesopores are dominant in CPA aggregates (Figure 4-17). A comparison between the size of Suwanne River NOM particles and CPA pore diameter can be made in Tables 3-4 and 4-6. Howe and Clark (2002) suggested that membrane foulants are small colloids ranging from about 3-20 nm in diameter. This suggests that mesopores (1 nm < d < 50 nm) can be especially useful in the removal of membrane foulants from natural water sources.
2) PSf is a relatively hydrophobic polymer, and this should favor NOM adsorption. As Childress et al (2000) pointed out, hydrophobic interactions between membranes and humic substances dominte at higher pH values.

The adsorption mechanics should be investigated more in the future. The suggested methods could be to fractionate NOM according to molecular weight (size) and hydrophobicity/hydrophilicity, and compare the CPA adsorption capacity with different NOM fractions and at different pH values.

The CPA samples used for adsorption are purified by dialysis, as discussed in Section 4.2.1; the disadvantage of this method is that remaining residual solvents cannot be totally removed. The organic solvents could remain on the surface of the polymer colloids, compete with NOM for the adsorption site, or block the pores. This will affect the measured NOM adsorption capacity. Complete purification of CPA should be an immediate goal of future work.

4.4 CPA-Membrane hybrid system

Flux decline patterns in the hybrid CPA-membrane system are compared with flux decline patterns without CPA pretreatment. The results are listed in Figures 4-20 to 4-21. With the PES membrane, flux without CPA pretreatment declined to 70% of clean water flux after 1.5 hours filtration, while in the CPA-membrane hybrid system with a CPA concentration of 200 mg/l, the flux stabilized somewhat around 85% of clean water flux (Figure 4-20). The clean water flux after the sample filtration showed an 8% recovery in both curves (Figure 4-20), which accounts for the disappearance of concentration polarization. Figure 4-19 shows a series of flux decline curves with different CPA concentrations in the hybrid system. The 1, 10 and 100 mg/l experiments showed similar patterns of flux improvement, while the 25 and 50 mg/l experiments showed no improvement compared to un-pretreated SRNOM. There were two kinds of membrane foulants in the hybrid system, the remaining SRNOM and CPA particles. At the higher CPA concentration, larger amounts of SRNOM could be removed by pre-adsorption, and there would be less membrane fouling by SRNOM. However, higher CPA concentrations also mean more significant membrane cake layer fouling by CPA particles. At lower concentrations of CPA, there will be more fouling by the remaining SRNOM, but less fouling by CPA particles. Nevertheless, no clear trend was observed in these experiments, and separation and clarification of particulate and adsorption-related fouling deserves more study.

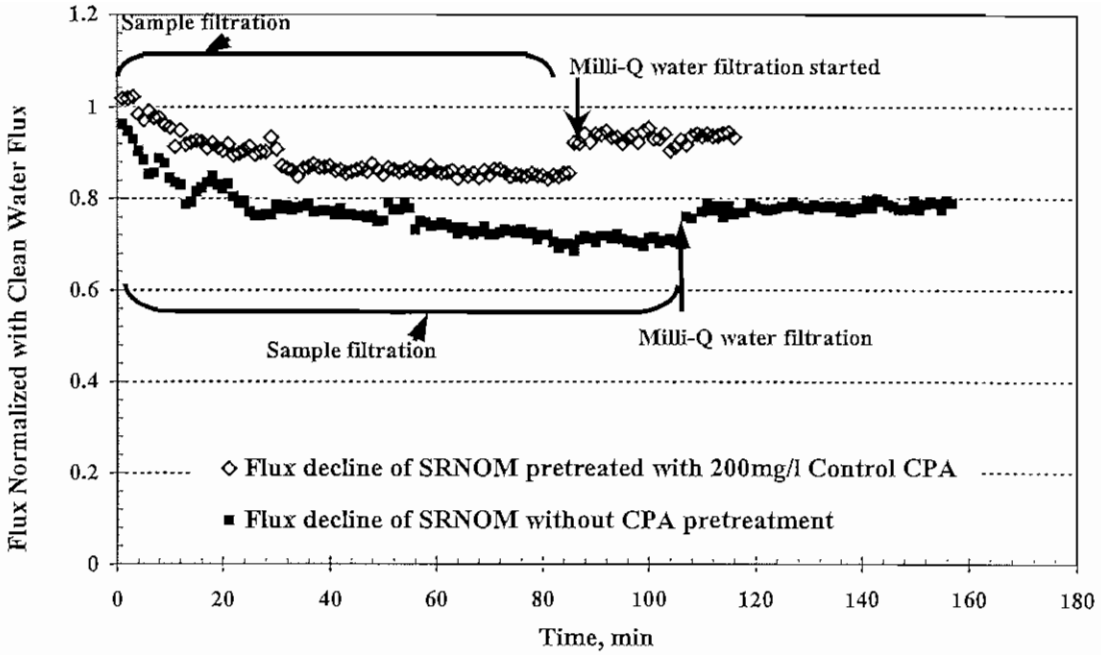

Figure 4-20. Flux decline curves. In CPA-membrane hybrid system, membrane is PES 20kD, CPA has a concentration of 200 mg/l. Raw SRNOM solutions is 7 mg/l. Dead-end filtration with continuous stirring at 30 psi.

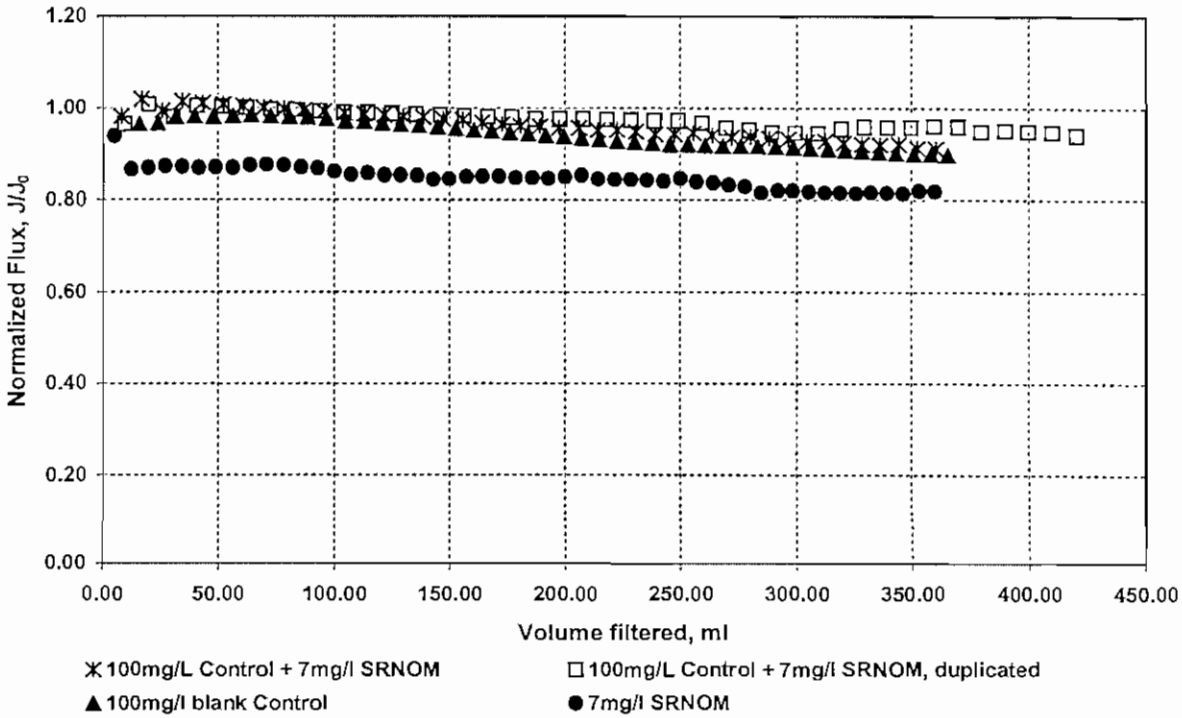

Figure 4-21. Flux decline curves. In CPA-membrane hybrid system, membrane is YM30, CPA has a concentration of 100 mg/l. Raw SRNOM solutions is 7 mg/l. Dead-end filtration with continuous stirring at 30 psi.

With YM30 membranes, an improvement in flux was also observed (Figure 4.21). The overall flux decline is less than that with PES membrane, because that regenerated cellulose membrane is relatively hydrophilic. Flux decline without CPA pretreatment is around 20%, and flux decline with CPA pretreatment is around 10%. In these experiments, the flux decline during SRNOM filtration in the hybrid system is very similar to the flux decline with blank CPA particles of the same concentration, which means that in the hybrid system, the flux decline is mainly caused by cake layer formation of CPA particles.

Membrane fouling by cake layer formation is supposed to be reversible, which is tested by back washing in this experiment. However, the water flux after back washing behaved abnormally. The recovered flux for all but one experiment was higher than the original clean water (Figure 4-19). Considering the fact that the PES membrane is an asymmetric membrane, this could mean there was damage to the membrane during backwashing. This damage could possibly be caused by the operating pressure during back washing. The back washing pressure in this study was chosen to be half of the normal filtration pressure, i.e. 15 psi. Future experiments might need to find a lower pressure to more properly backwash PES 20kD membranes.

In Figure 4-23, flux decline for a Norit-PAC-pretreated SRNOM solution is compared with SRNOM filtration without any pretreatment. Both showed a similar flux decline pattern. With a comparable adsorption capacity, CPA showed a slight improvement in membrane flux, while Norit PAC did not. There are two possible explanations for this phenomena: (1) CPA could selectively adsorb membrane foulants, while Norit PAC may not; or (2) membrane fouling could also be caused by the cake layer formation of CPA particles and Norit PAC particles, and CPA particles may cause much smaller particulate fouling effects than Norit PAC. Regarding the second explanation, CPA and Norit PAC fouling layers were examined with SEM. Figures 4-24

and 4-25 show very different cake layer structures; CPA formed a loose or diffuse layer, while Norit PAC formed a more compact layer containing large irregular particles. SEM imaging of membrane after backwashing was not performed in this work, but deserves study in the future.

EDX-SEM elemental analysis of foulant layers was also carried out in this work (Figures 4-26 to 4-28). The dry NOM powder was found to have large portions of C and O, and small portions of Na, Al, Si, S, and Cl. The virgin PES membrane surface was found to have large portions of C, O and S, and small portions of Na, results which are consistent with the chemical structure of polysulfone (Section 3.1.1). However, the results for the fouled PES membrane showed features very similar to that of the clean PES, and no additional elements are found. Apparently, the EDX signal recorded in this work was dominated by the underlying membrane material. Future work might determine if the EDX method can be better optimized in terms of penetration depth. Although the technique may be of limited value in studies of SRNOM fouling (because the SRNOM is highly purified) the technique should be pursued in future work with other unpurified sources of NOM. For example, Howe et al. (2002) used XPS to analyze foulants and found enrichment of Al and Si in NOM deposits from several rivers in the US.

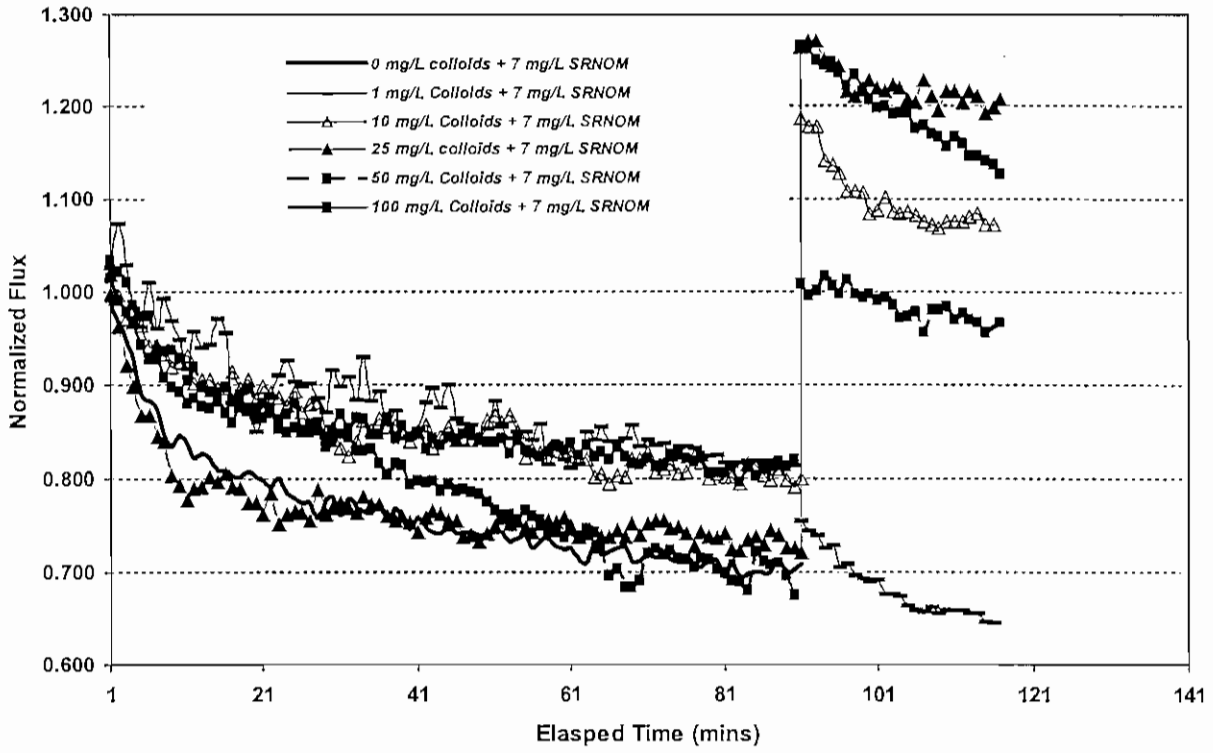

Figure 4-22. Flux decline curves. In CPA-membrane hybrid system, membrane is PES 20kD, CPA has a concentration of from 1mg/l to 100 mg/l. Raw SRNOM solutions is 7 mg/l. Dead-end filtration with continuous stirring at 30 psi.

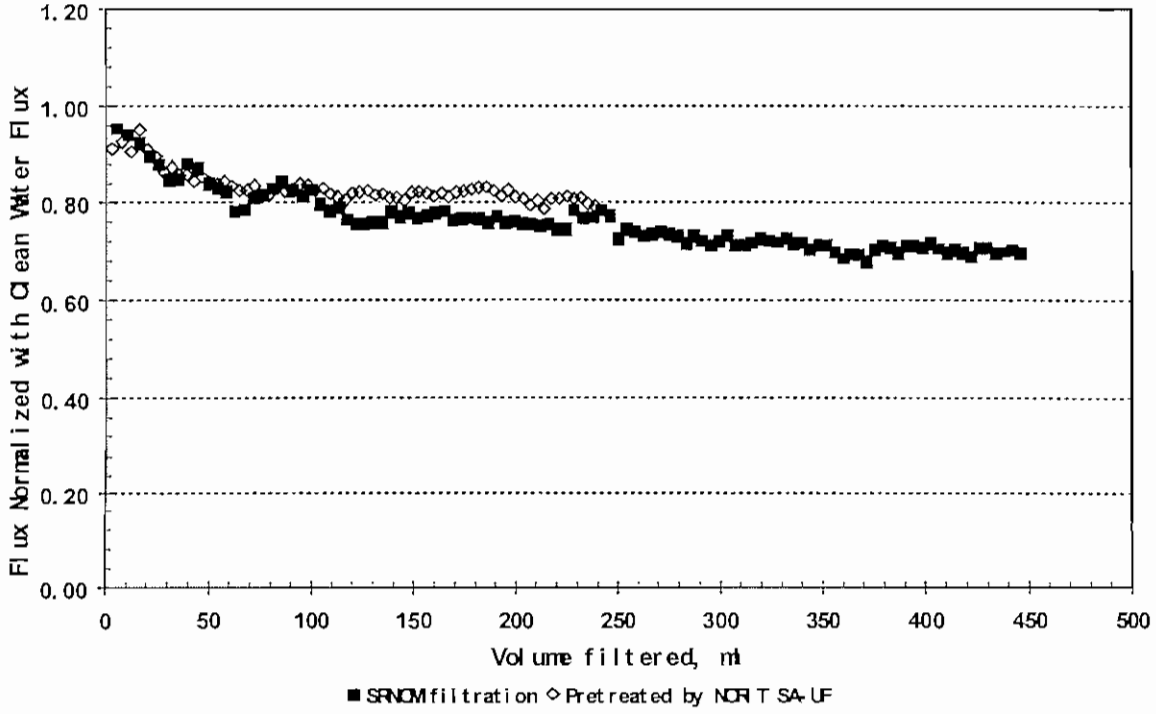

Figure 4-23. Flux decline curves. In Norit PAC-membrane hybrid system, membrane is PES 20kD, PAC has a concentration of from 100 mg/l. Raw SRNOM solutions is 7 mg/l. Dead-end filtration with continuous stirring at 30 psi.

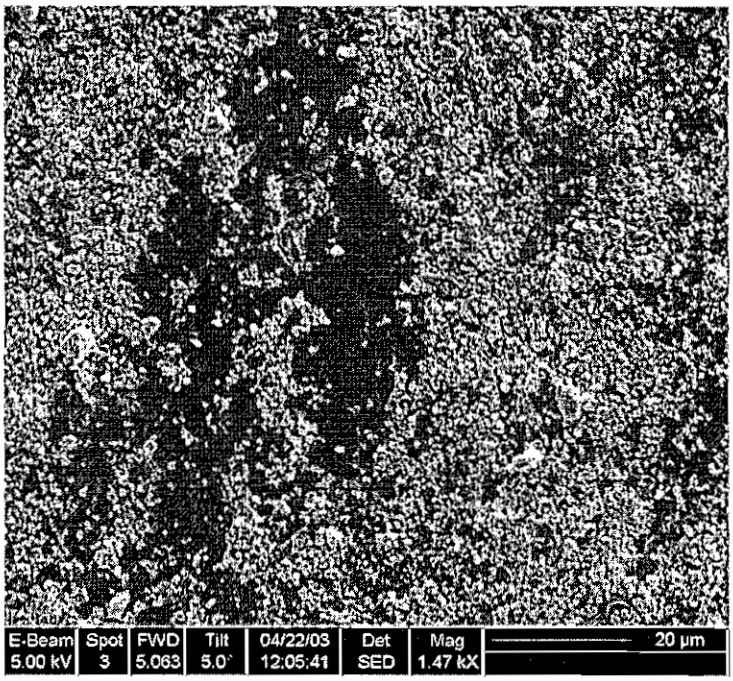

Figure 4-24. SEM image of CPA fouling layer on PES 20 kD membrane. CPA concentration is 100 mg/l. Dead-end filtration with continuous stirring at 30 psi for 1 hour.

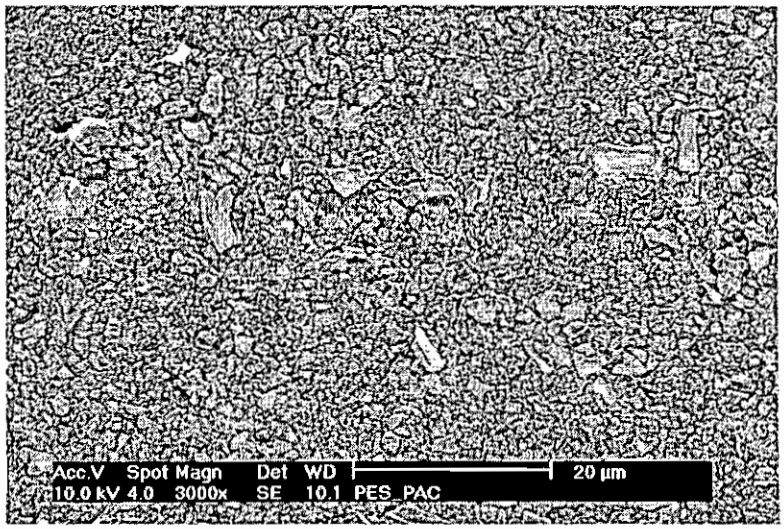

Figure 4-25. SEM image of Norit PAC fouling layer on PES 20 kD membrane. Norit PAC concentration is 100 mg/l. Dead-end filtration with continuous stirring at 30 psi for 1 hour.

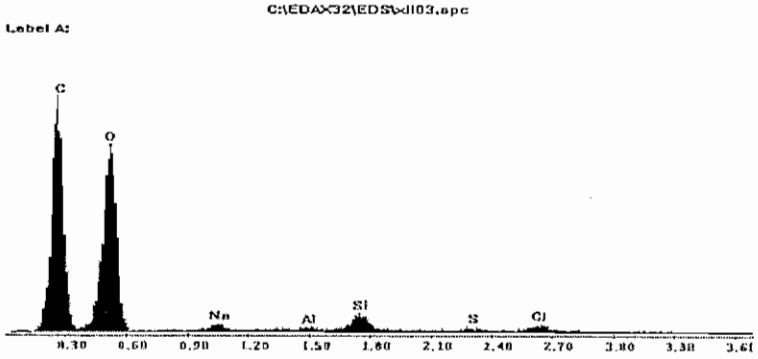

Figure 4-26. EDS elemental analysis of NOM powder.

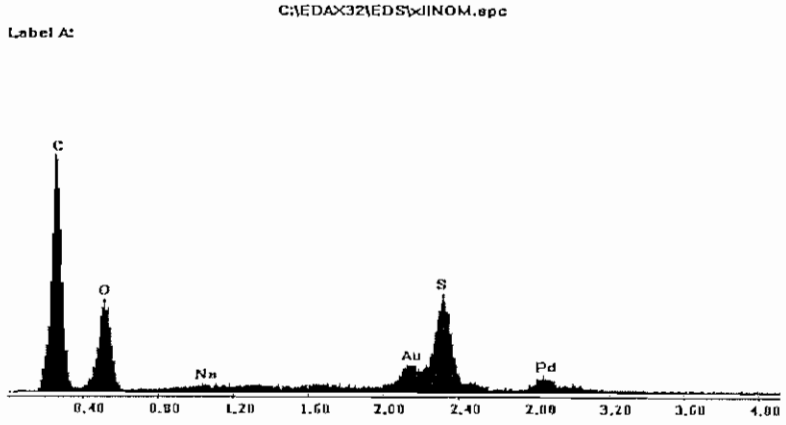

Figure 4-27. EDS elemental analysis of PES membrane after RNOM filtration.

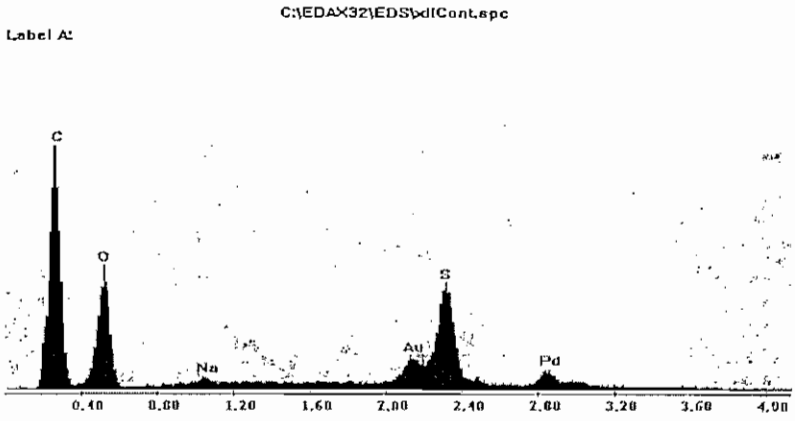

Figure 4-28. EDS elemental analysis of PES clean membrane.

5. Summary, Conclusions, and Perspectives

This work investigated a new NOM adsorbent, a colloidal form of polysulfone (CPA). The material is made from a common chemical formulation used in making polysulfone membranes, and is formed by direct injection into water. This work shows that the new material is mesoporous, with "pore" sizes on the order of 20-30 nm, and with a total surface area on the order of 70 to 90 m^2. Considering the fact that natural organic matter (NOM) is in the same range of sizes, it is felt that this material may be especially good at adsorbing NOM, either on its own or in a hybrid process incorporating membranes. Much work remains to be done on variation and optimization of the polymer chemistry and temperature. For example, in Murakami's (2000) research, it was shown that the amount of poor solvent (i.e. alcohol) in a binary organic solvent system can change precipitation rate and primary particle aggregation; likewise, in this work future experiments need to explore the effects of varying the NMP/PA ratio and temperature. A preliminary experiment performed at room temperature without any PA showed that long polysulfone fibers could be cast (Section 4.1). These early results are intriguing, as fibrous forms of the polysulfone adsorbent may be preferred over the colloidal form for some applications in water treatment. Work with polysulfone adsorbents will continue, in particular, we are interested in packing the fibrous material in columns which can be contacted with NOM-laden water. If successful, this could be an important advance in application of the new material, since regeneration-in-place will be much more easily achieved.

The project will soon abandon Suwannee River NOM as a model foulant. A number of issues have lead to this decision. First, Suwannee River NOM is expensive, about $1/mg. As we move into continuous flow experiments (say with packed columns of colloidal or fibrous polymer particles), we will need a cheaper source of NOM. Second, more and more studies are showing wide variations in membrane fouling by NOM from different sources (typically rivers and lakes).

In these studies, the full spectrum of (unpurified) NOM is typically applied. It is not surprising that fouling results for Suwannee River NOM are different than for wider spectrum NOM. Suwannee River NOM is a highly purified, mainly hydrophobic NOM, largely cleaned of all inorganic "contamination." However, it appears that the wide variation in fouling found with different water sources may be related to the fact that these sources of NOM are "dirty," including a wide spectrum of organic and inorganic materials (Howe and Clark, 2001). Therefore most of our future adsorption and fouling work will utilize full spectrum NOM from lakes and rivers.

Our work has recently shown that the colloid polymer material developed herein may be difficult to fully wet; a significant amount of unwetted area will decrease the adsorption efficiency of the colloidal adsorbent. In collaboration with Mr. Bob Riley (Separation Systems Technology), we have proposed new experiments that use a blend of polymers, sulfonated-polyether-sulfone and polysulfone. These blends were used in a previous NWRI funded project on membranes; in that project, we were able to cast membranes with varying hydrophobicity, porosity, charge, and NOM adsorption characteristics. Use of these polymer blends is underway in colloid production, and we expect the new polymer formulation will be another important variable, not only in wetting, but also in colloid charge and adsorption characteristics.

The polymer colloids developed in this work carry a significant amount of residual solvents (NMP and PA – Section 3.1.2). We have recently used NMR to explore contamination of the colloids. Through quite a bit of experimentation, we discovered that the colloids can be purified to a much greater extent than we previously though was possible by extended dialysis at elevated temperatures (below the glass transition temperature). This improved purification will now be part of standard operating procedure.

Several collaborations have developed during the course of this project. Timm Strathmann, an Assistant Professor in Civil and Environmental Engineering at UIUC, has trained some of the colloid project personnel in the use of the FTIR-ATR in his lab. In past work (Howe et al. 2002), we have used this technique to study organic material deposited on membranes during filtration of river water samples from around the US. As we move more into adsorption and fouling by unpurified NOM, FTIR-ATR will give us a new tool to study the functionality of NOM adsorbed on membranes and on polymer colloids. Just as pieces of membrane can be placed against an FTIR-ATR crystal, we feel that NOM-loaded colloidal polymer can be pressed against the ATR crystal. In fact, since the colloidal material has a much greater surface area than any membrane, we hope to get a clearer NOM signal with the loaded colloids. We have also started collaborations with Professors Andrey Kalimchev and James Kirkpatrick of the UIUC Geology Department. Kalinichev is using Molecular Dynamics simulations to study the association of organic and inorganic molecules and atoms with membrane surfaces. We have met several times, and we are hopeful that these simulations can explain some of the traditionally puzzling results from membrane electrokineitcs, e.g., why do membranes made from neutral polymers like polysulfone and polypropylene have a negative charge at natural water pH values? (This might then explain the negative charge of the polysulfone colloids fabricated in this study -- Section 4.2.4). Kirkpatrick is an expert on NMR, and we have supplied his group with samples of the polysulfone colloids, which will be used to concentrate NOM for NMR analysis.

6. References:

1. Adham, S. S., Snoeyink, V.L., Clark, M. M., Bersillon, J. L., 1991. *Journal of American Water Works Association,* 83(12):81-91
2. Adham, S. S., Snoeyink, V.L., Clark, M. M., Anselme, C., 1993. *Journal of American Water Works Association,* 85(12):58-68
3. Aiken, G. and E. Costaris, 1995, Soil and Hydrology: Their Effect on NOM. *Journal of AWWA,* 87(1):36-45
4. AWWA Committee Report. Membrane Processes for Potable Water Treatment: Research Needs. American Water Works Association Membrane Technology Research Committee, published in Journal American Water Works Association, 90, 4 (1998).
5. Amy, G. L., 1993, Using NOM characterization for the evaluation of treatment, *Natural organic matter in drinking water: origin, characterization, and removal,* Workshop proceedings, Chamonix, France.
6. Aoustin, E., Schäfer, A. I., Fane, A. G. and Waite, T. D., 2001, Ultrafiltration of Natural Organic Matter, *Separation and Purification Technology,* 22-23:63-78
7. Bai, R and Zhang, X., 2001, Polypyrrole-Coated Granules for Humic Acid Removal, *Journal of Colloid and Interface Science* 243: 52–60
8. Buffle, J., Deladoey, P. and Haerdi, W., 1978. The use of ultrafiltration for the separation and fractionation of organic ligands in fresh waters, *Analytica Chimica Acta,* 101(2):339-357
9. Chang, Y. and Benjamin, M. M., 1996. Iron oxide adsorption and UF to remove NOM and control fouling, *Journal of American Water Works Association,* 88(12):74-88

10. Childress, A. E., Elimelech, M., 1996. Effect of solution chemistry on the surface charge of polymeric reverse osmosis and nanofiltration membranes, *Journal of Membrane Science,* 119(2): 253-268

11. Childress, A. E., Elimelech, M., 2000. Relating Nanofiltration Membrane Performance to Membrane Charge (Electrokinetic) Characteristics, Environ. Sci. Technol., 34:3710-3716

12. Cho, J., Amy, G. and Pellegrino, J., 2000, Membrane filtration of natural organic matter: comparison of flux decline, NOM rejection, and foulants during filtration with three UF membranes, *Desalination*, 127(3): 283-298

13. Combe, C., Molis, E., Lucas, P., Riley, R., Clark, M. M., 1999, The Effect of CA Membrane Properties on Adsorptive Fouling by Humic Acid, *Journal of membrane science,* 154: 73-87

14. Fane, A.G., Fell, C.J.D., 1987, A Review of Fouling and Fouling Control in Ultrafiltration, *Desalination*, 62: 117-136

15. Gaffney, J. S., Marley, N. A. and Clark, S. B., 1996. Humic and fulvic acids: isolation, structure, and environmental role, *ACS symposium series 651*, Washington DC.

16. Gregg, S. J. and Sing, K. S. W., 1967, Adsorption, surface area, and porosity, London, New York : Academic Press

17. Hosoya, K., Kubo, T., Tanaka, N. and Haginaka, J., 2003, A possible purification method of DNA's fragments from humic maters in soil extracts using novel stimulus responsive polymer adsorbent, *Journal of Pharmaceutical and Biomedical Analysis,* 30(6): 1919-1922

18. Howe, K. J., and Clark, M.M. 2002, Fouling of Microfiltration and Ultrafiltration Membranes by Natural Waters, *Environ. Sci. Technol.*, 36: 3571-3576

19. Howe, K. J., 2001, Effect of coagulation pretreatment on membrane filtration and performance, thesis (Ph. D.), University of Illinois at Urbana-Champaign

20. Howe, K.J, Ishida, K, and M.M. Clark 2002, Use of ATR/FTIR Spectrometry to Study Microfiltration Membrane Fouling by Natural Waters, *Desalination, 147*, 251-255.

21. Hoy et al., 1981. Production of Aqueous Dispersion of Aromatic Polyethersulphone, US Patent, Patent number: 4,321,174

22. Ichikawa et al., Fuel Absorbent and A Process for Making the Fuel Absorbent, U.S. Patent, Patent number: 5,418,203

23. Jucker, C., Clark, M. M., 1994, Adsorption of Aquatic Humic Substnaces on Hydrophobic Ultrafiltration Membranes, *J. of Membrane Sci.*, 97: 37-52

24. Lahoussine-Turcaud, V., Weisner, M.R., and Bottero, J-Y., 1990a. Fouling in Tangential-Flow Ultrafiltration: The Effect of Colloid Size and Coagulation Pretreatment. *Journal of Membrane Science,* 52:173-190

25. Lau, W. W. Y., Guiver, M. D. and Matsuura, T., 1991, Phase separation in polysulfone/solvent/water and polyethersulfone/solvent/water systems, *Journal of Membrane Science*, 59: 219-227

26. Lee, S. J., Choo, K. H., Lee, C. H., 2000, Conjunctive use of ultrafiltration with powdered activated carbon adsorption for removal of synthetic and natural organic matter, *Journal of Industrial and Engineering Chemistry*, 6 (6): 357-364

27. Liang, L. and Morgan, J.J., 1990. Chemical aspects of iron oxide coagulation in water: laboratory studies and implications for natural systems, Aquatic Sci., 52(1) 32.

28. Lin, C. F, Huang, Y. J. and Hao, O. J., 1999, Ultrafiltration processes for removing humic substances: effect of molecular weight fractions and PAC treatment, *Water Research*, 33(5): 1252-1264

29. Maartens, A., Swart, P. and Jacobs, E. P., 1999, Feed-water pretreatment: methods to reduce membrane fouling by natural organic matter, *Journal of Membrane Science*, 163(1) a; 51-62

30. Maartens, A., Swart, P. and Jacobs, E. P., 2000, Membrane Pretreatment: A Method for Reducing Fouling by Natural Organic Matter, *Journal of Colloid and Interface Science*, 221(2): 137-142

31. McHugh, A. J., Miller, D.C., 1995, The dynamics of diffusion and gel growth during nonsolvent-induced phase inversion of polyethersulfone, *Journal of membrane science*, 105: 121-136

32. Morishima, K., Kawashima, Y., Kawashima, Y., Takeuchi, H., Niwa, T., Hino, T., 1993. Micromeritic characteristics and agglomeration mechanisms in the spherical crystallization of bucillamine by the spherical agglomeration and the emulsion solvent diffusion method, Powder Technology, 76(1): 57-64

33. Murakami, H, Kobayashi, M, Takeuchi, H and Kawashima, Y, 1999. Preparation of poly (DL-lactide-co-glycolide) nanopartilces by modified spontaneous emulsification solvent diffusion method, International Journal of Pharmaceutics, 187:143-152

34. Murakami, H, Kobayashi, M, Takeuchi, H and Kawashima, Y, 2000, Further application of a modified spontaneous emulsification solvent diffusion method to various types of PLGA and PLA polymers for preparation of nanoparticles, *Powder Technology*, 107(1-2): 137-143

35. Newcombe, G., Drikas, M., Assemi, S. and Beckett, R., 1997, Influence of Characterised Natural Organic Material on Activated Carbon Adsorption: I. Characterization of Concentrated Reservoir Water, *Water Research*, Volume 31, Issue 5, Pages 965-972

36. Niwa T., Takeuchi H., Hino T., Kunou N., Kawashima Y., 1993, Preparations of biodegradable nanospheres of water-soluble and insoluble drugs with D,L-

lactide/glycolide copolymer by a novel spontaneous emulsification solvent diffusion method, and the drug release behavior, J. Controlled Release, 25(1-2):89-98

37. Pontie, M., Durand-Bourlier, L., Lemordant, D., Laine, J.M., 1998. Control fouling and cleaning procedures of UF membranes by a streaming potential method, *Separation and Purification Technology*, 14(1-3): 1-11

38. Rabiller-Baudry, M., Le Maux, M., Chaufer, B., Begoin, L., 2002, Characterisation of cleaned and fouled membrane by ATR-FTIR and EDX analysis coupled with SEM: application to UF of skimmed milk with a PES membrane, *Desalination*, 146: 123-128

39. Ritchie, J. D., Perdue, E. M., 2003. Proton-binding study of standard and reference fulvic acids, humic acids, and natural organic matter, Geochimica Et Cosmochimica Acta, 67 (1): 85-96

40. Schäfer, A. I., Fane, A. G. and Waite, T. D., 2000. Fouling effects on rejection in the membrane filtration of natural waters, *Desalination*, 131: 215-224

41. Stevenson F.J., 1982. *Humus Chemistry*, Wiley, New York, pp. 337–354

42. Tadamier, C. J., Berry, D. F., and Knock,e W. R., 2000, Dissolved Organic Matter Apparent Molecular Weight Distribution and Number-Average Apparent Molecular Weight by Batch Ultrafiltration, *Environ. Sci. Technol.*, 34: 2348-2353

43. Thorn, K. A., 1994, Nuclear-Magnetic-Resonance Spectrometry Investigations of Fulvic and Humic Acids from the Suwannee River, Humic Substances in the Suwannee River, Georgia: Interactions, Properties, and Proposed Structures. Denver, Colo: U.S. G.P.O. Published. Page 142-182

44. Thurman, E. M., 1985, Organic Geochemistry of Natural Waters. Boston, MA: Martinus Nijhoff/ Dr W. Junk Publisher.

45. Yilmaz, L. and McHugh, A. J., 1986, Analysis of Nonsolvent -Solvent -Polymer Phase Diagrams and Their Relevance to Membrane Formation Modeling, *Journal of Applied Polymer Science*, 31(4): 997-1018

46. Yu, J. C., Jiang, Z., Liu, H., Yu, J. and Zhang, L., 2003, β-Cyclodextrin epichlorohydrin copolymer as a solid-phase extraction adsorbent for aromatic compounds in water samples, *Analytica Chimica Acta*, 477(1): 93-101

47. Wagoner, D. B., Christman, R.F., Cauchon, G., Paulson, R., 1997. Molar mass and size of Suwannee River natural organic matter using multi-angle laser light scattering, Environmental Science & Technology, 31 (3): 937-941

48. Wang, G. S., Hsieh, S. T. and Hong, C. S., 2000, Destruction of humic acid in water by UV light—catalyzed oxidation with hydrogen peroxide, *Water Research*, 34(15):3882-3887

49. Wayne, W.Y. Lau, Michael D. Guiver and T. Matsuura, 1991, Phase separation in polysulfone/solvent/water and polyethersulfone/solvent/water systems, *Journal of Membrane Science*, 59: 219-227

50. Won, J., Kang, Y. S., Park, H. C. and Kim, U. Y, 1998, Light scattering and membrane formation studies on polysulfone solutions in NMP and in mixed solvents of NMP and ethyl acetate, *Journal of Membrane Science,* 145(1):45-52

7. Appendix I --- Cost Analysis

Cost Estimation for the Production of a Polymeric Colloidal Adsorbent

John A. Westbrook

Department of Civil and Environmental Engineering

University of Illinois at Urbana-Champaign

1.0 Introduction

The following report explains the steps involved in estimating the batch production costs for polysulfone colloidal particles. The colloidal particles are proposed to be used as an adsorbent for a specific range of membrane-fouling components of source waters. Their use would be a novel step in traditional water treatment process, however, the use of adsorbents, e.g. activated carbon, is not. To demonstrate the economic viability of the proposed adsorbent system, the first step is to determine the cost to manufacture the polymeric particles. The cost of manufacturing may be used to estimate the batch cost of dry particles in $ / kg. This batch cost should then be used in further economic analysis which accounts for adsorption isotherms, recoverability and usability studies to give more meaningful cost information for comparison to existing adsorbent systems.

2.0 Background

The chemical engineering discipline has long been involved in the costing of industrial chemical processes. Engineers have developed empirical analyses for costing industrial processes ranging from highly specific and accurate evaluations and well-established industrial processes to rough order-of-

magnitude evaluations for novel, or untried industrial processes. A fundamental tool used by chemical engineers is the definition of a unit process. Each unit process describes a separate step in a chemical process strategy, whether it be thermodynamic, chemical, or other. To begin the costing analysis the process strategy is defined in terms of the unit processes. The following is the process flow diagram, *PFD*, for the production of the colloidal particles:

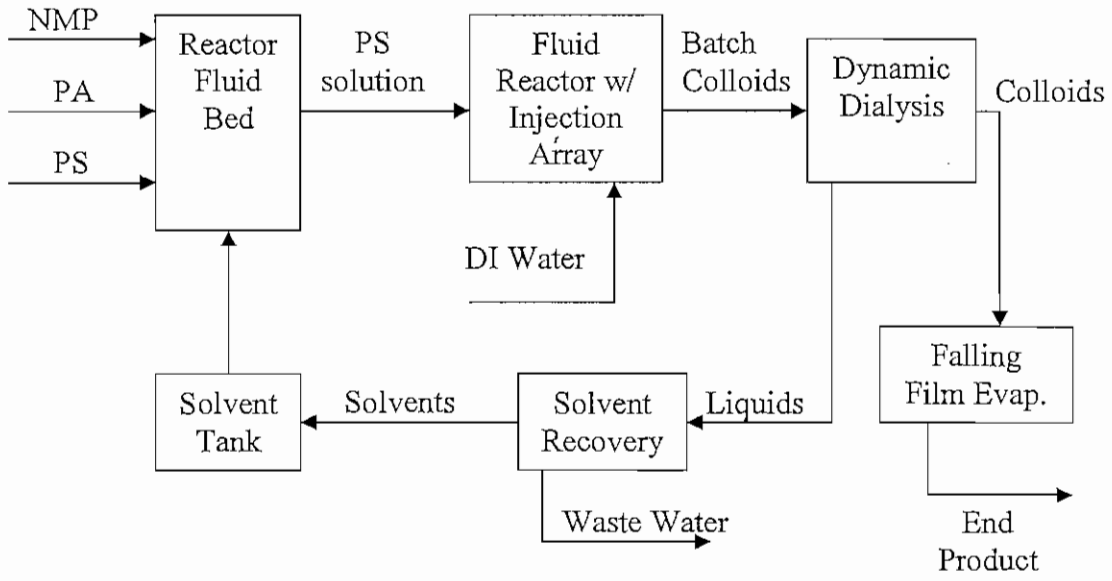

In the *PFD*, NMP and PA are the organic solvents n-methyl pyrrolidinone, and propionic acid, respectively, while PS is the polysulfone, deliverable as a granular (mm diameter) polymer resin. A primary costing on the basis of the input chemicals alone indicates that the two organic solvents make up the bulk of the cost of the raw materials, consequently, separation and recovery steps were added to recycle the solvents.

A dynamic dialysis module was chosen to separate the organic solvents from the particle-water stream as it will handle the colloids gently and, as a passive membrane process, with as little particle agglomeration, or microstructure alteration as possible. Once the organic solvents have been separated from the process stream the suspended colloids will be distributed through a falling-film evaporator which will operate at temperatures high enough to efficiently concentrate the solids while far below the glass transition of the polysulfone solid phase.

The waste stream leaving the dialysis module comprised of highly concentrated solvents will pass on to multi tray distillation columns for thermodynamic separation and purification. Purified solvent streams will combine with supply reservoirs for re-use while waste waters, the distillate top product will be passed as sewage, and should require minimal treatment by a public utility.

While the *PFD* above lacks many critical details that will go into the final design of the manufacturing plant, it contains all of the major unit processes in terms of the modules used in each of the steps of the processing strategy; this contains the necessary information to begin a rough costing [1].

Ulrich gives the following empirical relation for direct manufacturing costs, *DMC*, to the *COM*, or, the cost of manufacturing [2]:

$$DMC = C_{RM} + C_{WT} + C_{UT} + 1.33C_{OL} + 0.069FCI + 0.03COM \qquad \text{Equation 1}$$

In the previous equation, C_{RM} is the cost of the raw materials, C_{WT} is the cost of the waste (water) treatment, C_{OL} is the cost of operating labor and has a coefficient that reflects the costs associated with direct supervisory and clerical labor, and finally *FCI* stands for the fixed capital investment. The *FCI* can be approximated with the knowledge of the equipment and installation costs of each of the unit process modules required, it is preceded by a coefficient which accounts for maintenance, repairs, and operating supplies for each module.

In addition to *DMC*, one must also consider the fixed manufacturing costs, *FMC* which accounts for plant depreciation (which is assumed here to be 10%), local taxes, insurance, and plant overhead costs [2]:

$$FMC = 0.708C_{OL} + 0.068FCI + deprectiation \qquad \text{Equation 2}$$

Ulrich also gives an empirical relation between general manufacturing expenses and the *COM* [2]:

$$GE = 0.177C_{OL} + 0.009FCI + 0.11COM \qquad \text{Equation 3}$$

The *GE* includes administrative costs, distribution, and selling costs. By combining Eqns. 1, 2 and 3, and solving for *COM*:

$$COM = 1.16\left(C_{RM} + C_{WT} + C_{UT}\right) + 2.576C_{OL} + 0.286FCI \qquad \text{Equation 4}$$

Eq.4 gives a simple, empirical method for solving for the cost of plant operation with limited knowledge about the specifics of the plant.

The second major step in developing the batch cost is to determine the production capacity of the plant. Basically, Eq.4 gives the cost to run the plant for a specified amount of time, with a few assumptions about the production rates of the plant one can translate the cost per batch, or cost per unit weight.

3.0 Cost Estimation

3.1 Cost Estimation

The following sections describe the method for solving for each of the variables in Eq.4.

3.1.1 Fixed Capital Investment

The *FCI* term represents capital investments in the manufacturing plant. Here again empirical relations have been developed to determine capital costs based on the type of facility and specifically the modules involved in each of the process steps which can be found in the *PFD*. Determining the bare module costs, C_{BM}, or the cost to purchase a piece of equipment from a manufacturer, is the first step in calculating the *FCI*. Bare module estimates can be obtained directly from the manufacturers, or from industrial averages published in gray literature. In 2002 a software package called Capcost was released that readily performs capital module cost estimations based on industry averages from 2001, and can be run with relatively little information regarding module design. The next step is to factor in direct, indirect, contingency, and fee costs for obtaining the modules [1]:

$$C_p = C_{BM} F_{BM} \qquad \text{Equation 5}$$

where

$$F_{BM} = [1 + \alpha_L + \alpha_{FIT} + \alpha_L \alpha_O + \alpha_E][1 + \alpha_M] \qquad \text{Equation 6}$$

Values for the variables in Eqn. 6 are industrial averages reported in Guthrie's *Process Plant Estimating Evaluation and Control*, 1974 simply; they are the costs of materials, labor, freight, overhead and engineering for each module.

To develop the total module costs, C_{TM}, the cost for installation and interconnection of all of the modules is considered. Traditionally the Lang factor, F_{Lang}, is used to determine the cost to add modules to an existing facility:

$$C_{TM} = F_{Lang} \Sigma C_p \qquad \text{Equation 7}$$

[4], [5], and [6] discuss the derivation and use of the Lang factor, and give that for a solid-fluid processing plant the Lang factor is simply 3.63. Assuming that the plant is created from the ground up and is not an addition to an existing facility the capital costs are higher than C_{TM} alone:

$$FCI = C_{TM} + 0.5 \Sigma C_{BM} \qquad \text{Equation 8}$$

3.1.1.1 Vessel & Reactor Design

To efficiently develop the bare module cost of all reactors and vessels the basic set of design information required includes the diameter, length, maximum operating pressure (MOP), specification of horizontal or vertical arrangement, use of demister pad, and the materials of construction (MOC). However, because none of the reagents need to be stored at high temperatures or pressures and none of them are very corrosive, design of holding vessels is reduced to determining process flow rates and batch volumes. Demister pads should be included in the process costing.

Assuming a 50kg (colloidal solids) batch were desired the reactor in which the resin would be dissolved to 2% by 42% PA and 56% NMP, and which will be called R1, would need to be

50kg*(1/0.02)*[0.42*(1/988.1kg/m^3)+0.56*(1/1025.9kg/m^3)]/(0.42+0.56) = 2.47m^3

Likewise, the water filled vessel, where phase inversion will occur, and into which PS solution will be injected to 25% concentration will necessarily be

2.47m^3*(1/0.25) = 10m^3

These sort of calculations are permissible since the specific gravity for all reagents is near unity. The final two vessels for this process are the holding tanks for the solvents, NMP and PA. Their sizing will depend upon the recycle rate of the entire process, and the solvent demand per batch. In general it is prudent to design the vessels to hold twice the volumetric demand for single batch, in this manner, one batch may be processing while another waits in storage to begin processing once the former has passed any bottlenecks, and while a third process is recycling to storage. Therefore the NMP tank for 50kg (PS) batches will need to be

2*1400kg*(m^3/1025.9kg) = 2.72m^3

while a PA vessel for 50kg batches will be

2*1050kg*(m^3/988.1kg) = 2.13m^3.

3.1.1.2 Evaporator Design

The falling film evaporator operates by distributing a uniform film of process liquid along the inside wall of a column and allowed to fall down the column all the while increasing in temperature, and evaporating, by the transfer of heat through the column wall, and concentrating until being discharged at the bottom. To obtain a bare module estimate for the falling film evaporator only the operating pressure, the heat transfer area, and the MOC are required. Initially it is prudent to characterize the system according to its ability to transfer heat to the liquid which is to be evaporated. This is given by an overall heat transfer coefficient, U [8]

$$\frac{1}{U} = \frac{1}{h_i} + F_i + \frac{l_w}{k_w} + F_o + \frac{1}{h_o} \qquad \text{Equation 9}$$

where F_i is an inside fouling factor, F_o is and outside fouling factor, l_w is the wall thickness, and k_w is the thermal conductivity of the wall, and h_i is the falling film inside coefficient. The falling film coefficient, for water in turbulent flow is calculated as [8]

$$h_i = 120\left(\frac{W}{\pi D}\right)^{1/3} \qquad \text{Equation 10}$$

where W is the weight of the hot liquid and D is the inside diameter of the evaporator. Once the heat transfer coefficient is obtained, a simple economic evaluation may be undertaken, weighing the desired level of concentration against the energy input and size of the evaporator (a direct function of heat transfer area). If the concentration requirement is high enough, multiple evaporator columns may be warranted as their combined capital cost would be lower than the cost of a single very large module.

3.1.1.3 Distillation Design

Distillation design is one of the more involved steps in process costing. Accurate bare module costing of distillation towers require, at a minimum, tower diameter, length, MOP, orientation, need of demister pad, number of sieve trays, and MOC of the tower, trays, and if required, demister pad. The following, from Aerstin and Street, is one of the more efficient ways of determining each of the above parameters.

The distribution of components in the distillate and bottoms should be determined from the feedrate, initial composition, and desired recovery of products. Next, from the 'most desirable pressure and condenser system' the dewpoint of vapor at the top tray and the bubble point temperature of the bottom plate should be calculated. The relative volatility of the light to heavy keys should be calculated as

$$\alpha_{LK/HK} = \frac{P_{LK}}{P_{HK}} \qquad \text{Equation 11}$$

where P represents the partial pressure of the associated key at the average column temperature. Next the Fenske equation may be used to find the minimum number of plates required [9].

$$N_M = \frac{\log[(\chi_{LK}/\chi_{HK})_D(\chi_{LK}/\chi_{HK})_B]}{\log(\alpha_{LK/HK})_{avg}} \qquad \text{Equation 12}$$

Graphical relation, given by VanWinkle, which is not reproduced here, will yield N_{OPT}/N_M. Which is used to calculate N_{OPT}, the optimal number of trays required. Graphical methods are also used to find the optimum to minimum reflux ratio and Underwood's parameter which are used to calculate R_M, the minimum reflux ratio. Graphical relations are further used to find R_{OPT} from R_M and finally, using R_{OPT}, and N_{OPT} the column size and accessories may be determined.

3.1.1.4 Dialyzer Design

The dynamic dialysis module is so named because it employs passive, osmotic pressure to drive transmembrane diffusion as well as dynamic cross flow. The process is inherently slow and will likely be the bottleneck in the colloid production process, however, structural sensitivity of the colloidal particles demands a passive (as opposed to pressure driven) process. Dialysis membrane use at the industrial scale is relatively new and as such, industry wide averages do not exist in literature. The bare module cost of the dialyzer system was requested directly from a single manufacturer and is included in this cost evaluation. Therefore its presence as solitary data should be noted.

3.1.2 Cost of Operating Labor

To determine the cost of operating labor, C_{OL}, is to consider wage rates for all personnel at the facility. Minimizing operation costs requires continuous plant operation; the alternative, initializing and shutting down the plant daily would be very costly. Assuming each operating shift is 8 hours, and that there are 49 operating weeks / year * 5 shifts / week, there are 245 shifts / operator / year. Totally there are 24 hrs / day *365 day / year = 1095 shifts / year. Which means that a plant requires 1095 shifts / year * op-year / 245 shifts ≈ 4.5 operator units. By observing plant operations and noting operating labor requirements for typical unit processes, Ulrich [2] was able to develop the number of operators, x, required per module type so that the number of operators needed for plant operation is simply 4.5 * x.

Typically, chemical plant operators are well paid. In 1993 $USD a chemical plant operator made approximately $42,000 / year, in 1996 $USD that number was $46,800 / year giving an inflation rate equal to 3.67 %. By extending this analysis to 2003 a chemical plant operator would expect to make $58,108 / year, or ~ $30 / hour based on prior assumptions. Given one year of operation the C_{OL} is calculated as

$$C_{OL} = 4.5x * 58{,}108 \qquad \text{Equation 13}$$

3.1.3 Raw Materials Cost

Chemical Market Reporter lists bulk costs of raw materials. The web address is www.chemicalmarketreporter.com. As of February 2003, the cost of NMP was $5.612 / kg, PA was $4.188 / kg, and PS was $0.200 / kg. During the first step of the *PFD*, PS resin, NMP, and PA are mixed and stirred in a reactor at a 1:28:21 weight ratio. After the resin has completely dissolved the fluid is then pumped through an array of pipettes into a second, rapidly stirred, water filled reactor to a concentration of 500 mg/L. For product purity DI water is used in the second step and is estimated by Turton et al. as $1.00 / 1000 kg. No other raw materials are required for the process.

3.1.4 Cost of Utilities & Waste Treatment

In addition to raw materials, and capital expenses, the *COM* considers the cost of the utilities required to run the plant as well as the cost to treat its waste materials. Due to the fact that there are no relatively high temperature or high pressure processes in the process strategy, utility cost are solely a function of the electric energy requirements to run each of the module processes. Usage will be dictated largely by the demand for the thermal distillation process. This method will underestimate energy demands however as the plant will require auxiliary energy for lighting, digital monitoring, pumping, refrigeration, etc. Nationally, in 2003 the cost of electrical energy averaged $16.80 / GJ [1]. Energy costs are tracked and records kept by the Energy Information Administration.

As the *PFD* indicates, the major waste material is waste water. The water will be loaded with organics resulting from inefficiencies in the solvent reclamation step, and will require secondary waste water treatment, i.e. filtration and activated sludge treatment. Nationally secondary waste water treatment cost averaged $43 / 1000 m^3 in 2003 [1].

References

[1] Turton, Richard, R. Bailie, W.B. Whiting, and J.A. Schaewitz, Analysis, Synthesis, & Design of Chemical Processes, 2nd Edition. 2003. Prentice Hall, NJ.

[2] Ulrich, Gael D., A Guide to Chemical Engineering Process Design and Economics. 1984. John Wiley & Sons, New York, NY.

[3] Guthrie, K.M., Process Plant Estimating, Evaluation and Control, 1974. Solana, Solana Beach, CA.

[4] Lang, H.J., "Engineering Approach to Preliminary Cost Estimates," *Chemical Engineering*. 54, no. 9 (1947):130.

[5] Lang, H.J., "Cost Relationships in Preliminary Cost Estimates," *Chemical Engineering*. 54, no. 10 (1947):117.

[6] Lang, H.J., "Simplified Approach to Preliminary Cost Estimates," *Chemical Engineering*. 55, no. 6 (1948):112.

[7] Peters, M. S., K. D. Timmerhaus, Plant Design and Economics for Chemical Engineers, 4th Edition. 1991. McGraw-Hill, New York, NY.

[8] Aerstin, Frank, and Gary Street, Applied Chemical Process Design. 1978. Plenum Press, New York, NY.

[9] VanWinkle, M., and W.G.Todd, "Optimum Fractionation Design by Simple Graphical Methods," *Chemical Engineering*. (September 20, 1971):136-148.

8. Appendix II – US patent

US006669851B2

(12) **United States Patent**
Clark et al.

(10) Patent No.: US 6,669,851 B2
(45) Date of Patent: Dec. 30, 2003

(54) **WATER PURIFICATION BY POLYMER COLLOIDS**

(75) Inventors: **Mark M. Clark**, Urbana, IL (US); **Robert Riley**, La Jolla, CA (US)

(73) Assignee: **Board of Trustees of University of Illinois**, Urbana, IL (US)

(*) Notice: Subject to any disclaimer, the term of this patent is extended or adjusted under 35 U.S.C. 154(b) by 0 days.

(21) Appl. No.: **09/995,252**

(22) Filed: **Nov. 26, 2001**

(65) **Prior Publication Data**

US 2003/0100617 A1 May 29, 2003

(51) **Int. Cl.**[7] **B01J 2/26**; B01J 20/34; C02F 1/28; C08G 75/20; C08G 75/23

(52) **U.S. Cl.** **210/670**; 210/650; 210/661; 210/692; 252/180; 502/402; 516/77; 525/906; 528/391

(58) **Field of Search** 516/77; 252/180; 525/906; 528/391; 502/402; 210/661, 670, 692

(56) **References Cited**

U.S. PATENT DOCUMENTS

2,684,950	A	*	7/1954	Rivers et al.
3,272,782	A	*	9/1966	Lang ..... 516/77 X
3,272,784	A	*	9/1966	Lang ..... 252/180 X
4,247,432	A		1/1981	Huang et al.
4,321,174	A	*	3/1982	Hoy et al. ..... 525/906 X
4,451,424	A	*	5/1984	Tweddle et al. ..... 525/906 X
4,569,989	A	*	2/1986	Madison ..... 252/180 X
4,661,257	A		4/1987	Kreevoy et al. 210/638
4,990,248	A		2/1991	Brown et al. 210/136
5,041,335	A	*	8/1991	Inai et al. ..... 252/906 X
5,418,203	A	*	5/1995	Ichikawa et al. 502/402
5,434,226	A	*	7/1995	Nguyen et al. ..... 525/906 X
5,904,832	A	*	5/1999	Clifford et al. ..... 210/670 X
5,969,082	A	*	10/1999	Kuwahara et al. ..... 525/906 X
6,110,375	A		8/2000	Bacchus et al. 210/652
6,451,921	B2	*	9/2002	Weisse et al. ..... 528/391 X

OTHER PUBLICATIONS

Fritzsche, A.K., et al., The Effect of Free Volume on Enhanced Transport Rates of Polysulfone Hollow Fiber Membranes Spun from Lewis Acid: Base Solvent Complexes, *Journal of Membrane Science,* 46 (1989) 135–155.

Von Wandruszka, R., Final Report: The Secondary of Humic Acid and it Environmental Implications, at http://es.epa.gov/ncerqa/final/vonwandruszka.html Nov. 18, 1999.

Humic Acid, at http://www.greensmiths.com/humic.htm 1996.

Frost & Sullivan, "Activated Carbon: Sinking Market or Secure Opportunity?" at http://www.waternet.com/new.asp 2001.

Murakami, H., et al., "Preparation of poly(DL–lactide–co–glycolide) nanoparticles by modified spontaneous emulsification solvent diffusion method," International Journal of Pharmaceutics, vol. 187, pp. 143–152 (1999).

Berkland, C., et al., "Fabrication of PLG microspheres with precisely controlled and monodisperse size distributions," Journal of Controlled Release, vol. 73, pp. 59–74 (2001).

Fritzsche, A.K., et al., "The Effect of Free Volume on Enhanced Transport Rates of Polysulfone Hollow Fiber Membranes Spun from Lewis Acid: Base Solvent Complexes", *Journal of Membrane Science,* 46 (1989) 135–155.

Kociuk, et al., "Water Purification and Desalination, An AP Chemistry Project", printed from the Internet at: http://shell.rmi.net/~chill/chemistry/h2o/h20.html, dated Jan. 2, 2001, pp. 1–5.

Von Wandruszka, R., "Final Report: The Secondary of Humic Acid and it Environmental Implications", printed from the *U.S. Environmental Protection Agency* Internet website at: http://es.epa.gov/ncerqa/final/vonwandruszka.html dated Jan. 2, 2002, pp. 1–5.

"Humic Acid", printed from the Internet at http://www.greensmiths.com/humic.htm, dated Jan. 2, 2001, pp 1–3.

Frost & Sullivan, "Activated Carbon: Sinking Market or Secure Opportunity?" printed from the Internet at http://www.waternet.com/new.asp, dated Aug. 9, 2001, pp 1–2.

Solvay Advanced Polymers, "Radel®, Udel® Mindel® sulfone polymers pack a powerful punch", printed from the Internet at: http://www.solvayadvancedpolymers–us.com/ep_performance_amorphous.htm, dated Feb. 4, 2002, pp. 1–2.

Solvay Advanced Polymers, Udel® P–1700, printed from the Internet at: http://www.solvayadvancedpolymers–us.com/ep_datasheet.asp, on Feb. 4, 2002. pp. 1–2.

Solvay Advanced Polymers, Udel® GF–120, printed from the Internet at: http://www.solvayadvancedpolymers–us.com/ep_datasheet.asp, on Feb. 4, 2002, pp. 1–2.

Solvay Advanced Polymers, Radel® A–200, printed from the Internet at: http://solvayadvancedpolymers–us.com/ep_datasheet.asp, on Feb. 4, 2002, pp 1–2.

Solvay Advanced Polymers, Radel® A–300, printed from the Internet at: http://www.solvayadvancedpolymers–us.com/ep_datasheet.asp, on Feb. 4, 2002, pp. 1–2.

(List continued on next page.)

Primary Examiner—Richard D. Lovering
(74) *Attorney, Agent, or Firm*—Brinks Hofer Gilson & Lione

(57) ABSTRACT

A colloid comprises a sulfone polymer. The colloid may be used as a replacement for activated carbon or charcoal in water purification systems. Unlike activated carbon, the colloid is advantageously regenerated chemically and reused.

28 Claims, 4 Drawing Sheets

OTHER PUBLICATIONS

Solvay Advanced Polymers, Radel® AG-320, printed from the Internet at: http://www.solvayadvancedpolymers-us.com/ep_datasheet.asp, on Feb. 4, 2002, pp 1-2.

Solvay Advanced Polymers, Radel® AG-330, printed from the Internet at: http://www.solvayadvancedpolymers-us.com/ep_datasheet.asp, on Feb. 4, 2002, pp 1-2.

Solvay Advanced Polymers, Radel® R-5000, printed from the Internet at: http://www.solvayadvancedpolymers-us.com/ep_datasheet.asp, on Feb. 4, 2002, pp 1-2.

Solvay Advanced Polymers, Radel® R-5100 NT 15, printed from the Internet at: http://www.solvayadvancedpolymers-us.com/ep_datasheet.asp, on Feb. 4, 2002, pp 1-2.

Solvay Advanced Polymers, Radel® R-5500, printed from the Internet at: http://www.solvayadvancedpolymers-us.com/ep_datasheet.asp, on Feb. 4, 2002, pp 1-2.

Solvay Advanced Polymers, Radel® R-5800, printed from the Internet at http://www.solvayadvancedpolymers-us.com/ep_datasheet.asp, on Feb. 4, 2002, pp 1-2.

Solvay Advanced Polymers, Radel® R-7700, printed from the Internet at: http://www.solvayadvancedpolymers-us.com/ep_datasheet.asp, on Feb. 4, 2002, pp 1-2.

Solvay Advanced Polymers, Mindel® B-430, printed from the Internet at: http://www.solvayadvancedpolymers-us.com/ep_datasheet.asp, on 2/4/2, pp. 1-2.

Solvay Advanced Polymers, Mindel® S-1000, printed from the Internet at: http:www.solvayadvancedpolymers-us.com/ep_datasheet.asp, on Feb. 4, 2002, pp. 1-3.

Product Information Sheet for X-100: TRITON X-100™, printed from the Internet at: http://www.sigma.sial.com/sigma/proddata/t6878.htm, on Feb. 4, 2002, pp. 1-3.

Product Information Sheet for TRITON Detergents: Octylphenol Series, prited from the Internet at: http://www.sigma.sial.com/sigma/proddata/t6878x.htm, on Feb. 4, 2002, 1 page.

* cited by examiner

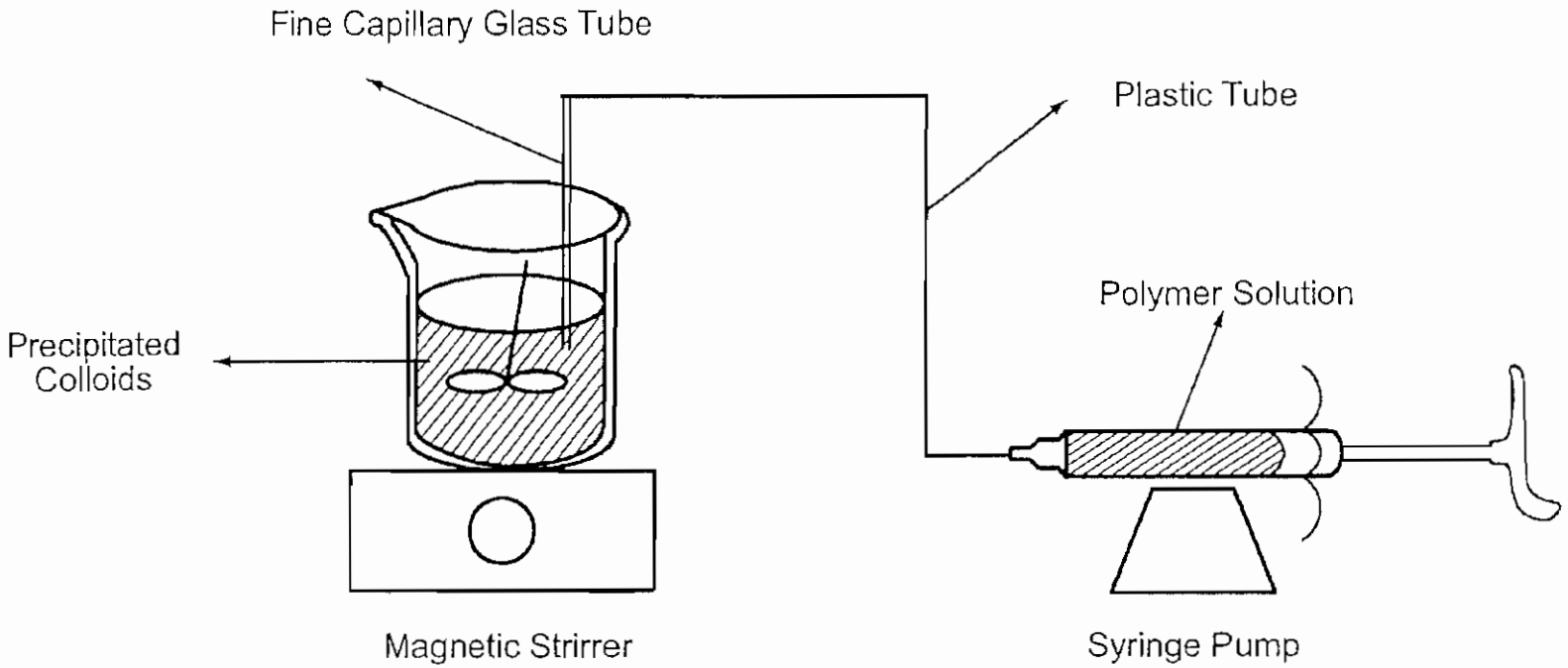

Laboratory Apparatus For Synthesizing The Sulfone Polymer Colloids

FIG. 1

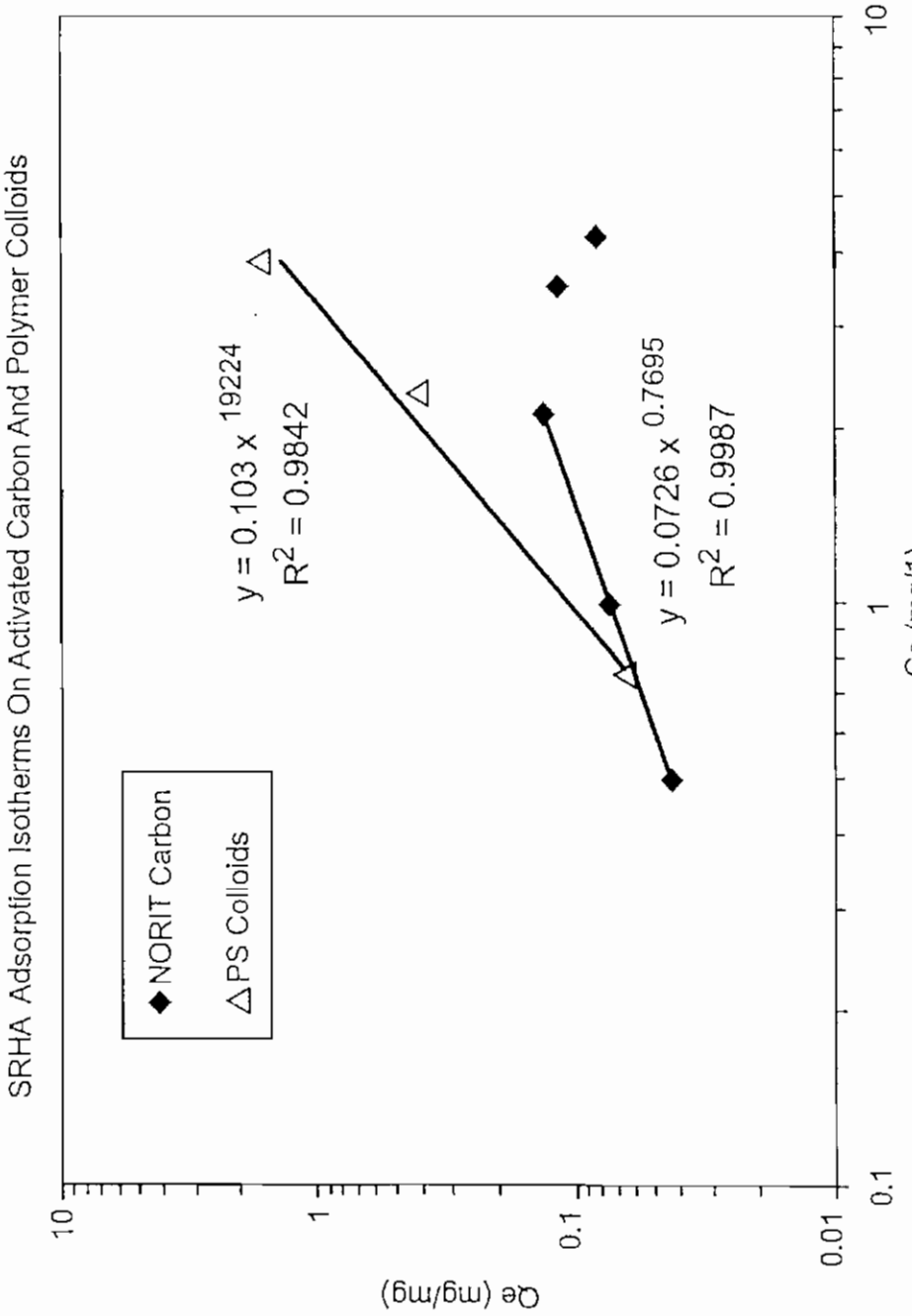
SRHA Adsorption Isotherms On Activated Carbon And Polymer Colloids
◆ NORIT Carbon
△ PS Colloids
y = 0.103 x 19224
R2 = 0.9842
y = 0.0726 x 0.7695
R2 = 0.9987
Qe (mg/mg)
Ce (mg/l)
10
1
0.1
0.01
0.1
1
10

FIG. 2

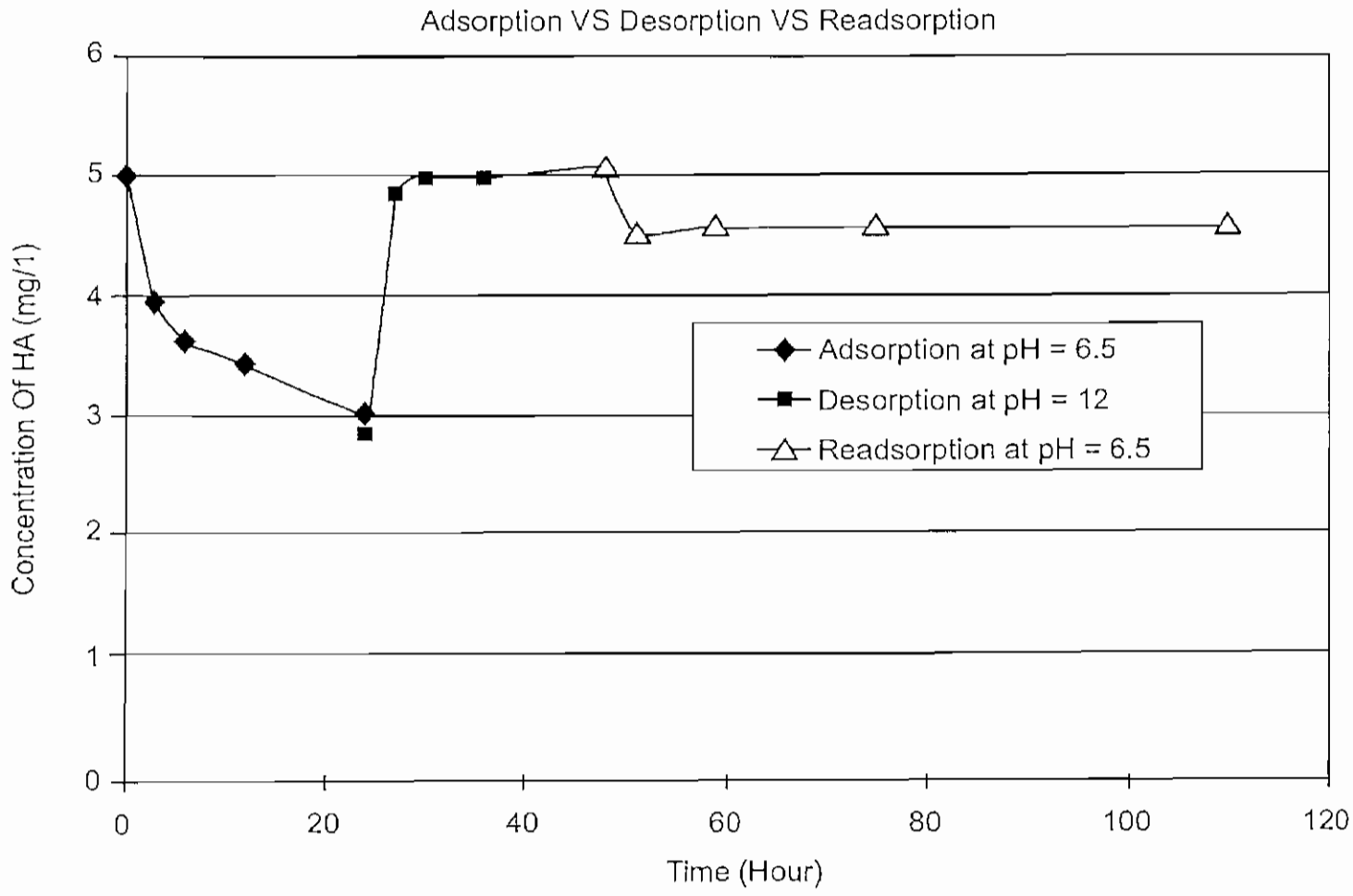
Adsorption VS Desorption VS Readsorption
Concentration Of HA (mg/1)
Time (Hour)
0
1
2
3
4
5
6
0
20
40
60
80
100
120
Adsorption at pH = 6.5
Desorption at pH = 12
Readsorption at pH = 6.5

FIG. 3

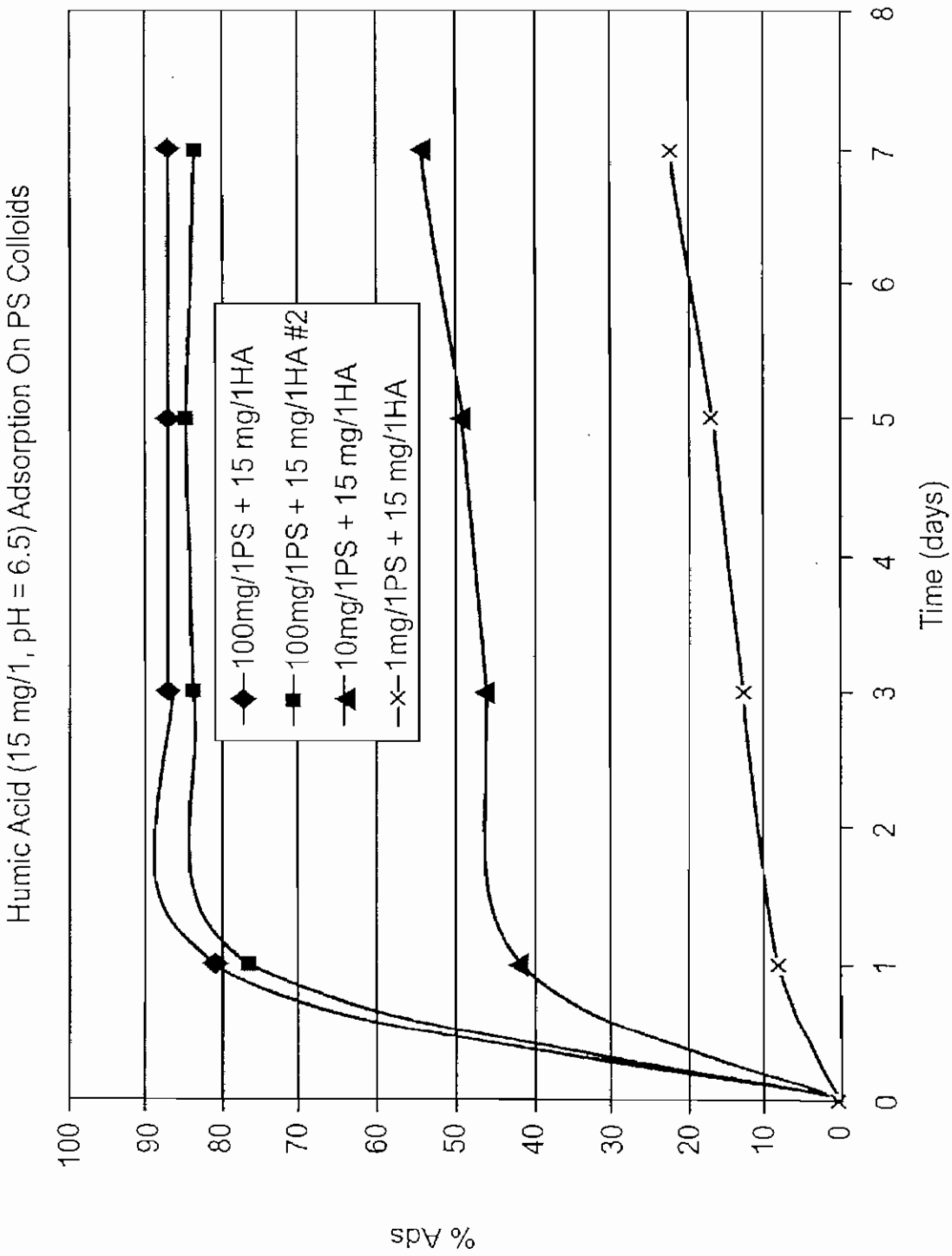
Humic Acid (15 mg/1, pH = 6.5) Adsorption On PS Colloids
100mg/1PS + 15 mg/1HA
100mg/1PS + 15 mg/1HA #2
10mg/1PS + 15 mg/1HA
1mg/1PS + 15 mg/1HA
% Ads
Time (days)
0
10
20
30
40
50
60
70
80
90
100
0
1
2
3
4
5
6
7
8

WATER PURIFICATION BY POLYMER COLLOIDS

BACKGROUND

The present invention relates to a novel process for the purification of water. Dissolved organic substances typically found in water supplies include man-made compounds and the natural products of plant decay, including humic acid, which can give undesirable color, taste, and odor to water. Dissolved organics also interfere with the water purification process by clogging filters and fouling resin beds. Furthermore, during treatment of the water supply at drinking water treatment facilities, natural organic matter can also react with chemical disinfectants, such as chlorine, to produce chlorinated-organic compounds, many of which are known carcinogens.

Activated carbon has long been used to adsorb organic compounds from water supplies. Typically, carbon filters are used prior to other purification processes to partially purify the water and prevent fouling of ion-exchange beds or membranes. Presently, activated carbon pre-filters are used before high performance water purification membranes, such as reverse osmosis membranes. Without a pre-filter, such membranes would rapidly clog with organic contaminants. However, all activated carbons have the disadvantage of requiring disposal or regeneration after their adsorption capacity is exhausted.

Many activated carbons, including those in powdered form, are never regenerated and remain in the residuals or sludges generated from water treatment. These residuals or sludges must then be disposed of as solid waste, usually in a landfill, which poses a secondary pollution problem.

Unlike their powdered counterparts, granular activated carbons can be regenerated using a high temperature process where the adsorbed organic materials are volatized or burned from the carbon. This process is energy intensive, and can cause secondary air and water pollution problems.

BRIEF SUMMARY

In a first aspect, the present invention is a colloid comprising a sulfone polymer.

In a second aspect, the present invention is a method for purifying water, comprising contacting a colloid comprising a polymer with water, the water comprising organic matter; and separating the colloid from the water.

In a third aspect, the present invention is a method of purifying a colloid comprising contacting a colloid further comprising organic matter with an alkali solution.

BRIEF DESCRIPTION OF THE DRAWINGS

FIG. 1 shows a representative laboratory scale synthesis apparatus for forming polymer colloids.

FIG. 2 shows the adsorption isotherm for humic acid on sulfone polymer colloids and NORIT powdered activated carbon.

FIG. 3 shows the regeneration of sulfone polymer colloids at increased pH and the readsorption of humic acid onto the colloids.

FIG. 4 shows the adsorption kinetics for humic acid at different sulfone polymer colloid concentrations.

DETAILED DESCRIPTION

The present invention includes using colloids, such as sulfone polymer colloids, to adsorb organic contaminants from water. The colloids may be made, for example, by dissolving a sulfone polymer in a solvent and precipitating the sulfone polymer as a polymer colloid. When the colloids are added to water containing organic contaminants, the contaminants are adsorbed onto the colloids. Removal of the colloids from the water results in removal of the organic contaminants, purifying the water. The colloids may be regenerated, or cleaned of the adsorbed organic contaminants, by exposing them to base. The regenerated colloids may then be reused.

The colloids may directly replace powdered activated carbon as it is presently used in drinking water treatment, for taste and odor control and adsorption of natural and synthetic organic pollutants. Rather than being discarded in the water treatment sludge, as is presently done with activated carbon, the colloids may be regenerated and reused. Additionally, the colloids can be used in place of an activated carbon pre-filter. When the colloids are made from the same or similar polymer as the purification membrane, superior pre-filtration is possible.

As described in Van Nostrand's Encyclopedia of Chemistry, pp. 272–276 (Douglas M. Considine ed., Van Nostrand Reinhold Co. 1984), colloids are disperse systems with at least one particle dimension averaging in the range of 10^{-6} to 10^{-3} mm. Particles may be defined as liquid or solid. Examples include sols (dispersions of solid in liquid), emulsions (dispersions of liquids in liquids), and gels (systems, such as jelly, in which one component provides a sufficient structural framework for rigidity and other components fill the space between the structural units). Preferably, the polymer colloids of the current invention are sols or sol-gels.

The polymer colloids may be precipitated when a solution containing the polymer is added to a liquid in which the polymer has lower solubility than the solvent of the solution. The solution is formed by dissolving the polymer in a solvent or mixture of solvents that has a higher solubility toward the polymer.

When the solution containing the polymer is added to a liquid having a lower solubility for the polymer, polymer colloids precipitate. Various solvents, solvent mixtures, surfactants, wetting agents, and acids can be used to tailor the morphology of the colloids. While many large scale production methods could be used, as known to those of skill in the art, a syringe pump is appropriate on the laboratory scale. A representative laboratory scale synthesis apparatus is shown in FIG. 1.

Polymers useful in the present invention include, sulfone homopolymers and copolymers such as polymers of polysulfone, polyethersulfone, polyphenylsulfone, and sulfonated polysulfone; homopolymers and copolymers of cellulose acetate, polyacrylonitrile (PAN), polyetherimide, and poly(vinylidene fluoride) (PVDF); and mixtures thereof. Such polymers may be purchased from AMOCO PERFORMANCE PRODUCTS, INC. (Alpharetta, Ga.) under the trade names of UDEL (polysulfone), MINDEL (sulfonated polysulfone), RADEL-A (polyethersulfone), and RADEL-R (polyphenylsulfone). They are also available from ALDRICH, Milwaukee, Wis.

Suitable average molecular weights for polysulfone useful in the current invention range preferably from 10,000 to 45,000, more preferably from 17,000 to 35,000, and most preferably from 26,000 to 27,000. Suitable average molecular weights for polyethersulfone useful in the current invention range from 8,000 to 28,000, preferably from 13,000 to 23,000, and most preferably from 16,000 to 20,000. Suitable

average molecular weights for poly(vinylidene fluoride) useful in the current invention range preferably from 100,000 to 600,000, more preferably from 180,000 to 534,000, and most preferably from 275,000 to 530,000. Suitable average molecular weights for polyacrylonitrile useful in the current invention range preferably from 30,000 to 150,000, more preferably from 60,000 to 110,000, and most preferably from 80,000 to 90,000. All average molecular weights are weight average molecular weights.

The solution containing the polymer includes the polymer and one or more solvents in which the polymer demonstrates solubility. Any solvent that permits colloid formation when the polymer solution is added to a liquid in which the polymers have lower solubility may be used. Additionally, the solution may contain an acid. Any acid which is compatible with the selected polymer and solvent system can be used if colloids form when the solution is mixed with a liquid in which the polymer has lower solubility. Although not intending to be bound by any particular theory, it is believed that the acid (a weak Lewis acid) complexes with the solvent (a weak Lewis base) to form a complex which breaks up when mixed with the liquid. Many acid/solvent systems are possible and are more fully described, for example, in Fritzsche, et. al., *Journal of Membrane Science,* 46, 135 (1989).

Suitable solvents include N-methyl pyrrolidine (NMP), N,N-dimethylformamide (DMF), dimethyl sulfoxide (DMSO), acetone, and dioxane, and are available from ALDRICH, Milwaukee, Wis. Suitable acids include organic acids, such as propionic acid.

Additionally, surfactants may be added to the solution to stabilize the colloids and otherwise vary their morphology. While any surfactant, including anionic, cationic, or non-ionic, may be used, preferable surfactants include sodium lauryl sulfate, TRITON X-45, and TRITON X-100, or mixtures thereof. Wetting agents, such as alcohols, may also be added.

Scanning electron micrographs show that small, relatively uniform spherical particles of colloids with average individual diameters of preferably from 10 to 1000 nanometers (nm), more preferably from 25 to 500 nm, and most preferably from 50 to 100 nm, are formed during precipitation. Aggregates of the colloid particles attain various shapes and sizes with a wide size distribution. Average aggregate diameters are from 10 μm to 1000 μm, preferably from 25 μm to 500 μm, and most preferably from 100 μm to 500

When the polymer colloids are added to water containing organic matter, the contaminating organic matter is adsorbed. The addition may be carried out in any appropriate agitated vessel or fluidized reactor. Although variables, including temperature, contaminant concentration, and colloid concentration affect the rate of adsorption, the organic matter is typically adsorbed onto the colloids within minutes to hours.

Organic matter includes hydrocarbons, hydrophobic pollutants, or pollutants with mixed hydrophobic/hydrophilic properties that pollute water by imparting an undesirable color, taste, or odor, as well as any other carbon-containing compound. Preferably, the present invention removes natural organic matter; natural organic matter includes carbon containing material typically found in drinking water supplies. Although many types of organic matter contaminants may be found in water, humic acid is one of the most common. Other organic matter contaminants include benzene, toluene, proteins, geosmin (a natural organic compound leached from soils), and 2-methylisoborneol (MIB) (a natural organic compound of aquatic biological origin).

Purified water is formed by removing the colloids that contain the organic contaminants from the water. As shown in FIG. 2, the colloidal polymers have a larger adsorption capacity for humic acid than activated carbon adsorbents typically used in the treatment of drinking water, including NORIT powdered activated carbon.

Any method may be used to remove the contaminated colloids from the water, such as centrifugation, filtration, gravity decantation, counter-current decantation, and packed column filtration. Filtration methods typically entail passing the purified water containing the contaminated colloids through a filter with pore sizes of a smaller average diameter than the average diameter of the colloids.

Gravity and counter-current decantation and fluidized bed methods rely on the colloids, or the substrates to which they are bound, having a greater density than the purified water. Gravity decantation describes methods where the colloids are allowed to settle due to gravity from the purified water, which is then removed without significantly disturbing the settled colloids. Counter-current decantation and fluidized beds suspend the colloids in the contaminated water stream using fluid movement.

Similarly, the colloids may be immobilized on a substrate which is then filtered out. Alternatively, the colloids are immobilized on a membrane or a packed column of substrate beads through which the contaminated water passes. Typically, a suspension containing the colloids are vacuum filtered through a membrane, thus trapping the colloids or their aggregates on the membrane. Suitable substrates include any material which is chemically compatible with the colloids and has the ability to bind the colloids while being physically larger, such as glass or plastic beads or mesh. The colloids may also be held in a container, such as a nylon mesh bag, which is permeable to water but not the colloids.

Once the contaminated colloids are removed from the purified water, they may be regenerated by chemically desorbing the organic contaminants. Unlike activated carbon, this allows reuse of the colloids for continued water purification and optional recovery of the organic contaminants (FIG. 3). In many instances, the organic contaminants have value as a fertilizer for plants.

The organic contaminants are desorbed from the colloids by exposing the colloids to an alkali solution. Although the alkali solution may be of any concentration, it preferably has a free hydroxide concentration of 1×10^{-4} to 10 N, more preferably of 1×10^{-3} to 5 N, and most preferably of 1×10^{-2} to 1 N. Any alkali solution may be used, such as a solution of sodium hydroxide, ammonium hydroxide, potassium hydroxide, calcium hydroxide, or mixtures thereof. Sodium hydroxide is most preferred.

Once the colloids are exposed to elevated pH, they are removed from solution using separation methods apparent to those of skill in the art, including those previously described, and are returned to the water source to remove more organic contaminants.

EXAMPLES

Example 1

Two grams of polysulfone (PS) (26,000–27,000 MW) was added to 56 grams of N-methyl pyrrolidine (NMP) solvent. The mixture was shaken in a gyrator until the polysulfone solids fully dissolved (approximately 1 day). Forty two

grams of propionic acid (PA) was added to the PS/NMP solution to form a mixture with a molar ratio of 1:1 PS/NMP to PA. The mixture was shaken until a homogeneous solution formed. The solution was stored at room temperature.

A syringe was then filled with 2.5-mL of the stored solution and placed in a syringe pump with a pumping rate of 1.5 mL/hr. A beaker was filled with 500 mL of deionized water which was stirred by a magnetic stirrer. The syringe pump was then used to pump the polysulfone containing solution through a capillary tube into the stirred water at about 25° C. Polymer colloids formed in the deionized water. When agitation was stopped, the colloids quickly settled to form aggregates.

Colloid samples were observed under ordinary optical mieroscopy (aus JENALaboval 4) with 200X magnification. Samples were also examined under Environmental Scanning Electron Microscopy (ESEM). The polysulfone colloids were concentrated onto 0.22-μm nylon filter paper by filtering the colloids solution with a syringe filter. The filter paper was then dried and coated with a gold-palladium sputter for ESEM analysis. ESEM analysis showed that the colloids are spherical in nature, having a diameter of about 50 nanometers, and are clumped into small aggregates.

Example 2

To test the performance of the PS colloids for water purification, Suwannee River Humic acid, obtained from the International Humic Substances Society, University of Minnesota, St. Paul, Minn. was used as a model. Humic acid was adsorbed by polysulfone colloids of varying concentration (100 mg/L, 10 mg/L, and 1 mg/L), but with constant humic acid concentration as follows:

A 15 mg/L humic acid solution was prepared by dissolving 15 mg of humic acid (Suwannee River Humic acid, International Humic Substanees Society) in a 1-Liter Erlenmeyer flask, with 10^{-3} M Na_2HPO_4 buffer. The solution pH was adjusted to 6.5 with 1 N HCl.

A 200 mL aliquot of each colloid composition (100 mg/L, 10 mg/L, and 1 mg/L) was mixed with 100 mL of the 15 mg/L humic acid solution in a glass jar. The jar was covered with a sheet of aluminum foil, and the cap was screwed on tightly over the foil. The glass jars were then put onto a gyrator shaker at approximately 22° C. A 10 mL sample was drawn from each jar on the 1st, 3rd, 5th, and 7th days and passed through a 0.22 μm nylon filter to remove the colloids. The percent of humic acid (HA) remaining in solution was then calculated from UV adsorption data at 254 nanometers. Recorded UV readings were the average of 10 replicates for each colloid concentration and are presented below in Table I.

TABLE 1

Time (days)		0	1	3	5	7
Control 5 mg/L HA	UV-ads	0.153	0.151	0.150	0.149	0.150
100 mg/L Colloid	UV-ads	0.153	0.029	0.02	0.0194	0.02
15 mg/L HA	% HA Adsorbed	0	80.79	86.67	86.98	86.67
100 mg/L Colloid	UV-ads	0.153	0.036	0.025	0.023	0.025
15 mg/L HA	% HA Adsorbed	0	76.16	83.33	84.56	83.33
10 mg/L Colloid	UV-ads	0.153	0.088	0.081	0.076	0.069

TABLE 1-continued

Time (days)		0	1	3	5	7
15 mg/L HA	% HA Adsorbed	0	41.72	46.00	48.99	54.00
1 mg/L Colloid	UV-ads	0.153	0.139	0.131	0.124	0.117
15 mg/L HA	% HA Adsorbed	0	7.95	12.67	16.78	22.00

The adsorption kinetics for humic acid at different polysulfone colloid concentrations are shown in FIG. 4. Almost 87% of the humic acid was adsorbed onto the 100 mg/L polysulfone colloids. Two trials of five aliquots each showed good reproducibility. The control samples demonstrated that the adsorption of humic acid on the wall of the glass jar was negligible, and that only polysulfone colloids contribute to the adsorption of humic acid over the 7 day period. Most adsorption occurred during day one and then plateaued. Based on the final sample taken on the 7th day, an isotherm was determined as shown in FIG. 2. Using the Freundlich isotherm to fit the data, a F=0.103 (mg HA/mg polysulfone) and a 1/n=1.9224 were obtained.

Example 3

In order to check whether the polysulfone colloids are reusable, a set of adsorption, desorption and readsorption tests were performed with 300 mL aliquots of 10 mg/L polysulfone colloids added to 150 mL of 15 mg/L humic acid solution. Humic acid adsorption was performed in accord with the method described in Example 2. The humic acid was then desorbed from the colloids by raising the pH of the solution to 12 with 1 N sodium hydroxide.

Readsorption of humic acid was performed by adjusting the pH of the solution down to 6.5 with 1 N HCl. Since most humic acid adsorption occurred on the first day, the experiments were performed with 1 day adsorption, 1 day desorption, and 1 day readsorption time periods.

Example 4

The adsorption eapacity of polysulfone colloids was compared to activated carbon as follows: A set of adsorption isotherms were performed with humic acid solution on activated carbon with carbon doses of 0, 5, 10, 20, 50, and 100 mg of activated carbon per Liter of humic acid solution.

NORIT SA-UF activated carbon, obtained from NORIT Americas, Atlanta, Ga., was used because it has the best adsorption capacity among the commercialized activated carbons. The initial concentration of humic acid was 5 mg/L and the solution pH was adjusted to 6.5. The experiment lasted 7 days and was considered to be in equilibrium on the 7th day.

Adsorption isotherms of humic acid on activated carbon versus polysulfone colloids are shown in FIG. 2. For activated carbon adsorption, the linear fit of the first three data excluding the curvature gives a F=0.072, and 1/n=0.7695 with Freundlich isotherm fitting. Compared to the activated carbon, the polymer colloids demonstrated greater adsorption capacity, approaching an order of magnitude, as shown by the npper line.

Prophetic Example 5

Colloids are incorporated into a membrane by vacuum filtering a water suspension containing the colloids through a 0.22 micron pore diameter nylon filter. Even though the

pore diameter of the filter is larger than the approximate 50 nm diameter of the colloid particles, the particles are trapped due to aggregation. Water contaminated with organic matter is then purified of organic matter by passing the contaminated water through the filter.

What is claimed:

1. A colloid comprising a sulfone polymer, wherein

the sulfone polymer is selected from the group consisting of copolymers and homopolymers of polysulfone, polyphenylsulfone, sulfonated polysulfone, and copolymers of polyethersulfone, or mixtures thereof; and where

particles of the colloid have an average diameter of 10 nm to 1000 nm.

2. The colloid of claim 1, wherein said polymer has a molecular weight of 13,000 to 23,000.

3. The colloid of claim 1, wherein said polymer has a molecular weight of 16,000 to 20,000.

4. The colloid of claim 1, wherein particles of said colloid have if an average diameter of 25 nm to 500 nm.

5. The colloid of claim 1,wherein said polymer is a homopolymer or a copolymer of polysulfone.

6. The colloid of claim 5, wherein said polymer has a molecular weight of 17,000 to 35,000.

7. The colloid of claim 5, wherein said polymer has a molecular weight of 26,000 to 27,000.

8. A method of purifying the colloid of claim 1, comprising:

contacting the colloid of claim 1 with organic matter to yield a colloid comprising organic matter; and

contacting the colloid comprising organic matter with an alkali solution.

9. The method of claim 8, wherein the organic matter comprises at least one member selected from the group consisting of humic acid, geosmin, and 2-methyl isoborneol.

10. The method of claim 8, wherein said alkali is selected from the group consisting of sodium hydroxide, potassium hydroxide, ammonium hydroxide, and calcium hydroxide, or mixtures thereof.

11. A colloid comprising a sulfone polymer, wherein particles of said colloid have an average diameter of 50 nm to 100 nm.

12. A method of purifying the colloid of claim 10, comprising:

contacting the colloid of claim 10 with organic matter to yield a colloid comprising organic matter; and

contacting the colloid comprising organic matter with an alkali solution.

13. The method of claim 12, wherein the organic matter comprises at least one member selected from the group consisting of humic acid, geosmin, and 2-methyl isoborneol.

14. The method of claim 12, wherein said alkali is selected from the group consisting of sodium hydroxide, potassium hydroxide, ammonium hydroxide, and calcium hydroxide, or mixtures thereof.

15. A method of making the colloid of claim 11, comprising mixing a solution and water, to form said colloid;

wherein said solution comprises the sulfone polymer, a solvent, and an acid.

16. The method of claim 15, wherein said polymer is selected from the group consisting of copolymers and homopolymers of polysulfone, polyethersulfone, polyphenylsulfone, and sulfonated polysulfone, or mixtures thereof.

17. The method of claim 15, wherein said solution further comprises a surfactant selected from the group consisting of sodium lauryl sulfate, octyl phenoxy polyethoxy ethanol 4.5, and octyl phenoxy polyethoxy ethanol 10, or mixtures thereof.

18. The method of claim 15, wherein said water further comprises a surfactant.

19. The method of claim 15, wherein said solvent is selected from the group consisting of N-methyl pyrrolidine, N,N-dimethylformamide, dimethyl sulfoxide, acetone, and dioxane, or mixtures thereof.

20. The method of claim 15, further comprising immobilizing the colloid on a substrate.

21. The method of claim 20, wherein said substrate is selected from the group consisting of a membrane and a bead.

22. A method of making a colloid comprising a sulfone polymer, comprising mixing a solution and water, to form said colloid;

wherein said solution comprises the polymer, a solvent, and an acid.

23. The method of claim 22, wherein said polymer is selected from the group consisting of copolymers and homopolymers of polysulfone, polyethersulfone, polyphenylsulfone, and sulfonated polysulfone, or mixtures thereof.

24. The method of claim 22, wherein said solution further comprises a surfactant selected from the group consisting of sodium lauryl sulfate, octyl phenoxy polyethoxy ethanol 4.5, and octyl phenoxy polyethoxy ethanol 10, or mixtures thereof.

25. The method of claim 22, wherein said water further comprises a surfactant.

26. The method of claim 22, wherein said solvent is selected from the group consisting of N-methyl pyrrolidine, N,N-dimethylformamide, dimethyl sulfoxide, acetone, and dioxane, or mixtures thereof.

27. The method of claim 22, further comprising immobilizing the colloid on a substrate.

28. The method of claim 27, wherein said substrate is selected from the group consisting of a membrane and a bead.

* * * * *